Development of novel TRIP strip steel grades for automotive applications.

Moody, Mark K

Moody, M. K.

Swansea University

Development of Novel TRIP Strip Steel Grades for Automotive Applications EngD

2009

DECLARATION

This work has not previously been accepted in substance for any degree and is not being concurrently submitted in candidature for any degree.

Signed .... (candidate)

Date .....28/10/09.....

STATEMENT 1

This thesis is the result of my own investigations, except where otherwise stated. Where correction services have been used, the extent and nature of the correction is clearly marked in a footnote(s).

Other sources are acknowledged by footnotes giving explicit references. A bibliography is appended.

Signed .... (candidate)

Date .....28/10/09.....

STATEMENT 2

I hereby give consent for my thesis, if accepted, to be available for photocopying and for inter-library loan, and for the title and summary to be made available to outside organisations.

Signed .... (candidate)

Date .....28/10/09.....

ABSTRACT

One of the advances in materials used in the manufacture of body panels, structural and crash components is the development of advanced high strength sheet steel. However, one drawback found when using such high strength levels is that these high strength alloys generally have lower ductility levels. This is a particular disadvantage when it comes to metal-forming operations.

Low-alloy transformation induced plasticity (TRIP) aided multiphase steels, which have a microstructure of intercritical ferrite, retained austenite, bainite and sometimes martensite, have been found to be a potential and promising substitute to conventional high strength dual-phase steels These TRIP steels give a good combination of high strength and excellent formability. There is also a potential for improved crash performance over dual phase steels due to the presence of retained austenite, which can transform to martensite during a crash event helping to absorb energy.

TRIP steels have a very good potential to be used in automotive applications if their shortcomings can be overcome. One of the largest problems is the coatability due to the formation of a silicon oxide layer. The main aim of this work is to see if using increased aluminium is feasible whilst still maintaining good properties with the aim to reduce the amount of silicon.

In addition this work looks to optimise the TRIP steel properties by changing the steel chemistry with the aim to produce a TRIP 800. A base steel of 0.2wt%C, 0.4wt%Si, 1.3wt%Mn, 0.8wt%P, 0.3wt%Al is used and 3 steels with an increase of 0.5wt%Al, 0.5wt%Mn and 1wt%Cu respectively. To further this, the processing route will also be examined concentrating isothermal holding to see how the aluminium additions affect this. The processing route is based on the current industrial capabilities available in South Wales looking at isothermal holding temperatures of 250^{o}C, 350^{o}C, and 460^{o}C and times of 100s, 200s, and 370s.

The addition of aluminium performs well giving good strength and very good elongation. Combining this with the increase on surface coatability that should arise from being able to reduce the silicon content, it is a good choice. However, the increased aluminium steel still needs additional manganese alloying content in order to meet the strength requirements for a TRIP 800.

An over-age time of 100 seconds is enough to produce the required amount of bainite to retain enough austenite at room temperature to produce good formability within the steel. It was seen at this over-age time that the best total elongations were achieved and generally better n-values were seen at shorter over-age times of 100 seconds. Any less than this and there is a drop off in elongation due to the lack of bainite formation, any more and the strength of the material is effected due to tempering of the bainite.

An over-age temperature of 250^{o}C produced the best tensile strengths. Whilst a higher over-age temperature of 460^{o}C produced better elongation values there is a marked decrease in strength for these temperatures. If TRIP steel is used based upon an aluminium chemistry, which exceeded the elongation requirements, with additional manganese to increase the strength. Then using lower over-age temperatures will also help increase the strength to meet TRIP 800 requirements whilst still meeting the required elongation values.

ACKNOWLEDGEMENTS

The author would like to acknowledge and give thanks to both supervisors of this project giving much of their time and advice; Dr. George Fourlaris for the metallurgical and scientific knowledge he has provided and to Laura Baker, who was always happy to meet give advise and help in any way she could.

I would also like to make a special thanks to Nick Silk for his help at the beginning of the project. Also to Bryan Jones who was always happy to talk over any aspect of my work.

Without the funding of EPSRC and Corus this research programme would not have been possible.

Thanks also to everyone at Testing Solutions Wales, Port Talbot. Their experience and time was a great help for the metallographic aspect of this project. Special thanks to Malcolm Westacott. Also a big thanks to the Port Talbot CSPUK RD&T team in particular Peter Evans for all his time and advice.

Finally, a massive thank you to my family friends and parents, Ken and Mary Moody, whose support throughout my academic career has been invaluable.

LIST OF TABLES

LIST OF FIGURES

1. INTRODUCTION

Within the automotive industry safety and environmental regulations combined with customer expectations have lead to a requirement for new technologies. These include energy sources, structural design and the materials used in manufacture.

Material development has focused on reducing overall vehicle mass. When applied to vehicle design the weight saving can be utilised to implement additional improve safety features, which leads to a better passenger safety through improved crash-worthiness, without impacting upon fuel consumption and emissions.

One of the advances in materials used in the manufacture of body panels, structural and crash components is the development of advanced high strength sheet (AHSS) steel. However, one drawback found when using such high strength levels is that these high strength alloys generally have lower ductility levels. This is a particular disadvantage when it comes to metal-forming operations. Currently dual phase (DP) steels are the favoured advanced high strength steel used to produce higher strength components or to reduce the thickness of the steel and therefore produce lighter components.

Low-alloy transformation induced plasticity (TRIP) aided multiphase steels, which have a microstructure of intercritical ferrite, retained austenite, bainite and sometimes martensite, have been found to be a potential and promising substitute to conventional high strength dual-phase steels [1]. These TRIP steels give a good combination of high strength and excellent formability with higher n-values than dual phase steels and can be used to answer the demand for weight reduction in the automotive industry. There is also a potential for improved crash performance over dual phase steels due to the presence of retained austenite, which can transform to martensite during a crash event helping to absorb energy.

The TRIP effect was first discovered by Zackay et. al. [2], and is the strain induced transformation of retained austenite to martensite, which results in a ductile material and final high strength material. However, to achieve the full potential of the increased ductility in TRIP steels, the uniform elongation during plastic straining needs to be maximised. Rapid austenite to martensite transformation in the early deformation stages has been reported to decrease the ductility. As such, one of the most important elements to control is the stability of the retained austenite [1]. The properties of these TRIP-aided steels were found to be particularly suitable for demanding automotive applications and could be beneficial when used for parts that require a combination of high strength, high formability and high dynamic energy absorption during high strain rate deformation (e.g. crash components).

Although a general understanding of these materials has been developed, a number of fundamental issues remain to be solved [4]. It has been found that these steels are considerably more sensitive to production variations when compared to conventional steels. Careful control of processing conditions and the identification of critical processing steps is crucial to the success of these products [4]. The challenge, therefore, is to develop industrially relevant processing routes that will lead to the desired properties with minimum variation. The cooling path and composition of these steels must be carefully optimised to minimize transformation back to ferrite or the pearlite and bainite reactions.

Conventional TRIP steels use high silicon levels to retain the austenite phase at room temperature. This can result in a Mn_2SiO_4 layer upon the surface of the steel causing problems with coatings. Aluminium can be used as a replacement for silicon in retaining austenite at room temperature and should overcome the problems with the oxide layer. The main aim of this thesis is to produce a TRIP steel substituting silicon with aluminium and finding a suitable steel chemistry and processing route to optimise the TRIP steel properties.

2. REVIEW OF LITERATURE

This section will review TRIP steels looking at the role that the processing route and different alloying elements have upon creating a TRIP steel microstructure. The commonly associated problems with TRIP steels will be looked at and potential ways to overcome these problems will be Identified as well as investigating processing routes that will optimise TRIP steel properties and the mechanisms by which this can be achieved.

2.1 Processing Route of TRIP Steels.

A simple chemical composition for a low-alloy TRIP-aided steel is Fe-0.15C-1.5Si-1.5Mnwt% [1]. Even though this is a fairly simple chemical composition, a wide variety of microstructures and mechanical properties can be achieved by applying different annealing routes. Figure 2.1 shows the wide range of mechanical properties that can be obtained in low-alloy TRIP-aided steel [5]. As can be seen there is a wide variety of mechanical properties that can be obtained from TRIP steels by using different chemistries and processing routes. An understanding of how changing these parameters affect the final properties needs to be developed.

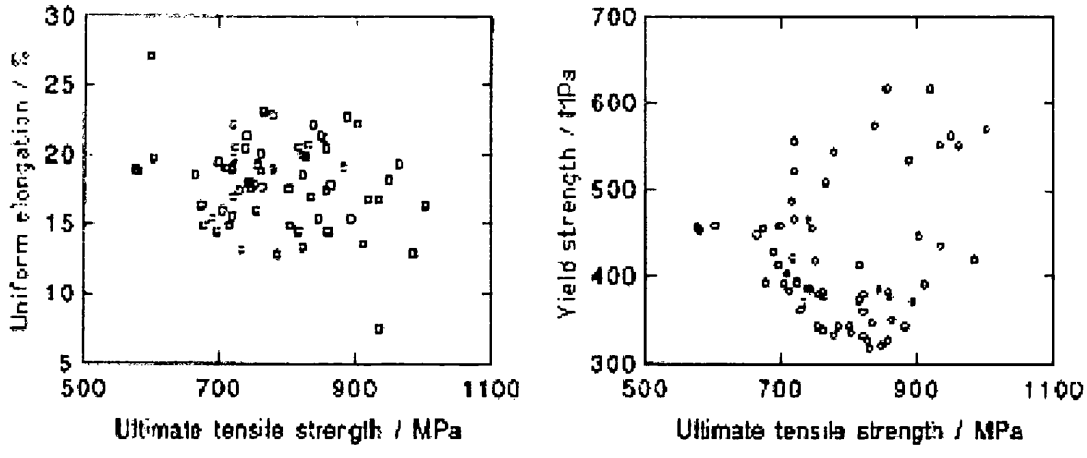

Figure. 2.1: Plot showing the wide range of mechanical properties achievable in low-alloy TRIP-aided steels [1].

The most important processing parameters are the intercritical anneal to produce the initial amount of retained austenite within the microstructure for the TRIP effect followed by the isothermal holding to enrich the austenite with carbon therefore retaining the austenite at room temperature.

Up to now, the most extensively investigated steels have been the TRIP steels for sheet production. By using a suitable combination of mechanical and thermal processing conditions followed by cold deformation, TRIP steels could be used for manufacturing a broader range of components such as crash and structural components.

2.1.1 Coiling Temperature.

In general the effect of coiling temperature for TRIP steel has not been shown to have any significant effect on either yield stress or tensile stress for a variety of annealing cycles [6]. However using a composition of 0.22C-0.1P-0.02Nb-0.1Ti-0.1Al did show an effect. The yield strength was affected more significantly than tensile strength. A lower coiling temperature of 450^{o}C was observed to give a rise in yield strength of 150MPa compared to a coiling temperature of 615^{o}C [6].

2.1.2 Intercritical Anneal.

Whatever the alloy, it is the quantity, distribution, grain size and stability of the austenite in the final microstructure that will determine the extent of the TRIP effect. The mechanical response of TRIP alloys cannot be optimised without due consideration of the intercritical annealing temperature in relation to the respective transformation range [6].

The first stage in any heat treatment for TRIP steels is an intercritical anneal. The intercritical anneal will produce the required amount of austenite in the microstructure. The intercritical anneal is achieved by heating the steel from room temperature into the region between Ae_1–Ae_3. This has been identified

as the intercritical region within the iron-carbon equilibrium phase diagram figure 2.2

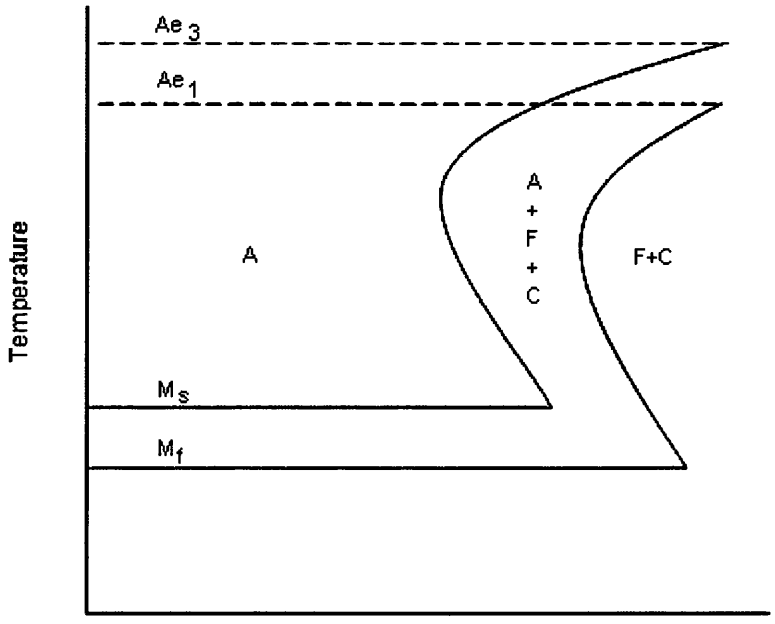

Figure 2.2: Time-temperature-transformation diagram representing phase transformations in steels [1].

At temperatures between Ae_1 (temperature at which austenite begins to form) and Ae_3 (temperature at which the microstructure is completely austenitic) the microstructure is typically allotriomorphic ferrite plus austenite. At temperatures above Ae_3, the microstructure is fully austenitic as is the case with hot-rolled steels. Applying the heat-treatment processes starting straight from the hot-rolled condition can be beneficial especially from an economical standpoint as there is no need to reheat the strips from room temperature.

Matsumura et. al. [7] has investigated the effect of varying the annealing temperature on the mechanical properties of a C-Si-Mn TRIP steel. They showed that an increase in the tensile strength could be obtained in the alloy by raising the annealing temperature from below Ae_1 above Ae_3 to 840℃. The tensile strength was increased more than 60% when a final microstructure of 90% bainite was produced by annealing at 840°C, which lies above the Ae_3

temperature when compared with a ferrite plus pearlite microstructure when annealing was carried out at below Ae_1. It was also shown that by annealing the steel at a temperature just above Ae_1, a significant increase in elongation was achieved due to the presence of the austenitic phase in the microstructure. However, there was a drop in the elongation when the annealing temperature was increased above this, this was due to a decrease in the volume fraction of ferrite along with an increase in bainite volume fraction and a slight decrease in the retained austenite content. This drop in the elongation may be explained due to the dependence between the volume fraction of ferrite and the carbon content in the austenite [8]. Therefore the nature of the second phase also contributes to the overall ductility of the alloy. The holding time in the intercritical annealing region has also been found to be important. If the holding time is too short it will result in low tensile strength and elongation levels [7]. This means it is important to select the optimum intercritical annealing conditions for a certain bainitic transformation processes. Matsumura et. al. [7] suggested that, for the alloy studied, and for the given bainitic transformation, optimum strength-ductility combination was at an annealing temperature just above Ae_1.

A larger amount of retained austenite can be achieved by increasing the intercritical holding time. However; a large fraction of retained austenite is not desirable as this will result in a reduced carbon content within the retained austenite in turn making it less stable [9]. At ~800^{o}C the fraction of retained austenite formed during the intercritical annealing can be up to approximately 50%. TRIP steels that have a lower percentage of austenite due to shorter holding times at intercritical annealing temperatures do not show good formability despite high elongation [9]. The stability of retained austenite goes up when the carbon solubility in retained austenite goes beyond adequate levels due to appropriate intercritical annealing temperature and higher holding time at that temperature.

Increasing Al content significantly increases the transformation finish temperature whilst the transformation start temperature remains largely

unaffected [6]. Steels that show the most attractive properties generally have higher transformation finish temperatures. Ignoring any direct effects from the chemistry on tensile properties. This implies that TRIP characteristics are promoted by intercritical annealing at temperatures low to the transformation range [6].

TRIP steels are cooled on the hot mill to allow ferrite formation. The cooling is interrupted to allow time for the ferrite fraction to stabilise before further cooling to meet the coiling temperature.

Dilatometer work [10] has shown that the optimum intermediate temperatures for ferrite formation are 660-720^{o}C depending on the composition. Ferrite formation will level off after five seconds. This means that a minimum of five seconds is needed to allow a consistent proportion of ferrite to be formed at most of the intermediate temperatures used. The most consistent ferrite formation over a range of temperatures has been found from high phosphorus steels [10] giving a wide intermediate processing range on the hot mill.

2.1.3 Isothermal Holding.

The second stage in the processing route for TRIP steels involves a controlled cooling rate to the bainitic transformation temperature region where the steel is isothermally held, Figure 2.3 [11]. During isothermal holding in the bainite transformation temperature range, the free energy of ferrite is lower than the free energy of the austenite at the start of the transformation and this provides the driving force for the bainitic transformation.

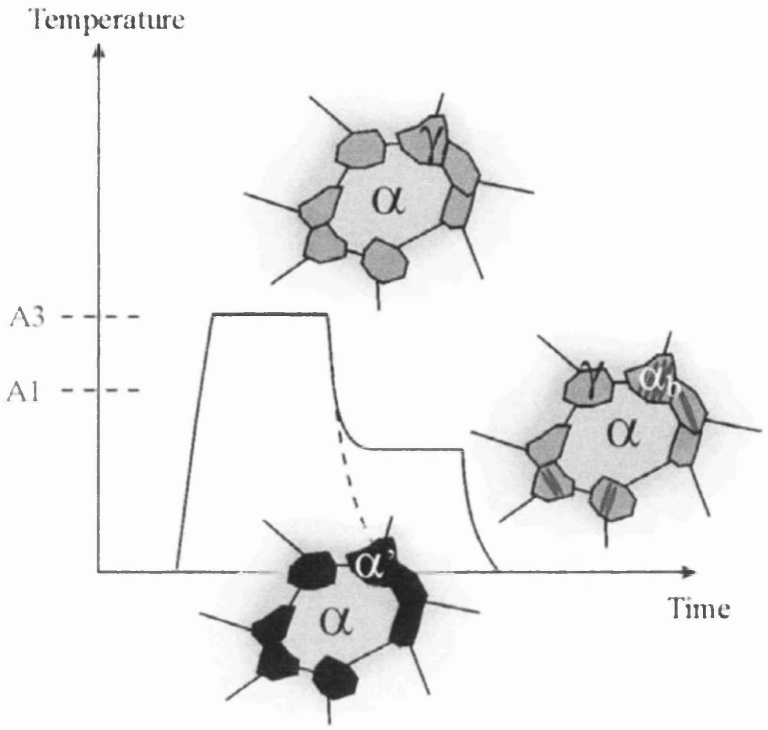

Figure 2.3: Schematic representation of the annealing route for TRIP steels.

ferrite(α), bainite(α_b), and austenite(γ), [11]. Typical time of annealing cycle ~12 minutes. A1~730°C, A3~1000 °C.

The final microstructure after the two-stage heat-treatment process is typical of intercritical ferrite and austenite resulting from the first stage, the intercritical annealing, and upper bainite resulting from bainitic transformation in the second stage [1]. The bainitic transformation is used to partition the carbon into the residual austenite. This is done because the austenite enriched with carbon will stabilise the austenite making it more resistant to transformation to martensite when cooling to room temperature. The stabilising effect is also essential as it makes the alloy less sensitive to any applied chemical or mechanical driving forces during the plastic deformation of the steel. Many authors have reported the effect of varying the holding time in the bainite transformation temperature region on the mechanical properties especially on the total elongation, for example as reported by Matsumura et. al. [7]. It has been reported that by changing the holding time during bainitic transformation, the carbon concentration in austenite changes as a carbon re-distribution process takes place. Varying the holding time in the bainite

transformation temperature region has a strong correlation with the stability of austenite and so affects the mechanical properties of the alloy, in particular the total elongation that can be achieved. It is well known that by increasing the carbon content within the austenitic phase the temperature at which martensite starts to form by cooling can be decreased [12]. This means that the austenite becomes more resistant to transformation into martensite.

In work done by S. Zaefferer et. al. [13] differently heat treated samples were compared and it was found that an appropriately long isothermal holding time at relatively high bainite formation temperatures leads to optimum stabilized austenite with a high and homogeneous carbon content in a ductile, well recovered ferritic matrix. This material showed optimum mechanical properties. Shorter isothermal holding times result in less bainite and leads to a less stabilized austenite due to heterogeneous carbon distribution. When decreasing the isothermal holding temperature, a lower amount of bainite is formed which contains a higher defect density due to high carbon-super saturation and little recovery. The remaining austenite has a low carbon content therefore is less stabilized and results in less attractive mechanical properties.

By increasing the isothermal holding time the mechanical stability of the retained austenite is significantly increased as more carbon, which has been partitioned from the bainite, then enriches the intercritical austenite. However if the steel is kept at the bainitic transformation range for too long a period, the total elongation decreases due to the volume fraction of retained austenite decreasing with increasing bainite growth. [14].

The mechanical stability of austenite due to carbon enrichment supports the approach of M.Y. Sherif [1], who looked at the austenitic chemical composition. The composition of the alloy has a direct effect on the free energies of the phases and in turn on the strain-induced transformation behaviour of the alloy. Retained austenite morphology has an effect on the mechanical stability and on the total elongation of the alloy. The desired

morphology of the phases in the microstructure can be obtained by changing the heat treatment parameters.

Sugimoto et. al. [15] have investigated how the morphology of both austenite and the second phase, which is a mixture of bainite and retained austenite particles, effects the mechanical properties of a TRIP-aided dual-phase steel of the composition 0.17C-1.41Si-2.00Mnwt%. They found that the best elongation behaviour was achieved when the retained austenite is in the form of thin films. These austenite films were embedded between the bainite sub-units. Also, the size of the retained austenite grain may have an effect on the transformation behaviour as the alloy undergoes plastic deformation. When the grain sizes were below 10μm, the interfacial energy due to the forming of a martensitic plate within an austenitic grain increases exponentially, which results in the austenite becoming more stable. However, it is also important to note that the transformation into martensite will not occur if the austenite grain size is about 0.01μm or smaller, this is because of the driving force required to accomplish the transformation to martensite being impractical [8]. Relatively large retained austenite grains were also reported to transform into martensite easily with a significant drop in the total elongation. However, reducing the temperature at which the bainitic transformation is conducted can eliminate these blocky austenite grains. Therefore adjusting the heat-treatment parameters affects the microstructure, the transformation behaviour of the retained austenite and consequently, the overall mechanical properties of TRIP-aided steels.

2.1.4 Cooling Rate.

In industrial processing lines, both the intercritical annealing temperature and time can be limited [16], this means that reaching the equilibrium phase fractions and the equilibrium content of substitutional solutes in the different phases can never be achieved. A high cooling rate of 30°C/s or more between the two annealing stages is needed to prevent new ferrite or pearlite forming.

The initial cooling rate may be lower when the temperature is still higher than the Ar_1 temperature, this will allow further enrichment of the austenite with carbon. The cooling rate and bainite transformation time and temperature can also be limited due to the process windows of the industrial continuous annealing or continuous galvanizing lines [16].

The effect of changing the cooling rate after intercritical annealing has been shown to have no significant effect [6]. Some TRIP steel compositions have shown a trend of moderately increasing yield and tensile strength with increasing cooling rate. However they were not significantly greater than the error associated with tensile testing. Therefore extending the cooling rate capacity on the processing line for TRIP production would not be beneficial [6].

2.2 Phases and Microstructure of TRIP Steels.

The precise characterization of the complex microstructure of multiphase steels, and the understanding of its formation mechanisms are of great importance for the interpretation and optimisation of the mechanical properties of these materials. In the case of low alloyed steels with transformation induced plasticity, the small grain size and the homogeneous distribution of the different phases lead to strong hardening and therefore to excellent elongation and strength [17].

The major phases present in the microstructure of hot rolled and cold rolled TRIP steels are: ferrite(α), bainite(αb), and austenite(γ), figure 2.4 [18]. The microstructure of TRIP steels are quite complex and optimising these steel products requires a good understanding of the mechanisms of the phase transformation, during thermo mechanical treatment, as well as during mechanical testing or metal forming [19].

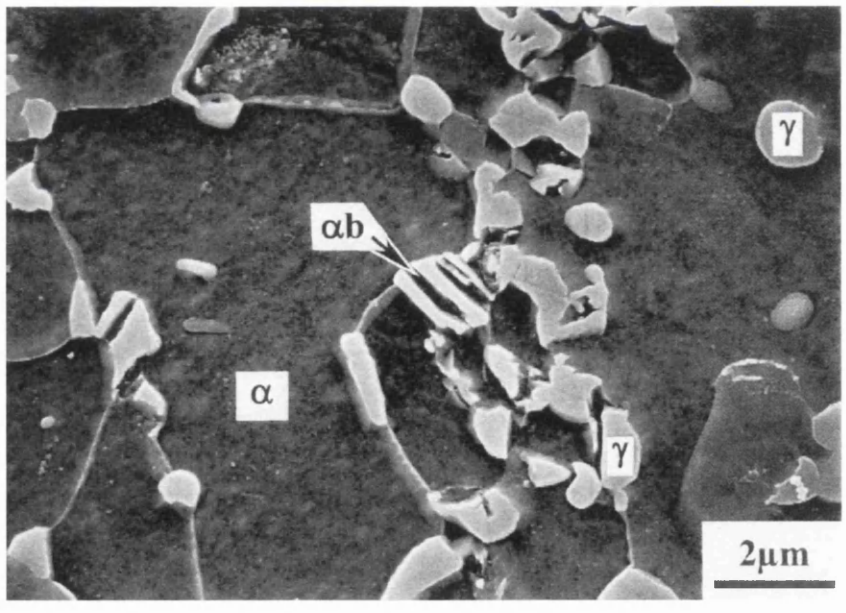

Figure 2.4: Typical microstructure obtained after the heat-treatment. Austenite appears in white, ferrite in black [18].

Ideally low-alloy TRIP steels should contain only the three phases: ferrite, bainite and retained austenite. Retained austenite particles exhibit a mean

size of 0.8μm [20]. Metallographic investigations show that retained austenite is mainly located at the ferrite grain boundaries and is frequently surrounded by bainite. The ferrite grain structure is characterized by a non-equiaxed morphology and may contribute to the strength by both smaller grain size and increased dislocation density compared to a morphology [21]. The bainite structure can be difficult to describe due to the complexity of the transformation reaction. The "classical bainite" morphology is characterized by ferrite laths of high dislocation density and includes carbide precipitates.

TRIP steels are made up of fine multiphase microstructures. Due to this it can be difficult to identify the different phases of multiphase high strength steels, as well as the varying density of carbides in bainite and tempered martensite. Finding the composition of each constituent is fundamental in helping to understand TRIP steels [19]. The composition of cementite is a key point for austenite stabilisation during bainitic transformation. The analysis of the composition of retained austenite is also of importance in particular the carbon content is of great interest, as it is one of the major elements that control the austenite thermal and mechanical stability.

The strength obtained with TRIP steels is usually between 600 and 1000 MPa. The usual carbon content for this level of strength is about 0.15-0.2% [19]. TRIP steel contains generally around 50 to 70% ferrite, which ensures good matrix ductility. Whichever process route is used the steel will reach a two-phase ferrite-austenite state during final cooling. At this stage because of carbon enrichment due to the growth of bainite during the isothermal holding, the austenite will contain about 0.5%C.

As is often the case the microstructure will also contain minor amounts of carbides and, depending on the chemical composition, martensite. The presence of carbides is of major importance, as it means that the cementite may not have been fully dissolved during the intercritical annealing, and so not all of the available carbon has been able to precipitate in the carbon enrichment of the austenite during the bainitic transformation.

One of the most difficult aspects of TRIP steel research is still the exact quantification of the phases, the carbon distribution and the properties of the different phases. The distinction between ferrite and bainitic ferrite is very difficult to make, and has yet to be done experimentally [16]. The problem is usually avoided by assuming equilibrium phase distribution during intercritical annealing and ignoring the formation of new ferrite in the fast cooling stage. The carbon content of the bainitic ferrite is still being debated [16].

Ferrite may be divided between intercritical ferrite existing before cooling and proeutectoid ferrite, which may be created during cooling. Austenite has a face centred cubic structure. Bainite is a constituent consisting in the current case of ferrite, austenite and, sometimes, various forms of cementite. Different characterization methods for the complex microstructure of these steels are available. Light microscopy with a colour etching allows the distinction of ferrite, bainite and austenite. However, an important drawback is that martensite usually cannot be distinguished from austenite [13]. The stability of austenite can therefore not be controlled. Also, the two sorts of ferrite are not distinguished and the separation of bainite and ferrite is not in all cases unambiguous.

2.2.1 Ferrite.

Work done by I.B. Timokhina et. al. [22] found the ferrite in different steels showed a different behaviour during straining. For an Nb steel sample a strain of ~0.14 corresponded to the onset of necking, while at the same strain; the strain hardening of non-Nb steel demonstrated a second maximum. At different stages of straining, the ferrite grains in non-Nb steel elongated by almost two times more than in Nb steel. This shows that the strain was concentrated in the ferrite matrix, which caused it to flow around the bainite and martensite islands. The ferrite in Nb steel showed a lesser amount of deformation than in non-Nb steels and did not flow around the bainitic region during straining. This could be a direct result of the Nb addition promoting

precipitation hardening of the ferrite and possibly through grain refinement, which leads to the strengthening of ferrite [22]. Another observation was the higher volume fraction of martensite between the ferrite grains as well as at the ferrite/bainite interface in Nb steel. The presence of as-quenched martensite in a soft ferrite matrix led to the formation of a plastic-deformation zone in the ferrite surrounding the martensite islands [22]. As reported by Goel *et al.*, [23] this could contribute to an increase in the strain hardening of the ferrite. Also having a hard phase in a soft matrix could increase the strength of the matrix by itself and affect the stress partitioning between the phases. The interaction between the ferrite and martensite during straining also should lead to the formation of an additional plastic deformation field in the soft matrix that will increase the strain hardening of the ferrite.

The strain-induced transformation also affected the deformation behaviour of the ferrite. As mentioned previously, the retained austenite present between ferrite grains and at the ferrite/bainite interface transformed to martensite at an early stage of deformation. These new strain-induced martensite islands could lead to extra plastic-deformation zones in the adjacent ferrite grains, due to the volume expansion of martensite during the transformation and the new dislocations generated in the ferrite [23]. This could increase the strain hardening of ferrite and decrease the mean stress level within the retained-austenite islands, which will in turn delay the austenite-to-martensite transformation. This could be responsible for the presence of coarse untransformed blocks of retained austenite in ferrite after a 0.1 strain in the Nb steel. Hence, the contribution of ferrite to the stress-strain behaviour during deformation should be considered as interaction between ferrite, retained austenite, and martensite.

2.2.1.1 Effect of Volume Fraction of Ferrite

With the formation of ferrite the rejection of carbon and if enough time is allowed of silicon and manganese, occurs in the remaining untransformed austenite. A higher concentration of carbon increases austenite stability, while higher levels of Si inhibit carbide precipitation. When the intercritical anneal in recrystallised samples is at 725°C in work by E. V. Pereloma et. al. [24], the pearlite formation was completely by-passed. However this leads to a lower fraction of ferrite, which means there is a lower level of carbon in the remaining austenite. Therefore, as further transformation takes place the austenite will be less stable which results in a higher amount of martensite and reduced retained austenite in the final microstructure. If the intercritical anneal is reduced to 670°C in order to increase the volume of ferrite, a small amount of pearlite was formed which resulted in a decreased amount of retained austenite. Increasing the amount of proeutectoid ferrite should mean an increase in the hardenability of the remaining austenite, which will in turn make it easier to avoid the formation of other phases during cooling [24]. If this is possible then the higher carbon content and the higher under cooling promote the formation of finer low temperature transformation product. This in combination with high silicon content, which suppresses carbide formation in the intermediate temperature bainite, leads to a higher volume of retained austenite in the final microstructure. Therefore, holding the temperature to increase the amount of ferrite in temperature ranges where pearlite forms, leads to a fine balance between the need for increased hardenability of the remaining austenite and the potential to form pearlite, which will reduce the amount of retain austenite in the final microstructure.

2.2.2 Bainite.

2.2.2.1 Bainite Reaction

For TRIP steels we define bainite as a plate-like microstructure, which consists of a sheaf of one or several sub-plates [25]. Within an individual sub-plate or between two sub-plates, carbides or grains of retained austenite may be present. Figure 2.5 shows typical bainite microstructures. Neither the presence of carbides nor that of retained austenite is an essential component of the bainitic structure.

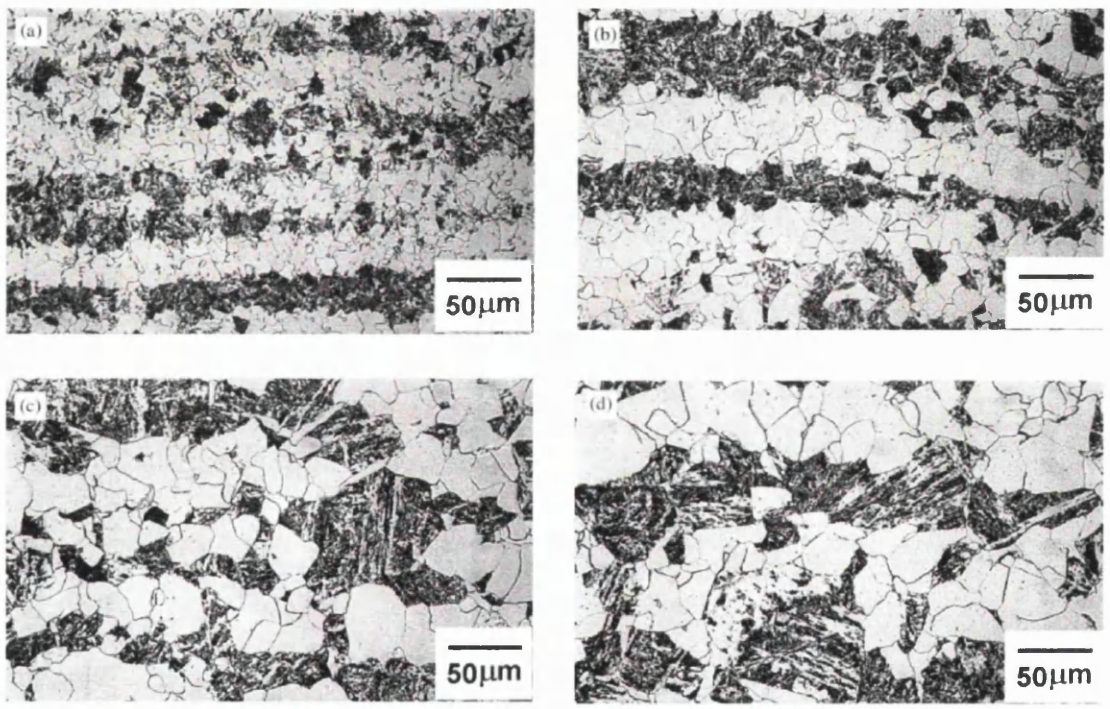

Figure 2.5 Typical Bainite microstructures, bainite showing as the darker phase [26].

The austenite stability depends on a range of factors [27], such as the bainitic holding time, figure 2.6. However as has been discussed the most important factor is the carbon concentration of the austenite [8]. The carbon concentration in the retained austenite results from both the proeutectoid ferrite formation [28] and the bainite formation [29]. As the carbon content of the retained austenite in a typical Fe–0.2C– 1.5Mn–1.5Si wt% TRIP steel is

around 1.5 wt%, the redistribution of carbon atoms must take place at the bainite reaction temperature. Therefore proeutectoid ferrite formation alone cannot achieve high carbon concentration within the austenite alone. Further austenite enrichment must occur during bainite formation. If during the bainite growth the carbon was trapped within the bainite, it would be unlikely that it could diffuse over long distances in order to enrich the austenite to the levels that have been experimentally determined [30]. Hence, in TRIP steels, bainite formation is accompanied by an immediate carbon rejection from the bainite during its formation [30].

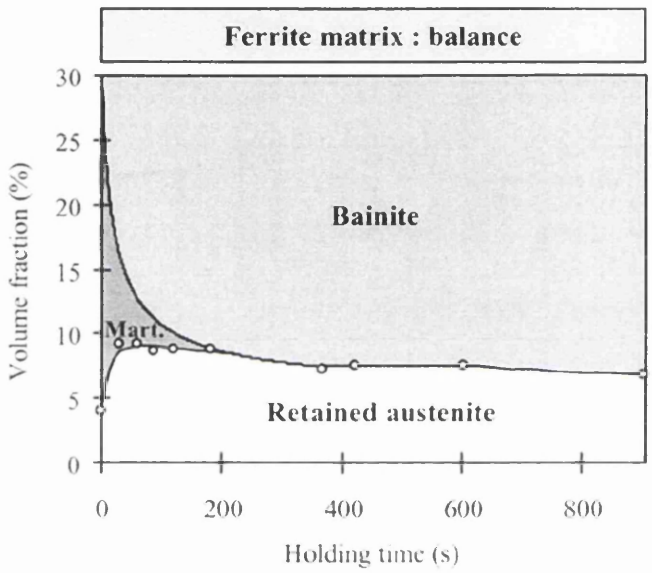

Figure 2.6: Evolution of the final microstructure with increasing bainitic-holding time at a temperature of 370^{O}C [18].

As the isothermal holding time is increased, the volume fraction of retained austenite will initially increase and then decrease. The reason for this is that when the holding time is short, the volume fraction of bainitic ferrite is small and therefore the carbon content in austenite is low. This in turn means that the martensite start temperature (Ms) temperature of the austenite is above room temperature, so when cooling to room temperature, the austenite transforms into martensite with less retained austenite left in the final microstructure. By prolonging the holding time, the volume fraction of bainitic ferrite will increase and reject more carbon into the austenite, this means the

Ms temperature of the austenite will be under room temperature. When cooling to room temperature, more retained austenite will remain. Increasing the isothermal holding time further will lead to the presence of a large amount of bainitic ferrite, so the carbon content in the austenite increases correspondingly. At the same time, the carbide precipitates from the austenite, and then decomposes into cementite during the subsequent cooling process.

With an increase in the isothermal holding time, the tensile strength will first increase followed by a decrease then an increase again. With a shorter isothermal holding time, the structure will have much more martensite with large internal stress after cooling [31]. Therefore, the tensile strength is lower. With an increased isothermal holding time, carbide-free bainite, martensite, granular bainite and a little retained austenite are formed, this kind of structure has high tensile strength and better ductility because the volume fraction of the retained austenite is at a maximum [31]. With an isothermal holding time of ~10 minutes, much more granular bainite is formed and martensite distributed in the lath-shaped bainitic ferrite. Thus, the mechanical properties are at their worst due to the large internal stress in the structure [31]. With a further increase in the isothermal holding time to 20 or 30 minutes, the carbon rich austenite will transform into ferrite and cementite in the following cooling to room temperature [31]. The precipitation of carbide improves the tensile strength. Furthermore, the increasing volume fraction of ferrite improved the ductility.

S. Zaefferer et. al. [32] investigated the bainitic transformation on an intercritically annealed and isothermally held Fe–0.11C–1.50Si–1.53Mn steel and they came to the following conclusions. The bainitic transformation that takes place during isothermal holding will stop before all of the austenite is consumed, and so exhibits an incomplete reaction phenomenon. The carbon concentration of untransformed austenite measured when the bainite formation finishes correlates fairly well with the calculated T_0 line. T_0 is the temperature at which austenite and ferrite of identical composition have the same Gibbs free energy. This fact suggests the contribution of a diffusionless

mechanism to the bainitic transformation. However, the overall rate at which the bainite formation occurs was found to depend on the transformation temperature. This is due to the fact that, inside the small intercritical austenite grains it is necessary for the adjacent development of the bainitic ferrite laths [32]. This transformation process was observed to cause a build-up of carbon in the austenite near the interface; this then goes on to significantly persist at low temperature and so hinders the progress of the reaction. Therefore, the kinetics of bainite formation that is seen in this study differs from that reported on fully austenitised grades and seems to be typical of multiphase TRIP-assisted steels.

2.2.2.2 Behaviour of Bainite During Straining

It was found in the work done by I.B. Timokhina et. al. [22] that the bainite morphology also affects the structure-property relationship in TRIP steels. Similar to the ferrite behaviour, the bainitic ferrite of non-Nb steel also flowed and elongated around the hard martensite islands during straining. The bainitic ferrite in Nb steel was more rigid and demonstrated a lower degree of elongation. The higher resistance of bainitic ferrite in Nb steel to the tensile deformation could be explained by the refinement of the bainitic ferrite laths in the Nb steel. Theoretically, the refinement of the bainitic ferrite laths with different crystallographic orientations should increase the mechanical stability of the retained austenite [22]. As mentioned previously, if the residual austenite is closely surrounded by the relatively rigid and refined bainitic ferrite, the mechanical stability of the retained austenite also increases due to the geometrical restrictions of the bainitic ferrite laths. [33] This also increases the strain hardening of the bainitic ferrite, preventing the elongation of bainite. In addition, the martensite between the bainitic ferrite grains or laths could also strengthen the bainite and affect the overall deformation behaviour of this microstructure.

It was observed for Nb steel that the retained austenite between long, parallel bainitic ferrite laths transforms to martensite at the beginning of straining [22].

Furthermore, the part of the austenite crystal in close proximity to the bainitic ferrite laths transformed faster than the core. This could be due to the rigidity of bainitic ferrite laths caused by the higher level of carbon [22], the increase in the dislocation density due to the displacive type of transformation, and by the morphology of the bainitic ferrite. This might stimulate the retained austenite-to-martensite transformation at a low strain due to the concentration of the stress at the interface with its further propagation into the retained austenite crystal during testing in Nb steel. Thus, the interaction between the bainitic ferrite laths and the retained austenite during straining, on one hand, influences the strain-induced transformation of retained austenite and, on the other hand, affects the behaviour of bainite [22]. The retained austenite with optimum stability, which showed the gradual transformation to martensite during straining, was found in non-Nb steel within granular bainite. It is suggested that the bainitic ferrite present in the form of grains propagates less stress to the retained austenite during deformation and does not stimulate the rapid transformation of the retained austenite to martensite [22]. Since non-Nb steel contains higher amount of granular bainite, it demonstrates greater elongation.

Due to the complexity of the microstructure, the mechanical properties of the TRIP steels are more dependent on the deformation mode of each phase and the interaction between phases present rather than just the volume fraction and stability of the retained austenite, although this is a function of the surrounding phase morphology [22].

The mechanical properties of the complex multiphase microstructures are determined not only by the strain-induced transformation of retained austenite, but also depend on the characteristics and interactions of all phases present in the microstructure. Both ferrite and bainite are responsible for a good combination of strength and ductility in the TRIP steels [22].

Moreover, the morphology of the bainitic ferrite plays a vital role in the retained-austenite stabilization. The coarse blocks of retained austenite

located in the ferrite or at the ferrite/bainite interface transform to martensite at an early stage of deformation, while the retained austenite present between the bainitic ferrite laths is more stable and can remain in the microstructure even after the testing to failure [22]. This is due to its higher chemical and mechanical stability. The granular bainite, as the dominant second phase, provides the optimum stability of the retained austenite and shows the maximum contribution to the elongation.

2.2.3 Retained Austenite.

An enhancement of the formability of cold rolled TRIP-assisted steels is mainly determined by the characteristics of the retained austenite [34]. The chemical composition and such processing parameters as cold rolling, intercritical annealing and subsequent austempering treatment affect the volume fraction, distribution and carbon concentration of the retained austenite [35].

2.2.3.1 Austenite Formation.

The formation of austenite has been widely investigated. Speich *et al.* [36] investigated austenite formation in 1.5 wt% Mn steels containing 0.06 to 0.20 wt% carbon and concluded that austenite formation could be separated into three stages:

(1) Very rapid growth of austenite into pearlite until complete pearlite dissolution,
(2) Slower growth of austenite into ferrite primarily controlled by carbon diffusion in austenite, and
(3) Very slow equilibration of austenite and ferrite controlled by manganese diffusion in austenite.

In general, the nucleation of austenite is associated with cementite precipitates and, thus, potential nucleation sites are ferrite/pearlite interfaces

and cementite particles at ferrite grain boundaries [37]. These generally accepted mechanisms of austenite formation are based primarily on isothermal studies on hot-rolled or fully annealed steels. Petrov *et al.* [38] have suggested that in a C-Mn-Si TRIP steel, austenite formation occurs in non-recrystallised ferrite during ultra-fast heating (~1000°C/s) leading to a refined microstructure as compared to more conventional heating rates (~50°C/s). The substantial role of the degree of ferrite recrystallisation is confirmed by an earlier study by Yang *et al.* [39] who observed a strong influence of ferrite recrystallisation and rapid spheroidisation of cementite in the deformed pearlite on the formation and distribution of austenite in intercritically annealed C-Mn-Si steel. In this case, austenite forms initially on grain boundaries of elongated ferrite grains and later, *i.e.*, after completion of recrystallisation, on carbides in the ferrite matrix. Despite these important findings and their potential practical relevance, there is still a lack of detailed quantification on how heating rate will affect the austenite transformation during the isothermal portion of intercritical annealing.

The microstructures of the steel will feature pearlite colonies with a banded morphology surrounded by equiaxed ferrite grains. After cold rolling, both phases will become elongated; *i.e.*, the ferrite grains become elongated and contain deformation bands and other substructures, while the pearlite will also be deformed. Cold working has the following effects on the steel:

(1) There is an increase in the stored energy of the material due to the high dislocation density and this provides the driving pressure for the ferrite recrystallisation upon annealing
(2) The total ferrite grain boundary area is increased
(3) The cementite laminar structure in pearlite is broken down.

The last point has been shown to promote spheroidisation of cementite during subsequent annealing processes [39]. Upon annealing of the cold-rolled material, the stored energy is released by recrystallisation. In general, recrystallisation of ferrite is completed before the intercritical temperature

range is reached. However, for sufficiently high heating rates, ferrite recrystallisation can be delayed to temperatures above the start temperature, at which austenite formation in ferrite was first experimentally observed as a function of heating rate [4]. Sometimes there can be significant overlap between ferrite recrystallisation and austenite formation at higher heating rates. This is dependent upon the chemistry of the steel, which can give rise to slower recrystallisation and lower start temperature. It might be expected that there would be important implications on the formation of austenite when it occurs simultaneously with ferrite recrystallisation. However, the effect of heating rate on subsequent isothermal transformation can also be observed for hot-rolled material for example in the absence of recrystallisation. Therefore, it appears that there is an important intrinsic effect of thermal history on austenite formation [4].

Austenite formation starts from the pearlite colonies by nucleation at the cementite-ferrite interface followed by quick growth consuming the dissolving pearlite. Subsequently, austenite may nucleate at ferrite grain boundaries in competition with austenite growth from the prior pearlite areas. It appears that the competition between austenite formed at these different sites is responsible for the marked heating rate effect on the transformation kinetics [4]. Slower heating rates will favour substantial growth of austenite nucleated at pearlite sites, whereas faster heating rates will promote additional nucleation at ferrite grain boundaries.

For the hot-rolled material at a heating rate of 100^{o}C/s, the extent of austenite nucleation at ferrite grain boundaries is such that an almost complete network of austenite along the boundaries connecting to the pearlite nucleated austenite emerges. Thus, there is no growth competition between pearlite and grain boundary nucleated austenite, thereby promoting larger transformation rates at holding temperature [4]. The higher transformation rates for this condition are also consistent with the larger ferrite-austenite interfacial area associated with the observed austenite morphology. In the case of the cold-rolled sample, the situation is different for several reasons. First, the

distribution and shape of the pearlite colonies, where the majority of the carbon is located, have been geometrically modified by cold rolling. Second, at the higher heating rates, recrystallisation occurs concurrent with austenite nucleation [4]. This situation can then be expected to resemble that of the hot-rolled sample. However, the morphology of the austenite is different due to the fact that the cold rolling process has substantially modified the shape of the initial pearlite colonies. The most complex situation is the one where the cold rolled material experiences a high heating rate [4]. In this case, much larger elongated austenite islands are observed. The shape and geometric arrangement of these islands corresponds to the as-rolled pearlite distribution; however, the austenite islands are considerably larger. Moreover, there is a striking absence of austenite formed at ferrite grain boundaries [4].

2.2.3.2 Effect of Heating Rate on Austenite Formation.

Very significant effects of heating rate on both the fraction of austenite and its distribution and morphology have been observed. These observations are of importance since intercritical annealing represents the first step of the annealing route of TRIP steels. The microstructure produced in this step is inherited through the remainder of the process and is thus reflected in the final microstructure [4].

Fundamentally, heating rate clearly affects the nucleation and growth of austenite both for hot-rolled and cold-rolled materials, although the effect is greater for cold-rolled materials. The interaction between the microstructure of the ferrite/pearlite mixture and austenite formation is complex and requires further understanding. The basic trends can be rationalized by the competing mechanisms for nucleation and growth of austenite and how these depend on the starting microstructure. The interaction between ferrite recrystallisation and austenite formation is strong, and it affects not only the kinetics of austenite formation but also the spatial distribution and morphology of austenite.

From an industrial point of view, a range of heating rates, 1°C/s to 100°C/s, are typical of continuous annealing lines used for galvanizing. It appears that it is possible to tailor microstructures by control of processing conditions and alloy design. The level of cold rolling is expected to be important since it determines the initial spatial distribution of carbon, which is predominately found in the pearlite islands and will also effect the rate of ferrite recrystallisation [4]. The interaction between ferrite recrystallisation and austenite formation can be controlled by changing heating rates but also by alloy design. For example, the addition of elements such as Mo, Nb, or B, which are known to retard ferrite recrystallisation, would promote the overlap between these phenomena.

2.2.3.3 Effect of Austenite Condition

The austenite condition before transformation to martensite affects the amount of ferrite and the nature and amount of the other phases that will be present in the final microstructure [24]. Recrystallised austenite has an equiaxed shape and is coarser than the elongated grains of the pancaked (non-recrystallised) austenite. The number of sites for ferrite nucleation is significantly higher in non-recrystallised austenite as there is a higher surface area per unit volume.

In work by E. V. Pereloma et. al. [24] the differences of recrystallised austenite and non-recrystallised austenite were looked at in order to see how they affected the final microstructure and properties of TRIP steel. There are some fundamental differences between the two that had to be taken into account during the study, as the pancaked austenite will have a higher density of defects such as deformation bands and other dislocation structures. These will promote diffusion, particularly of any substitutional elements, which may then go on to affect any subsequent transformation reactions, while also providing potential intra-granular nucleation sites. However, accepting these differences E. V. Pereloma et al. found three clear trends:

(1) The amount of retained austenite is similar at a similar ferrite content for both conditions
(2) The microstructure is more uniform in the transformation from pancaked austenite.
(3) There is a tendency to lower transformation temperature second phase products in the pancaked austenite.

They also found that the time required to form approximately 50% ferrite was much shorter for the pancaked austenite, this means there is less time spent at temperatures, which promote the formation of pearlite. The formation of pearlite markedly reduces the amount of retained austenite, and the amount of pearlite formed in the pancaked austenite was reduced. The more uniform microstructure in the pancaked austenite suggests that the distribution of the elements, which partition to the austenite, is more uniform for the pancaked structure. This could be due to the higher defect structure and the shorter diffusion distances required to achieve composition uniformity [24]. This role of local composition was highlighted in some large blocks of the retained austenite/martensite constituent where the retained austenite was preserved near the lower bainite or ferrite interface, while the centre of the blocky phase had transformed to martensite due, it is proposed, to a lower carbon concentration.

2.2.3.4 The Effect of Carbon Concentration in Austenite.

The carbon content of retained austenite is a major factor on the chemical stability of the retained austenite [40] and, therefore, on the TRIP behaviour. By retarding the transformation of austenite to bainite, the carbon content of the austenite increases and the volume fraction of retained austenite decreases. At higher intercritical annealing temperatures, an increase of the bainite phase leads to some decrease in the retention of austenite and the carbon content of the retained austenite increases significantly. The higher carbon content of Al-TRIP steels compared with Si-TRIP steels reflects the higher carbon content of the retained austenite in the former steel.

In studies on the effect of intercritical annealing temperature on two types of TRIP-assisted steels [40] the following were concluded:

(1) Al-TRIP steel with higher carbon compared to Si-TRIP steel contains a higher volume fraction of retained austenite and, consequently, higher carbon content in the retained austenite.
(2) The optimum intercritical annealing temperature in order to achieve the maximum amount of retained austenite was higher for Al-TRIP steel compared to Si-TRIP steel.
(3) An intercritical annealing of cold rolled TRIP assisted steel sheet at a temperature of $(Ae_1+Ae_3) / 2 +20^{o}C$ is the optimum condition for increasing the volume fraction of retained austenite.

2.2.3.5 The Effect of Austenite Grain Size.

In principle, the transformation kinetics of austenite can be affected significantly by the austenite grain size. As has been reported, [41] the effect of grain size on transformation products differs from one transformation to another. These can influence the characteristics of the retained austenite and therefore the TRIP steel properties.

It has been well established that austenite with a finer grain size usually transforms to finer grained ferrite and finer pearlite, bainite, or martensite plates. [42] In addition, an increase in the austenite grain size decreases the rate of bainite formation [41]. Furthermore, it is believed that the bainite packet size decreases with austenite grain size refinement [43]. These can all be used to explain the observed austenite grain size effects.

The average packet size in the finer austenite grain structure is smaller than that of the coarser one. It was shown that [44] for the same cooling rate and isothermal holding temperatures, coarser austenite grain sizes led to bainite morphologies closer to the lower temperature morphologies *i.e.*, higher

volume fraction of bainitic ferrite platelets per unit volume of bainite, and a lower quantity of the interlayer regions at the end of the isothermal bainite holding period. On the other hand, as was mentioned previously, the coarser the austenite grain size, the bigger the size of bainite packets. This, in turn, results in coarser austenite particles trapped in between the bainitic packets, which are less stable, *i.e.*, more prone to transform to lower bainite or Martensite on subsequent cooling to room temperature.

Thus, the lower amounts of retained austenite in coarse-grain austenite occur for two reasons. First, the larger bainite packets with higher volume fraction of bainitic ferrite platelets per packet reduces the volume fraction of inter-packet and interlayer remaining austenite at the end of isothermal bainite holding duration. Second, the coarser remaining austenite particles are more likely to transform to lower bainite and/or martensite during subsequent cooling to room temperature (the finer the austenite particle size, the lower the Ms and therefore the higher the stability of parent austenite) [45]. The Ms temperature is an accepted criterion for austenite stability. The lower the Ms temperature, the higher the stability of austenite and hence the higher the retained austenite volume fraction at the end of the process. This rationale however, does not follow with the introduction of Nb into the steel. The higher the level of Nb in solution, the higher the stability of parent austenite, thereby increasing the volume fraction of retained austenite obtained at the end of the process [45]. This is true of coarser austenite grain sizes rather than the finer grain sizes, the latter being generated by deformation, which promoted the kinetics of Nb precipitation during subsequent treatment, removing Nb from solution.

2.2.3.6 Morphology, Distribution, and Stability of Retained Austenite

When ferrite, bainite, and retained austenite are coexisting, ferrite undergoes strain hardening, and so strain energy is accumulated by dislocation pile-up inside the ferrite grains. The resulting accumulated strain energy provides the mechanical driving force needed for the strain-induced transformation of retained austenite. Upon this strain-induced transformation, the accumulated energy is absorbed, dislocation pile-up is relaxed, and ferrite grains are again softened. The softened ferrite grains can then be strain-hardened again by the strain-induced martensite [96]. This process repeats throughout the process of strain-induced transformation of retained austenite. If the stability of the retained austenite is high, the strain-induced transformation can proceed at a steady rate even under high strain. This will then enhance the formability because the abrupt drop in strain hardenability can be prevented [96]. Therefore, the stability of retained austenite is an important factor directly affecting the formability.

It has been reported that an increase in the volume fraction of retained austenite increases the strain-hardening coefficient, which leads to an increase in elongation. [46] On the other hand, a number of articles have shown that a higher amount of retained austenite does not necessarily result in a higher uniform elongation, because the higher amount of retained austenite may have a lower average carbon content, leading to low stability during deformation. Hence, there is an optimum amount of the retained austenite required to increase the elongation of TRIP steels [47].

The main variables that can dictate the stability of the retained austenite during deformation are the carbon content, size, morphology, and distribution of the grains within the microstructure. The carbon content determines the chemical driving force for the transformation of retained austenite to martensite, the stress-free transformation strain and the flow behaviour of the retained austenite [48]. It has been found that retained austenite with a low carbon content of 0.06wt.% or lower can transform to martensite more rapidly

during plastic straining and does not contribute to an increase in elongation. [49] On the other hand, if the carbon content is a lot higher, 1.8wt% or above, it will result in the incomplete transformation of the retained austenite to martensite after deformation and also does not lead to an increase in elongation [50]. It has also been shown that retained-austenite grains larger than 1μm are unstable and do not contribute significantly to the ductility of the material, since smaller retained austenite crystals contain fewer potential nucleation sites for the transformation to martensite and, consequently, require a greater total driving force for the nucleation of martensite [51]. On the other hand, the retained-austenite islands, which are smaller than sub-micron size, have a low tendency to transform to martensite, even if necking occurs, and, thus, do not contribute to the ductility [52].

The morphology of the retained austenite is also important for its stabilization. The best elongation behaviour has been observed when the retained austenite is present as films between the sub-units of bainite, rather than as blocky regions between sheaves of bainitic ferrite [53]. The blocks of austenite tend to transform to martensite under a small strain and, consequently, do not contribute to the TRIP effect [53]. The kinetics of the deformation-induced transformation can also be affected by the location of the retained austenite in the microstructure. According to Tsukatani *et al.*, [54] the presence of martensite near retained austenite diminishes the TRIP effect because martensite propagates stress directly to the retained austenite, which may then easily transform to martensite at an early stage of straining [54]. Bainitic ferrite can also act as a barrier against the autocatalytic propagation of the austenite to martensite transformation [55].

Recent publications have also revealed the importance of the effect of ferrite and its interaction with, retained austenite, and strain-induced martensite during straining on the structure-property relationship in TRIP steels. [56] However, since TRIP steel microstructures also contain bainite with different morphologies, it is proposed that the effect of the interaction of all phases

present in the microstructure on the microstructure property relationship should also be considered.

2.2.3.7 Retained Austenite in Dual Phase Silicon Steels

Research by M.H. Saleh et. al. [57] looked at retained austenite in dual phase silicon steels. They found that after interrupted quenching, the primary factor for the amount of retained austenite is the silicon concentration and this could be optimised at a quenching temperature of 400°C. By increasing the silicon content between 0.24 and 1.44wt.% they were able to increase the amount of retained austenite significantly to a maximum of 1.44 to 1.96%. This in turn meant the tensile strength was increased and the uniform elongation was reached at 25% in 1.44% Si steel, the morphology of the austenite formed at the intercritical annealing temperature affected its morphology after interrupted quenching. This meant that isolated austenite would give rise to isolated retained austenite volumes, and continuous austenite would give rise to interlath retained austenite with bainitic ferrite. During straining, the steels, which contained small amounts of retained austenite and had low mechanical stability transformed completely to martensite early on during the straining process. This caused the maximum incremental strain-hardening exponent (n_1) of this steel to occur at a low strain, this will account for the lower uniform elongation and tensile strength that was observed. When increasing the silicon content the transformation from retained austenite to martensite would occur at a much higher strain. This in turn resulted in a higher n_1 value at high strain, a higher work hardening rate, a high uniform strain and high ultimate tensile strength. However, for steel that contained more than 1.44% Si the maximum n_1 value decreased and accounted for lower uniform elongation and low tensile strength.

2.2.4 Martensite.

2.2.4.1 The Austenite to Martensite Transformation (TRIP effect)

Knowledge and understanding of the impact-dynamic properties of materials used in the structural parts of cars are essential to guarantee a controlled dissipation of the energy released during a crash. Transformation behaviour of retained austenite is influenced by its chemical composition and grain size as well as deformation mode.

Martensitic transformation is a solid-state diffusionless phase transformation. Only atomic movements over very small areas less than the inter-atomic distance are required for the martensitic transformation to take place [1]. Since there is no diffusion, the chemical composition of the parent phase (austenite) and the product phase (martensite) is identical. The martensitic transformation is also a displacive transformation and so structural changes take place. The atoms, which are involved in the transformation process, will retain their neighbourhood relationships because of the co-ordinated atomic shifts [3]. Many diffusionless displacive phase transformations can be found in materials other than TRIP steels, which form a subset of a larger class of phase transformations sharing common features. Martensitic transformations have also been known to take place in minerals, crystals and compounds, which can undergo a martensitic transformation as long as that the rate of heating or cooling is high enough to prevent the alternative diffusion-controlled transformation [12]. This means a rapid cooling of the steel from the austenitic region is required to result in a martensite formation, sometimes with retained austenite in the microstructure. The transformation process into martensite seems to be at random since the density of the formation of martensitic plates throughout the steel appears to be independent from the austenite grain size [12]. The newly formed martensitic plates will generally be smaller in size than the austenite grains as the transformation process proceeds due to an austenite partitioning caused by the previously transformed martensitic plates [12].

The martensitic transformation from austenite can also be achieved by applying a stress or strain instead of rapid cooling. The stress-assisted transformation of austenite has already been established in research as in work by Tamura et. al. [58] and Yu et. al. [59]. Applied mechanical loading can therefore contribute to the overall free energy needed to start the transformation, via its introduction with the shape deformation [3]. It is therefore possible to nucleate martensite at temperatures above Ms as long as there is a sufficient mechanical driving force

The following features defined by Cohen [60] are necessary and sufficient to define the martensitic transformation:

1) There must be a displacive lattice distortion involving a shape change with a dominant shear mechanism.
2) It is diffusionless.
3) Transformation kinetics must be dominated by sufficiently high shear-strain energy.

2.2.4.2 Effect of Deformation Mode.

The strain-induced martensitic transformation is dependent not only on the temperature and strain rate but also on the deformation mode imposed. To obtain the expected mechanical properties of TRIP steels through the metal-forming process, where the material undergoes complicated deformation, prediction and control of the change in material characteristics due to the deformation are indispensable [61].

This means that TRIP steels should be deformed under suitable strain rate and deformation mode to achieve preferable formability [62]. This could be understood from two aspects. On one side, strain rate influences the nucleation and birth rate of martensite, from which the hardenability is improved and homogeneous formability of TRIP steels is also achieved. If it

deforms too fast, more retained austenite would transform to martensite, which might result in the insufficient supply of plasticity improvement from the TRIP effect in the successive deformation, and bring about necking. If it deforms too slowly, the transformation rate of retained austenite would be too small and result in insufficient plasticity supplement in the early deformation stage, which might foster early thickness thinning [62]. The intrinsic good formability of TRIP steels could not be made full use of which would go against expanding the application of TRIP steels in automobile panels. On the other side, the occurrence of a suitable deformation mode is a predominant factor that determines the usage of the TRIP effect. Since the stamping parts could not be obtained from single deformation mode, TRIP sheet steels should be deformed under appropriate combination of deformation modes, which could be described as strain path. The most suitable strain path for different stamping parts is different and should be designed according to the part geometry, material properties and forming condition [62]. For example, first plane strain tension then uniaxial tension might be sufficient for a simple part but be harmful to complex panels due to different drawing depth and part geometry.

2.2.4.3 Strain Rate Behaviour

The deformation of steels during high-strain-rate loading is the result of an interaction between two opposing processes: strain-rate hardening and thermal softening due to adiabatic heating. For TRIP steels, thermal softening is more complex because the temperature affects the austenite to martensite transformation. The increased temperature reduces the transformation rate. During high-strain-rate loading, the austenite is not fully transformed into martensite and it contains numerous deformation twins. [63] The three phases each have individual responses. The BCC phases, ferrite and bainite, have a strong temperature and strain-rate dependence. For the FCC austenite, the strain-rate and temperature dependence are less pronounced, but its transformation behaviour is temperature dependent.

2.2.4.4 Stress-Strain Relation

The influence of the strain rate is material dependent, but positive for both CMnSi-TRIP and CMnAl-TRIP steels. Stress levels rise as the strain rate increases. Differences between the static and dynamic stress-strain curves are most pronounced for CMnAl-TRIP steel. CMnAl-TRIP steels show lower strength compared to CMnSi-TRIP steels [64]. The contribution of Al to the strengthening of the BCC phases, ferrite and bainitic ferrite, is limited. However, as could be expected, Al alloyed TRIP steels exhibit high deformation values [64].

Different parameters can be used to evaluate the crash resistance performance of steels. Since, for most applications, the material rarely deforms up to fracture, the yield stress and energy absorbed by the material at certain levels of deformation gives valuable information. It is clear that the strain-rate dependency is more pronounced at larger strains [64]. The strain-rate dependency of the flow stress is positive and more pronounced at higher strain levels.

2.2.4.5 Hardening Behaviour

Due to void formation and the formation of carbides in CMnSi-TRIP steel, more obstacles are introduced in the material than in CMnAl-TRIP materials. Therefore, CMnSi-TRIP steel has lower elongation values, but higher strength levels. When comparing steels with differing carbon content, those steels that have the higher carbon content will increase energy absorption [64]. This can be attributed to the fact that carbon is an important solid solution strengthening element for bainite, martensite, and austenite. By increasing the carbon content of TRIP steels, its strength increases without deteriorating the formability of these steels [64].

In the early stages of deformation, the strain hardening is highest for CMnSi-TRIP steel, followed by CMnAl-TRIP. Temper-rolled TRIP steel shows the

lowest strain hardening in the beginning. After approximately 14% true strain, the strain-hardening coefficient of CMnSi-TRIP steel begins to decrease. The decrease of the strain hardening of aluminium materials begins later during the deformation [64]. CMnAl-TRIP steel shows an important increase in strain hardening at the end of the deformation, before strain localization occurs at the highest strain rates. The strain-hardening coefficient is calculated at different values of true strain, ranging from 5 to 20% true strain. The strain-hardening coefficient at 5, 10, and 20% true strain increases significantly as a function of the strain rate. Moreover, the higher the strain, the steeper the increase is. This can be correlated to the increase of the energy absorption in function of the strain rate shown earlier [64].

2.2.4.6 Microstructure During Strain.

The retained austenite phase in low-alloy TRIP steels is a metastable high-carbon austenite with low stacking fault energy. It has relatively low yield strength and higher work hardening than ferrite. This higher work hardening is related to both the difficulty in cross-slip of dislocations and the strain-induced austenite/martensite transformation [64].

The high-strain-rate deformation processes, which determine the mechanical behaviour of retained austenite in dynamic loading, are as follows: dislocation glide, the formation of stacking faults, twinning, and transformation to martensite.

The effect of strain rate on the austenite/martensite transformation has been studied in detail in single-phase metastable austenitic steels. [65] In these steels, the transformation decreases when the strain rate increases. The results obtained under high-strain-rate loading indicate that adiabatic heating affects the mechanical stability of the austenite.

When the stress level increases from the Ms temperature, heterogeneous pre-existing nuclei of martensite can be activated with increasing temperature

[64]. When the Ms temperature is reached, plastic deformation further assists the transformation by creating additional martensite nuclei. Thus, the Ms temperature determines the transition between stress and strain-induced martensite nucleation, and is dependent on the yield stress of the retained austenite. The latter is influenced by the strain rate during the test and the temperature of the sample, both having an opposite effect on the yield stress.

At low strains, when the temperature rise is relatively limited, a higher transformation rate and lower dislocation mobility can be observed. It is likely that both deformation twinning and martensite formation might occur in high-carbon austenite, as is the case in austenitic stainless steels. At larger strains, when the temperature rise is important, dislocation glide will be favoured, the transformation rate will be reduced, the stacking fault energy will be increased, and the solid solution strengthening effect of certain alloying elements may be reduced.

It is known that low-alloy TRIP steels combine high strength levels with an excellent formability in quasi-static conditions. It is shown that TRIP steels preserve these excellent properties during dynamic or high strain rate loading [64]. From the results of an extensive experimental program on the high-strain-rate properties [64], it is clear that as the strain rate increases, higher yield stresses, higher strengths, and higher energy absorption levels are found. As in the static case, aluminium increases the ductility significantly in high-strain-rate conditions, and silicon has a positive influence on the strength level. The bake hardening of the TRIP material causes the disappearance of the yield peak of the stress-strain curve.

The low-alloy TRIP-steel properties are due to the multiphase microstructure in which the combination of the high-strain-rate properties of the ferrite, bainite, and austenite phase results in a composite effect. There is a large and uniform deformation of the phases at high strain rates. The strain and temperature dependent transformation of the metastable retained austenite into martensite is responsible for the excellent high-strain rate properties.

2.2.4.7 Rate of Mechanically Induced Martensitic Transformation

Typically, a transformed grain contains between two and five martensitic variants. Partially transformed grains are rarely observed in low silicon steels [65], meaning that the transformation is almost instantaneous. The size of the austenite grains thus seems to be sufficiently small for the autocatalytic effects to overwhelm the local drop of hydrostatic stress during transformation (a drop of the hydrostatic stress would, in principle, reduce the driving force for continuing the transformation) [65]. The continuous increase of the transformation with increasing strain in low silicon steels is thus not merely due to a step by step transformation inside each retained austenite grain. The kinetics of the mechanically activated transformation of retained austenite depends on the chemical composition of the grain, the morphology, size and location of the grain, the crystallographic orientation of the grain, the stress state and the strain state.

The relative importance of these parameters remains difficult to evaluate. Low silicon and high silicon steels differ not only in the amount of retained austenite but also in other factors such as the carbon content of austenite. A larger accumulated plastic strain is needed to transform retained austenite high silicon steels, this suggests that retained austenite in high silicon steel is more stable [65]. This result is in good agreement with previous studies. Solid-solution strengthening of the ferrite matrix can be achieved by silicon or “shielding” of austenite from the external load in high silicon steel as a result of load transfer to high strength bainite.

A strong dependence of the rate of martensitic transformation on stress triaxiality has been found [65], the transformation rate increases with increasing triaxiality. This strong stress triaxiality effect originates from the volume expansion accompanying martensitic transformation, which results in the mean stress being the main driving force for the transformation. Even though shear deformation is the main deformation associated with martensitic

transformation, a volume expansion also occurs which depends on the carbon content.

Stress triaxiality affects more predominantly the transformation of the last 50% of retained austenite. In the case of uniaxial tension, the strain-induced martensitic transformation becomes progressively exhausted and some retained austenite was found strained up to true uniform strain. Metallographic observation revealed that this part of the austenite that transforms the last corresponds to the film type austenite lying along bainitic ferrite plates. It was already reported that the higher stability of this type of austenite should be ascribed to a higher carbon content, a size stabilizing effect and a constraint effect due to the presence of adjacent, finely grained bainitic ferrite [66].

The mechanically induced martensitic transformation improves strength and ductility by both a composite strengthening effect resulting from the progressive increase of the amount of hard martensite, and a dislocation strengthening of the ferrite matrix as a consequence of the transformation strain accompanying martensitic transformation.

2.2.4.8 The Coupling Between Transformation and Damage

Martensitic transformation is responsible for the creation of damage sites. This behaviour is very different from the behaviour of steels for which the volume expansion associated with the transformation hinders damage by postponing the nucleation of voids [67]. However, the onset of the martensitic transformation is not a sufficient condition for damage initiation. Low silicon steels, which show faster martensitic transformation, do not suffer higher levels of damage than high silicon steels. It is actually seen that the onset of damage is earlier in high silicon steels. The first reason is the high carbon content of the austenite, which transforms into a high strength martensite [66]. The ensuing larger strain incompatibilities between ferrite and martensite induce more rapid de-bonding. Higher carbon contents also render martensite more brittle and martensite cracking therefore becomes easier. The non-

intercritical ferrite phases, i.e. bainite and retained austenite, constitute a nearly continuous network along the ferrite grain boundaries. Martensitic transformation of more than 75% of the initial retained austenite content creates an almost continuous brittle network consisting of high strength bainite and martensite into the ferrite matrix. This network allows brittle crack propagation inside the material without crossing the ductile phase. This means that, for the levels of mechanical stability of austenite involved in TRIP-aided steels, damage is governed not only by the transformation rate but also by the amount of martensite.

2.2.4.9 Testing Conditions

At high strain rates the strain-hardening rate is initially higher. However, with the decrease of stress concentrated at the induced martensitic transformation interface caused by the transformation dilatation, the effect of dislocation hardening decreases and strain-hardening rate is rapidly reduced [68]. During deformation, high strength martensite, which inherits the high alloy and carbon content of austenite and ferrite with numerous dislocations, makes the work hardening rate decrease slowly. Strain-hardening rates decrease slower at lower strain rates [68].

Because of the very fast deformation, the associated adiabatic temperature rise should be appreciable. Masaaki Itabashi [69] indicates that temperature rise of a *0.*44C-0.23Si-0.75Mn steel is about 62°C at a strain rate of $1000s^{-1}$. The adiabatic temperature rise rates per unit time of steel samples with different heat treatments are almost the same. The higher the strain rate, the higher the rate of the adiabatic temperature rise [68]. A strain rate of $1600s^{-1}$ causes the adiabatic temperature to rise 30°C within 0.1 ms for steel deformed at this strain rate, the deformation time is about *0.*2–*0.*3 ms; this implies that the adiabatic temperature rise is about 60°C to 90°C. The effect of the temperature rise on the increase in total elongation cannot be ignored [68]. The adiabatic temperature rise during high strain rate tests retards the nucleation of new martensite, and makes retained austenite more stable [70].

More stable retained austenite will gradually transform with increasing strain. It has been shown that there is no rapid rupture taking place after necking for high strain rate tests. This may be caused by the gradual transformation of retained austenite after necking, subsequently increasing the strength of the material matrix and retarding the necking [68].

Test temperature has a major influence on the mechanical properties of low silicon TRIP steel, and it may be caused by retained austenite transformation [68]. The strain rate has little influence on the retained austenite transformation when testing at temperatures of $110^{o}C$. The energy absorption increases with the strain rate. This increase of energy absorption is mainly due to an increase in total elongation. Three factors affect the total elongation in dynamic tensile tests [68]. First, the strain rate increase retards cross slip and multiples slip of dislocation, subsequently increasing the resistance to ductile rupture and slowing the abrupt rupture after necking [71]. Second, the temperature rise leads to a softer material matrix at medium strain rates [71]. Third, the retained austenite transformation plays an important role at the same strain rate.

Retained austenite transformation has become one of the three major factors affecting the total elongation. It is strongly related to the volume fraction of untransformed retained austenite [68]. Long impulse duration time at low strain rate promotes defect production in alloys, which is beneficial for the austenite transformation to martensite [71]. Uniform elongation is at its highest when retained austenite has fully transformed to martensite, but samples will generally rapidly fracture after necking. X-ray diffraction has indicated that there are numerous retained austenite grains remaining at deformation in the rupture area after tests at high strain rates [68]. This type of austenite will partly increase the plasticity after necking, slow down hole formation at the interface of ferrite and second phase, and further increase uniform retained austenite which will also be more stable when the test temperature is raised [68].

2.3 Alloying Elements Used in TRIP Steels

Carbon, which exhibits the austenite-stabilizing effect, is the most important alloying element in TRIP steels. However, its content cannot be increased too high due to further technological requirements such as weldability, which is adversely effected by high carbon levels. Other austenite-stabilizing elements used in TRIP steels include manganese and silicon. Manganese enhances the solubility of carbon in austenite and so retards the formation of pearlite. Both of these elements can improve the strength of the material. Alloying with aluminium has been extensively investigated, as adding aluminium both inhibits cementite precipitation and provides effective solid solution strengthening [72]. Niobium can be used as an austenitisation-delaying element; this inhibits grain growth and will affect phase transformation and recrystallisation.

Controlled cooling after intercritical annealing creates the retained austenite in a bainitic ferritic matrix. The intercritical annealing creates a microstructure that consists of about equal volume fractions of ferrite and austenite. Cooling occurs by quenching the material into the temperature regime of bainite formation where it is held until a certain amount of bainite is formed. During intercritical annealing and the following bainitic phase transformation the remaining austenite is enriched with carbon due to carbon partitioning. The stabilisation of austenite has to be well balanced in order to prevent the formation of martensite during cooling and to allow the continuous martensite formation over a large straining range [13]. The important point in the alloying concept and the heat treatment procedure of TRIP steels is therefore to achieve a relatively high carbon content in the austenite. An appropriate alloy composition for TRIP steel consists of a sufficiently high carbon content of 0.15–0.2wt% and small additions, in the range of 0–2wt% of silicon, aluminium and manganese [73]. Small amounts of phosphorus may also be added.

Current low alloy TRIP-aided steels are typically characterized by their very low content of alloying elements, for example in current 800MPa TRIP steel, the total content of alloying elements is around 3.5wt%. Conventional TRIP steel compositions are usually based on the original 0.12–0.55wt%C 0.2–2.5wt%Mn 0.4–1.8wt%Si that was proposed by Matsumura et al. [74]. The carbon content plays a key role in the composition. Its distribution between the main micro-structural constituents is fundamental to the properties of the material. It should be enriched as much as possible in the retained austenite to obtain the best mechanical properties. Whereas original laboratory TRIP steels could have a carbon content as high as 0.4 wt%, current TRIP steels contain typically 0.20–0.25wt%C or less for reasons of weldability [16]. Another major alloying element is Mn, the content of which in low alloy TRIP steel is ~1.5%, Mn is required to achieve hardenability. Manganese has a dual role, as it is also an austenite stabiliser therefore lowering the temperature at which the cementite starts to precipitate. High manganese contents of around 2.5wt% are not favourable as they lead to banding in the microstructure and excessively stabilized retained austenite [75]. Silicon significantly increases the carbon activity coefficient in both ferrite and austenite and reduces the carbon solubility in ferrite. Silicon also increases the temperature at which the cementite starts to precipitate in ferrite at a given ageing time. Silicon is a major alloying element particularly in earlier TRIP chemistries as silicon also inhibits the formation of cementite during the austempering stage. This is usually explained by the fact that silicon has an extremely low solubility in cementite.

From an industrial point of view, it is important to realize that silicon reduces the kinetics of the bainitic transformation considerably; this implies that cold rolled C, Mn and Si type TRIP steel can only be produced on a line with a long over-ageing section, in which a long austempering stage can be carried out [16].

Although low silicon and even silicon free compositions have been proposed, silicon is the most effective alloying element to prevent the formation of cementite during the austempering stage. This means there should only be a partial replacement of ~1wt%Si by ~1wt%Al [76]. The high aluminium content in C, Mn, and Al TRIP steels results in a high carbon content in the retained austenite [77]. Both silicon and aluminium are insoluble in cementite and greatly retard cementite formation. Aluminium decreases the carbon activity coefficient in ferrite and increases the solubility of carbon in ferrite. Aluminium increases the temperature for the initiation of cementite. More importantly, aluminium accelerates the bainite formation. The increased bainitic transformation kinetics are very relevant to industrial production, as many continuous galvanizing lines for automotive sheet products were often originally designed with interstitial free steels in mind and therefore do not have long over-ageing sections which is needed for the austempering process to be carried out. The disadvantage of using aluminium over silicon is its lower solid solution hardening [78] and the fact that aluminium destabilizes the austenite.

The critical alloying elements of TRIP steels manganese, silicon, and aluminium form oxides internally and at the surface, which are difficult to reduce. Phosphorus does not cause any problems and aluminium causes fewer problems than silicon for coatability. But aluminium cannot completely replace silicon [79].

Phosphorus can be used to limit the use of aluminium if the full replacement of Si is restricted. Phosphorus alloying additions can perform several roles; it suppresses the formation of cementite. It is also very effective as a solid solution hardening element and, when low silicon content is used, it has been shown to increase the amount of retained austenite [80]. Phosphorus also significantly increases the carbon activity coefficient in ferrite. Only small amounts of phosphorus are required (0.05–0.1wt%) to achieve significant improvements.

Currently the development of TRIP steel is focused on steel with strengths ranging from 500MPa to 800MPa. In order to achieve strength levels higher than this of around 1000MPa or more other micro-alloying concepts have been proposed. Nb, Ti and V, have all been used in various combinations and have been found to refine the microstructure and form carbide precipitates.

Ti additions provide precipitation strengthening in the hot band. After cold rolling and annealing it is expected that some of this will be lost due to coarsening of precipitates. More promising is V with N, where this combination will allow precipitation during annealing, and therefore give better control of the precipitation sequence to yield optimum strengthening. Using Al in conjunction with V will also affect its precipitation behaviour, as it is also a strong nitride former [79].

An increase of 150MPa can be achieved when using V and N micro alloying additions while ~230MPa can be achieved when using Ti micro alloying, and in addition cause significant grain refinement [79]. V is the best element for precipitation strengthening of cold rolled TRIP, and an increase in strength can be achieved without a reduction in ductility. Using low coiling temperatures with a V and N micro-alloyed steel can give a tensile strength increase of 35MPa and 80MPa to the Ti micro-alloyed steels [79]. Lowering the coiling temperatures can also increase the work hardening rate. All micro alloying also increases toughness.

2.3.1 Silicon.

It is a common practice in low-alloy TRIP-aided steels to add large concentrations of silicon. The higher silicon content will reduce the chances of cementite precipitation occurring in the microstructure during the growth of upper bainite [1]. By preventing the growth of cementite it will ensure higher ductility levels, by forcing the carbon to enrich the austenite rather than forming into cementite. It has been shown that achieving retained austenite in these low-alloy TRIP steels is almost impossible when the silicon

concentrations are much below 1 wt% [81]. The kinetics of cementite precipitation in TRIP steels depends on the carbon concentration of bainitic ferrite during the bainitic transformation [5]. Carbon that is partitioned from bainitic ferrite will either enrich the residual austenite or form carbides. Both of these processes can occur at the same time, however, one process will dominate depending on the choice of isothermal holding temperature and alloy composition. It has been noticed that in high silicon TRIP steels, carbide precipitation is slower than the formation of the bainitic ferrite, and in fact, the microstructure of alloys with high silicon content is carbide-free even after holding for several hours in the bainitic transformation region [1].

The mechanism by which silicon retards cementite precipitation has been proposed by Pichler et. al. [82]. In their research they found the mechanism for the suppression of cementite precipitation was that silicon has a low solubility in cementite. It is well established that the composition of upper bainite cementite has a substitutional solute content, which is close to or slightly higher than that of the alloy bulk composition [5]. In work by J. Chance et. al. [83], which looked at upper bainite in a Fe-0.81C-1.41Cr wt% alloy, they found that the chromium partition coefficient, which is the ratio of chromium concentration in cementite to that of the austenite, was almost equal to unity. These findings mean that the mechanism by which cementite grows is displacive. This fact is interesting since the carbon diffusion, which is partitioned from austenite, can only occur in the process of cementite precipitation. However, the diffusion involved in the process of cementite precipitation is of the interstitial not the substitutional solutes [5]. This leads to the conclusion that it is still possible for the interstitial solutes to diffuse at as low a temperature as -60°C. As such, the ratio of the concentration of iron to that of carbon remains constant throughout the steel, and this leads to the carbon chemical potential achieving equality throughout the alloy. Therefore, cementite grows by a para-equilibrium transformation mechanism [5]. If cementite is forced to retain the silicon due to the para-equilibrium transformation mechanism, therefore, to a large extent, the driving force for

cementite precipitation is decreased which has the effect of retarding cementite precipitation [5].

A study by P. Jacques et. al. [84] looked at two steels: a conventional 0.29C–1.40Mn–1.50Si TRIP-assisted multiphase high silicon steel, and a new low silicon 0.16C–1.30Mn– 0.38Si multiphase steel. Bainite transformation in the high silicon steel showed the typical behaviour of silicon-rich steel, giving an incomplete reaction phenomenon, which corresponds to a maximum carbon enrichment of austenite. The bainite transformation will stop before the complete transformation of the intercritical austenite. The bainite transformation is accompanied by carbon enrichment of the residual austenite up to a maximum level attained at the transformation stasis. It was noted that the silicon content of the high silicon steel was sufficient for holding up the decomposition of austenite by cementite precipitation during long isothermal holding at 360 or 410°C. However, notwithstanding the displacive nature of the bainite transformation, it was also shown that the kinetics of the bainite transformation of the intercritical austenite is influenced by the isothermal holding temperature. As also observed in other TRIP-assisted multiphase steels, the temperature at which the isothermal bainitic holding is carried out will influence the bainite transformation rate when the initial microstructure obtained at the end of intercritical annealing is constituted by a mixture of fine grains of ferrite and austenite [84]. This behaviour is quite different from the bainite transformation of an initial fully austenitic microstructure and experimental results have shown independence of the holding temperature on the bainite transformation kinetics. It can be said that the small grain size of the intercritical austenite, which were found to be approximately 1mm, and their isolated nature in the intercritical ferrite matrix will largely influence the progress of the bainite transformation [84]. Because of the small size of the intercritical austenite grains, the first steps of the bainite transformation will enhance the heterogeneities of carbon redistribution along the broad faces of the sub-units in the small austenite grains. This will then restrict the opportunities for nucleation of the next ferrite sub-units. Due to the thermal activation of carbon diffusion, the heterogeneities in the redistribution of

carbon are smaller so that the global kinetics appears to be faster at higher isothermal holding temperature. For the low silicon steel, the incomplete reaction phenomenon was not observed. In this case, a complete inhibition of cementite precipitation during the growth of bainitic ferrite cannot be explained in the same way that the bainite transformation and decomposition of austenite occurs simultaneously. It was shown that a maximum carbon level in the residual austenite is rapidly achieved and that any further progress in the bainite transformation is also accompanied by a decrease in the carbon content. Due to the lower silicon content, cementite precipitation from austenite cannot be avoided in the low silicon steel so that it overlaps with the formation of bainitic ferrite. As a consequence, the maximum amount of retained austenite is observed in the microstructure of the low silicon steel in the early stage of the bainite transformation, when a part of the residual austenite also transforms into martensite during quenching to room temperature. The formation of cementite will reduce the carbon content in the austenite, and so will promote the bainite transformation in such a way that no incomplete reaction phenomenon can be observed. The carbon content of residual austenite during bainitic holding is highly influenced by both the redistribution of carbon from bainitic ferrite and by the cementite precipitation. Therefore, the bainite transformation kinetics of the low silicon steel is dictated by both these phenomena, by their own kinetics, and by their influence on the nucleation and growth of bainitic ferrite plates. Cementite precipitation leads to more carbon being depleted, residual austenite is faster and more pronounced at 430°C. Despite comparable maximum carbon contents of austenite at 370 and 430°C, the faster decrease of carbon content at 430°C leads to easier nucleation of new bainitic ferrite plates and, therefore, to faster kinetics when the isothermal bainitic holding temperature is higher [84].

2.3.2 Aluminium.

The standard silicon TRIP aided steel contains about 0.15% C 1.5% Mn 1.5% Silicon which will result in the formation of a Mn_2SiO_4 oxide film on the surface [85] This can then be easily rolled into the surface during hot rolling. This oxide is also difficult to remove and will generate poor surface characteristics for the hot rolled steel. After cold rolling and continuous annealing, these surface oxides will result in poor coatability for the steel [86]. Since corrosion protection will become a safety aspect of great importance when it comes to higher strength automotive sheet steel, they must be coat-able by means of current conventional electroplating or continuous galvanizing technologies [86]. The high silicon content in conventional C-Mn-Si TRIP steels are expected to give rise to galvanizing problems, and have also been known to cause low ductility levels in the as-cast condition, and this is an additional reason to keep the Si content of TRIP steels low

The free energy of the austenite and the ferrite is a function of both the temperature and their composition. At any temperature there is a common composition at which the free energy of the ferrite equals the free energy of the austenite of identical composition [85]. The bainitic transformation can only take place below the T_0 line as Si effectively suppresses the formation of cementite. The isothermal transformation in high Si alloys will lead to the progressive decrease of the difference in the free energy between ferrite and retained austenite, and the transformation will stop when the carbon content in the retained austenite reaches its maximum attainable value. Silicon is therefore required in TRIP- aided steel as it will effectively suppress the formation of cementite during the isothermal transformation and contributes to the stability of retained austenite. It is well known that aluminium acts in the same manner as silicon as this element is also insoluble in the carbide Fe_3C [85], it is known to have a very large effect on the growth rate of the carbide. Therefore, aluminium increases the carbide formation time and decreases the thermodynamic stability of the cementite. Aluminium can therefore be used to substitute silicon.

2.3.3 Comparison of Silicon and Aluminium in TRIP Steels

Etienne Girault et. al. [18] compared the effects of silicon and aluminium on the tensile behaviour of TRIP steels. To do this they chose a high silicon steel 1.5wt% Si a lower silicon steel 0.78 wt% Si and an aluminium steel 0.06 wt% Si 1.5 wt% Al. It was found that the three developed microstructures mainly differed by their retained austenite volume fraction.

Etienne Girault et. al. [18] found evidence of a significant decrease for austenite in the microstructure during deformation of optimised steel grades. Optical microscopy was used to confirm the gradual appearance of martensite at the expense of austenite, and so establishing the occurrence of strain-induced transformation. It was shown that retained austenite populations exhibit comparable mechanical stability. During deformation, the austenite to martensite transformation took place at about the same rate for all three steels. However, the strain-induced transformation proves to be relatively more extensive on the 1.5Si/1.5Al grades, since they contained greater amount of retained austenite.

In Dual-Phase and TRIP-assisted steels, the strains that are associated with martensite formation are known to generate some stresses and free dislocations in the neighbouring grains of ferrite matrix, near the ferrite/martensite interface [87]. When the matrix is subjected to straining such as tensile testing, the strain-induced transformation of austenite to martensite contributes to an enhanced formation of dislocations in the ferrite, compared to that achieved by the deformation of the matrix. Since flow stress in steels is proportional to the square root of the dislocation density, a significant strain-hardening rate arises, due to the large increase in dislocation density per unit strain. This means, the introduction of free dislocations favours the increase of dislocation tangles in the ferrite, which results in a substantial instantaneous work hardening.

In TRIP-assisted steels, the strain-induced transformation of austenite typically spreads out the formation of martensite all along the deformation and so the associated dislocations are introduced gradually, which allows it to steadily sustain the strain hardening. This enhancement of the work hardening causes the conditions for plastic instability to be met at higher strains, so that the onset of necking is postponed to large deformations [87]. The three steel grades developed in the work by Etienne Girault et. al. [18], were shown to have a high strength despite the remarkable uniform elongation achieved. The latter may be attributed to the occurrence of strain-induced transformation. The difference in strength levels achieved by the three steel grades investigated can be explained by their corresponding chemistry. It is known that when aluminium is present in solid solution it has a small effect on the strength of the ferrite, unlike silicon, which is one of the best substitutional strengtheners for ferrite [88]. The work-hardening rate of ferrite is known to increase with the addition of silicon and to be insignificantly affected by the presence of aluminium [88]. This shows that the 1.5Si grade and the 1.5Al grade in the work by Etienne Girault et. al. [18] manifests a similar work-hardening behaviour, which is consistent with the fact they experience a strain-induced transformation of comparable extent during testing. However, the 0.8Si grade, despite its silicon content, exhibits a strain-hardening rate barely above that of the 1.5Al steel. This lower work hardening can be explained by a less extensive strain-induced transformation for the 0.8Si grade, and therefore corresponding limited TRIP-effect. Looking at the respective uniform elongation obtained for the three TRIP steels, it can be said that both 1.5Al and 1.5Si steels, and to a lesser extent the 0.8Si steel, develop a remarkable TRIP-effect. However, the 1.5Al grade gives strength levels that are much lower than both the silicon containing grades. Thus, despite high interest in the use of aluminium in achieving the TRIP-effect, completely substituting silicon with aluminium in TRIP-aided steels will prove to be detrimental to the strength-ductility balance, owing to the weakness of the resulting ferrite matrix.

Pichler et. al. [89] suggested that since silicon is not soluble in cementite, the most important mechanism for cementite nucleation and growth is the diffusion of silicon from the particle. It is known that aluminium and phosphorus, which in addition to being strong ferrite stabilizers also retard the tempering reaction and inhibit the formation of cementite. Pichler et al also suggests that aluminium is an element, which is not soluble in cementite while phosphorous will reduce the precipitation kinetics of cementite. Aluminium and phosphorus are therefore expected to influence the bainitic transformation reaction in much the same way as silicon but without the adverse effects.

Chen et. al. [90] found for 0.07wt% phosphorus and silicon containing steel annealed at 800°C for 150 seconds and isothermally held at 450°C for 300 seconds, gave a volume fraction of retained austenite of 9.5% a high strength of 730MPa and a total elongation of 36% this shows that phosphorus is a possible alternative to partially replace silicon in TRIP steels. Also as the effect of cold work embrittlement caused by phosphorous only occurs for low and ultra low carbon steels no embrittlement is expected to take place because of the relatively high phosphorous additions [90].

The choice of the aluminium content of TRIP steel is a compromise between several factors. On one side, the substitution of silicon by aluminium is favourable, as high silicon contents will result in poor surface conditions and lower ductility. However, on the other hand it can be seen that by substituting silicon by aluminium it will extend the intercritical region. For a carbon content of 0.2wt%, the fully austenitic phase region is not even reached when silicon is totally substituted by aluminium. Therefore, the silicon content should only be partially replaced by aluminium. In addition, the carbon content can be increased to further extend the austenite phase region.

2.3.4 Partial Substitution of Silicon by Aluminium

It was found for two steels, a C-Mn-Al-Si and C-Mn-Si steel that the amount of retained austenite after tensile testing will not vary much for different combinations of temperature and time [86]. However, the level of retained austenite after straining takes place will be higher for the C-Mn-Al-Si steel composition, than for the C-Mn-Si steel. Chen et. al. [90] has reported that for phosphorus containing steel very small retained austenite particles less than 1μm will hardly transform to martensite, even if necking occurs. Therefore, small austenite grains are only expected to have a negligible effect on ductility. For aluminium-alloyed steel the amount of very fine austenite grains was greater than in the conventional TRIP steel. For the aluminium alloyed TRIP composition that was used, there were probably a larger number of fine retained austenite particles present within the fine bainite network structure [86]. Brandit ET. al. [91] have pointed out that smaller retained austenite particles will contain less potential nucleation sites for the transformation to martensite, and therefore require a greater total driving force for the nucleation of martensite.

By partially replacing silicon with aluminium in cold rolled C-Mn-Si TRIP steels it will lead to improved mechanical properties. Also for silicon TRIP steels a maximum n-value will be reached for low strains. However aluminium TRIP steels show more stable n-values with limited strain dependence and therefore result in a larger uniform elongation. This can be particularly valuable in stretch forming operations. The microstructure of the aluminium TRIP steel will show a larger amount of bainite resulting from a larger amount of austenite at the end of intercritical annealing. The volume fraction of retained austenite is larger for aluminium TRIP steels. Also the level of retained austenite after straining was higher for aluminium TRIP steels as well as having a higher carbon content in the retained austenite.

2.3.5 Copper, Chromium and Nickel.

In a study by Sung-Joon Kim et. al. [92] TRIP-aided multiphase low carbon steels that contained elements such as copper, chromium and nickel are designed, having high strength and ductility with a good recyclability. The addition of nickel will enhance the tensile strength and ductility along with the increase of retained austenite volume fraction. Nickel is a typical austenite stabilizer, and so will contribute to the formation of a large amount of retained austenite, and the enhancement of mechanical properties [92]. In addition, copper is an austenite stabilizer like nickel, and also gives a beneficial effect on the formation of retained austenite, resulting in the increase of the strength-ductility balance. It has been shown that nickel and copper might be used as beneficial tramp elements to improve the mechanical properties of low carbon TRIP steels. The addition of nickel in addition to chromium revealed a quite different behaviour from nickel additions by its self. In this case, while tensile strength increased remarkably, retained austenite volume fractions and elongations were decreased by a large amount, which is a-typical with the tensile behaviour of dual phase steels [92]. Chromium is a ferrite stabilizer. From the phase diagram of Fe–Cr, it is known that the addition of only a small amount of chromium 0.4 wt.% already stabilizes the ferrite in the temperature range of 780–790°C. This means the transformation from austenite to ferrite would proceed very actively, whilst being held in this temperature range, and other elements like carbon, manganese, and nickel could be put into solution into austenite and enhance the formation of retained austenite [92]. However, in chromium containing steels, retained austenite volume fractions were found to be lower than those of chromium-free steels. This result could be due to that though chromium is a ferrite stabiliser, it also causes an increase of austenite hardenability. The addition of chromium in order to increase hardenability is frequently applied in micro alloying steels [92]. If the cooling rate after isothermal holding is rapid, almost all the austenite will transforms to martensite. If this were the case then there would be little improvement of ductility due to the TRIP effect because of the decrease of retained austenite [92]. For chromium containing steels, the

cooling rate would have to be slowed down after isothermal heat treatment takes place to prevent the austenite from transforming to martensite.

In the meantime, mechanical properties of steel are superior to those of Cu-free steel, when they were intercritically annealed and isothermally transformed at the same condition [93]. Im et. al. [93] has reported that tensile strength and elongation of copper-containing Fe–0.15C–1.5Mn–1.5Si multiphase steel were 817MPa and 36.4% elongation, while those of copper free steel were 727MPa and 29.2% elongation, showing the superior tensile properties of copper-containing steel. Generally, when copper is used it is known to precipitate very fine ε-Cu in ferrite grains and so contributes to precipitation hardening [94]. In copper containing steels, precipitation of ε-Cu has been reported only in the specimens containing over 1.0 wt.% copper and after ageing tens of minutes in the temperature range 400–700°C [95]. As the copper content of the steel was only 0.5% and the isothermal transformation was carried out at 430°C for 20 min, it is unlikely that there will be precipitation of ε-Cu. Thus it can be said that the increase of yield and tensile strength in copper added steel when compared with Fe–0.15C–1.5Mn–1.5Si steel is considered to be due to the TRIP effect, from higher fractions of retained austenite and the solid solution hardening effect of copper in ferrite grains. In addition, copper is an austenite stabiliser like nickel and thus helps the formation of retained austenite resulting in the increase of the strength-ductility balance. Therefore, copper can be used as a beneficial tramp element in enhancing the mechanical properties of TRIP aided cold rolled sheet steels [92].

With the addition of copper alone, or copper and nickel, the volume fraction of retained austenite increases and results in an excellent combination of strength and ductility. Tensile strengths ranging 800–850MPa with large elongations of 34–38% were attained from copper or copper and nickel containing steels. The addition of chromium or chromium and nickel to the base steel shows a ferrite–martensite dual phase tensile behaviour, giving it a high strength of over 1000MPa and rather low ductility with an elongation

around 20% [92]. Copper and nickel are austenite-stabilizing elements, which gives beneficial effects on the formation of retained austenite. On the other hand, chromium increases the hardenability of austenite, which results in the formation of martensite after isothermal transformation. It has been confirmed that tramp elements like copper, nickel and chromium can be utilized to design an excellent material having various mechanical properties with good recyclability.

2.4 Applications for TRIP Steels.

TRIP steels have mainly been used in sheet production. One possible way to broaden the range of applications might be to combine an incremental deformation process with thermo mechanical treatment [97]. The semi product must possess suitable shape and appropriate microstructure, to allow the application of the TRIP effect. The breakdown of the total strain into incremental deformation steps will let the introduction of large total strains, leading to grain refinement and reduction of required forming force [97]. The final cold deformation should introduce sufficient strain to trigger the formation of strain-induced martensite, which will secure required strengthening. The cold deformation should be introduced in incremental steps as well. Two possible concepts for the use of incremental forming, which can be applied to low-alloyed TRIP steels, are currently being researched [97].

The first concept involves the production of a hollow semi product by a hot process, for example by cross wedge rolling on a mandrel. Subsequent heat treatment will result in a microstructure that will be suitable for the application of the TRIP effect. One way to achieve the final shape of the finished product would be cold metal spinning. Cold processing will impart strains necessary for transformation of retained austenite to martensite, which will provide the material with the required strength.

The second concept concerns thermo mechanical treatment used for preparation of the semi product [97]. This would result in the optimum shape for final forming operations and a suitable microstructure for utilizing the TRIP effect. Therefore, a heat treatment would not be needed and replaced with the thermo mechanical treatment. This process would bring improvement of mechanical properties in the steel and the energy, time and labour requirements. A properly designed process chain would be capable of producing high-strength components with favourable dynamic properties, and would not require any further heat treatment.

Both of these modified heat and thermo mechanical treatments proposed by H. Stankova et. al. [97] are consistent with the capabilities of actual technological procedures and permit the achievement of required microstructures in a low-alloyed TRIP steel, which can thus be used for processing routes which employ the TRIP effect. The existence of simple thermo mechanical treatment processes has been confirmed. These processes do not contain any lengthy soaking periods or sophisticated transition stages and particularly no abrupt changes in thermal gradients.

Results of the experiment carried out by H. Stankova ET. al. suggests a real possibility for the application of TRIP steels in production of components other than sheets. Products such as thin-walled parts made by forming, e.g. hollow bodies, etc. could be produced. The selected components must have a suitable shape to comply with the technological procedure. For this it will be possible to produce the required shape by thermo mechanical treatment and achieve suitable ferrite-bainite-retained austenite microstructure at the same time. The amount of incrementally introduced strain to be used presents the most important decision. Introducing incremental deformation will make it possible for the introduction of large strains simultaneously with the reduction of forming forces and tool stresses, which would otherwise be extremely high. Final deformation must then be introduced in a cold forming operation [97]. It must be designed in such a manner as to achieve the final shape of the product, whilst still maintaining the required amount of strain, which will induce the TRIP strengthening effect.

2.4.1 Automotive Applications

In the automotive industry, advanced high strength steels are being used mainly in structural, passenger safety-related parts of the body. In the engine area, advanced high strength steels can be used in the front structure to absorb frontal impacts, which are transferred by the bumper to longitudinal members.

In the side structure, the advanced high strength steel can be used for the B-pillar, A-pillar, and reinforcements to these pillars, rocker rails and cross-members. These parts are critical in preventing intrusion during side-impact collisions. In the rear, advanced high strength steel longitudinal rails should absorb the impact energy, in a manner similar to the front structure in the engine area [16].

During vehicle crash tests, strain rates can become quite high varying between $10s^{-1}$ and $30s^{-1}$ during frontal impact tests, to $60–200s^{-1}$ during side impact tests [16]. From a mechanical point of view, TRIP steels are composite materials and their behaviour can only be well understood if this composite behaviour is taken into account. On the fundamental level, the deformation of multiphase TRIP steel at high strain rates is the result of two interacting processes. The work hardening processes and temperature related softening effects, resulting from adiabatic heating [16]. The dynamic mechanical properties of low alloy TRIP-aided steels are related to dynamic behaviour of the three phases within the microstructure. In TRIP steels ferrite forms the soft matrix phase. The mechanical properties of ferrite have a high temperature and strain-rate dependence. Bainite is the strongest phase as a result of a very small lath size, a high dislocation density and a high carbon super saturation. The retained austenite is face centred cubic phase this results in a high strain hardening. In addition, the face centred cubic phase tends to have a much smaller temperature and strain-rate dependence of the mechanical properties [16]. As the retained austenite transforms to martensite, the temperature-dependence of the transformation rate will also play a role.

The dynamic testing of high strength automotive steel grades is therefore of great practical importance. During forming operations, steels are processed in a controlled dynamic manner. In collisions, the deformation is quite different as the steel is both in a pre-strained and in an aged condition [16]; the aged condition is a consequence of processes such as low-temperature paint baking treatment.

In laboratory tests, the split Hopkinson bar method or crash tests using hat or box-shaped beams are often used to reach high strain rates. Both dual phase and TRIP steels have been shown in these laboratory tests to possess high energy absorption at high strain rates [16]. Most studies on the evaluation of crash worthiness improvements have published comparisons between different conventional high strength steels and advanced high strength steels. In most of these studies, both dual phase and TRIP steels always yield the best energy absorption results [16].

There are different ways for determining the crash resistance performance of TRIP steel. For example the energy absorbed during the entire test can be plotted as a function of strain rate to evaluate the effectiveness of the TRIP steels in absorbing energy during dynamic tests. However there is currently no standardized method to measure the absorbed energy. Therefore it may be more appropriate to use the dynamic absorbed energy up to a strain of 10% to compare different steel grades, as the strains involved during a collision is usually much smaller than the fracture stress.

Automotive sheet thickness reductions of 10–15% and 20% can be achieved without loss in performance by the use of dual phase and TRIP steels, respectively [16]. Whereas their deep draw ability and stretch formability are excellent and comparable to those of low carbon steels [43], advanced high strength steel may still require some attention to specific manufacturing issues. In press forming, elastic recovery, springback (figure 2.7) and sidewall curling has been found to be a problem for high strength steels, and may result in the use of higher blank holder forces or the use of new die processes which emphasize stretching [16].

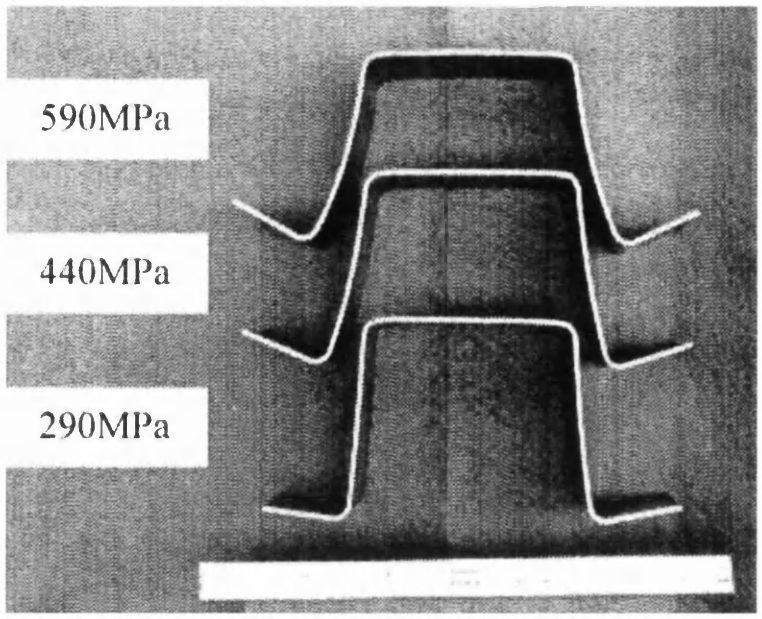

Figure 2.7: Spring back after U shaped forming [98]

Although not a critical point in most applications, the stretch-flangeability of TRIP steels is rather poor. The standard measure of stretch-flange-ability is the hole expansion ratio. For TRIP steels it is usually les than 50%. This is due to a combination of low strain rate sensitivity and the large difference in strength between the present phases [16].

The combination of large work hardening and strong bake hardening effects are additional reasons to use TRIP steel in automotive applications. This effect is very pronounced in TRIP steel, for which it routinely exceeds 100MPa. This pronounced bake-hardening effect is only observed after pre-straining [16].

2.5 TRIP Steels and their Associated Problems.

2.5.1 Welding

Welding is one of the reasons why TRIP steels are not widely used. Due to the higher carbon and alloying content of TRIP steel, welding was originally considered to require appropriate welding procedures. The composition of TRIP steels is such that adequate, yet relatively simple, welding procedures may be needed to avoid cold cracks. In the case of the resistance spot welding of TRIP steels, Cretteur et al. [99] have shown that excessive weld nugget hardness and cold cracks could easily be avoided by in situ short pre and post weld heat treatments for relatively high carbon TRIP sheet steel. This procedure can easily be carried out on conventional welding equipment. There have been no reports of critical difficulties encountered during the welding of TRIP steels; in fact even, the welding of TRIP sheet steel to non-TRIP sheet steel does not require any special precaution.

2.5.2 Galvanisability

The Si and Mn alloying elements form a very stable Mn_2SiO_4 oxide on the surface during the annealing process (figure 2.8) The surface tension properties of this oxide, when in contact with liquid zinc, inhibit the galvanisability and as a result the TRIP steels are currently generally electro-galvanised rather than hot dip galvanised [76].

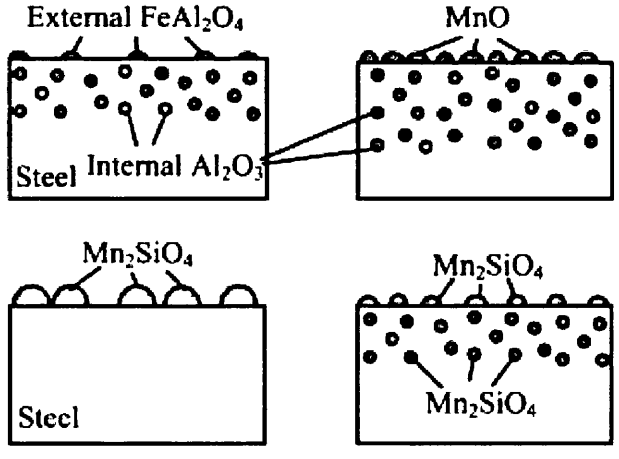

Figure 2.8: Schematic of oxide formation for TRIP steels [76]

Research efforts to improve the galvanisability of silicon containing steels focus mainly on annealing furnace atmosphere control and grinding or pre-plating before dipping in the liquid zinc [76]. Although these methods were used to prevent silicon from segregating to the surface, TRIP steels with a high amount of silicon cannot readily be galvanised by means of these methods. An alternative approach to obtain galvanized TRIP steels is the substitution of silicon by elements with similar properties.

According to De Meyer et al. [100] the partial replacement of silicon by aluminium in TRIP steel results in a much-improved galvanisability. Furthermore, the mechanical properties of cold rolled silicon free C Mn Al TRIP steel were comparable to those of conventional C Mn Si TRIP steels.

Silicon free C-Mn-Al TRIP steel shows improved wetting by the liquid zinc in comparison to a standard C-Mn-Si TRIP steel. This effect is even more noticeable after processing the steel in a low dewpoint -30^{o}C atmosphere. On the other hand, C-Mn-Si TRIP steel had a better wettability after processing the steel in a high dewpoint +10-50^{o}C atmosphere [76].

This improved wettability can be explained by the smaller amount of oxide on the surface before dipping in the liquid zinc as the aluminium is oxidised internally at the lower oxygen potential atmosphere [76]. Silicon forms a large amount of oxide on the surface of the steel when it is annealed in a low dewpoint atmosphere. Another beneficial effect when galvanising a C-Mn-Al TRIP steel is the formation of a subsurface Al depleted layer of about 5mm thickness. This is due to the selective internal oxidation of aluminium during hot rolling. The aluminium content of the C-Mn-Al TRIP steels should be high enough to form the aluminium depleted surface layer to improve the galvanisability as the aluminium content of the C-Mn-Al TRIP steel determines the thickness of this layer [76].

2.6 Summary

TRIP steels are potentially very good, being able to produce high strength parts whilst still maintaining high formability. However they do have some problems, which are keeping them from more widespread use. One of the main concerns is their coatability due to high silicon levels forming oxides upon the surface. Aluminium has been shown to perform a similar role to silicon in TRIP steels and can be used to reduce the silicon content. However removing silicon entirely in favour of aluminium has been shown to be detrimental to the properties. Some work has been done upon looking at a combination of silicon with aluminium but more work needs to be done to build upon a better understanding. With so many factors affecting the final properties of TRIP steel, with the steel chemistry and the way it is produced interacting to produce a complex microstructure. Although a high amount of retained austenite seems to be desirable the stability of the retained austenite is also a major factor and weather the stability of the austenite can be controlled sufficiently so that the degree of transformation to martensite can be predicted, perhaps keeping some untransformed to improve crash resistance.

3. AIMS OF STUDY

TRIP steels have a very good potential to be used in automotive applications if their shortcomings can be overcome. One of the largest problems is the coatability.

Aim one: To see if a increased aluminium alloying content is feasible, with the intention that reduced silicon levels can be used.

Aim two: Optimising the TRIP steel chemistry (adjusting elements such as manganese content) with the aim to produce a TRIP 800 i.e. Rp - 440-560, Rm >790, A > 20, n >0.14.

Aim three: investigating the effects of other austenising elements such as copper to be able to reduce silicon levels and enhance TRIP steel properties.

Aim four: Investigate processing route variables such as intercritical temperature and isothermal holding time to see how the aluminium additions affect this. The processing route will also be based on the current industrial capabilities available in South Wales with the aim of eventually producing viable commercial TRIP steel.

4. EXPERIMENTAL PROCEDURE

4.1 Material to Study

The cast chemistries (table 4.1) chosen were selected at a range of aluminium additions 0.33-1.57wt%, as the main focus of this work is to investigate aluminium for the same role that silicon plays in a traditional TRIP steel. Silicon levels were kept at 0.4wt%, which is a relatively low level (More than 1wt% silicon being typical for TRIP steels [76]). This means that the effects of Aluminium can be fully assessed. A range of manganese levels was also chosen 1.31-1.91wt%. Manganese can have a small effect on the amount of retained austenite but is mainly used for its strengthening properties. However too, much could detrimentally affect elongation and formability properties. A high carbon level of 0.2wt% was chosen as is typical for TRIP steels and is needed for the TRIP effect. A small amount of phosphorus was added, 0.08wt% as it has several beneficial roles in TRIP steels, such as its solid solution strengthening effects. Phosphorus also increases the amount of retained austenite in low silicon steels such as those that are being investigated in this work. A steel chemistry with an addition of 1wt% copper was also chosen as again copper can have benefits for TRIP steels. In Table 3.1, the chemistries in white (VS4296-VS4303) were provided by Corus strip products research and development team and so only limited material was available. The highlighted casts in grey (VS4378-VS4380) were experimentally cast for this work. All the steel was produced as strip and cold rolled to 1mm.

Table 4.1: List of the steel chemistries looked at in this work in wt%.

Steel No.	Characteristic	C±0.001	Si±0.01	Mn±0.01	P±0.001	Al±0.01	Cu±0.01
VS4296	Base	0.21	0.4	1.53	0.087	0.36	<0.01
VS4297	0.6%Al	0.21	0.41	1.54	0.09	0.64	<0.01
VS4298	1%Al	0.205	0.42	1.54	0.085	1.01	0.01
VS4299	1.3%Mn, 1.3%Al	0.205	0.42	1.35	0.087	1.28	0.02
VS4300	1.3%Al	0.2	0.43	1.55	0.09	1.29	0.01
VS4301	1.7%Mn, 1.3%Al	0.205	0.42	1.72	0.09	1.27	0.01
VS4302	1.9%Mn, 1.3Al	0.205	0.42	1.91	0.085	1.28	0.01
VS4303	1.6%Al	0.215	0.41	1.53	0.084	1.57	<0.01
VS4378	1.3%Mn, 0.8%Al	0.2	0.4	1.33	0.08	0.86	<0.01
VS4379	1.3%Mn	0.195	0.39	1.31	0.077	0.33	<0.01
VS4380	1.8%Mn, 0.8%Mn	0.205	0.4	1.82	0.079	0.32	<0.01
VS4381	1.3%Mn, 1%Cu	0.21	0.4	1.34	0.081	0.33	1

4.2 Annealing Simulations

4.2.1 Gleeble

Steels VS4296-VS4303 were selected in for Gleeble annealing trials, using a Gleeble 3500. Due to the small size of the samples used for the Gleeble it allowed for a large selection of annealing routes to be used on the limited amount of material available.

In the Gleeble the steel is heated up to the intercritical temperature, between Ae_1 and Ae_3 in figure 2.2, at which point there will be a microstructure consisting of ferrite and austenite. It is then held at this temperature. During the intercritical holding period there may be an increase in the amount of austenite as the heating rate is quite fast and there may not have been initial equilibrium. The sample will then be cooled down to the over-age temperature. At this point some of the austenite will have transformed to bainite and there should be a general increase in bainite during the over-age holding period (moving into the A+F+C region of figure 2.2). Upon cooling to room temperature some of the austenite will transform to martensite (moving through the M_s and M_f temperatures of figure 2.2). However, some will remain as retained austenite due to carbon enrichment during bainite growth.

For each of the first eight steels a twelve-cycle Gleeble programme was established. Table 4.2 shows the annealing cycles used for the Gleeble, which is also graphically represented in figure 4.1. The cycles used were focused on looking at variations in the over-age section of the annealing route, selecting three different over-age temperatures (250, 350, and 460°C), and holding for three different over-age times (100, 200 and 1000s), for each steel chemistry. They were all held at an intercritical temperature of 850°C for 100 seconds. Additionally three annealing cycles were used to look at taking the intercritical annealing temperature high enough to produce a fully austenitic microstructure, before being brought back down into the intercritical annealing temperature used in the previous cycles. These are shown in the

last three rows of table 2.2 where the second number in the first column is the amount of time in seconds that the steel was held for at 900°C before being brought back to 850°C for the remainder of the 100 seconds. The idea behind this is that normally before cooling down to the over-age temperature the microstructure would consist of austenite grains within a ferrite matrix. By taking it up to the fully austenitic range, before bringing it back down to the intercritical temperature, it is hoped that an austenite matrix with ferrite grains will be formed, and the effects of this on the final microstructure and properties can be assessed. There is only a small amount of variation of temperature across the samples ~1°C due to their small size and accuracy of the Gleeble.

Table 4.2: The annealing cycles used with the Gleeble for each of the eight RD&T materials.

Intercritical Temperature for 100s (°C)	Over-age Temperature (°C)	Over-age Time (°C)
850	460	100
850	460	200
850	460	1000
850	350	100
850	350	200
850	350	1000
850	250	100
850	250	200
850	250	1000
900, 5s	460	200
900, 15s	460	200
900, 30s	460	200

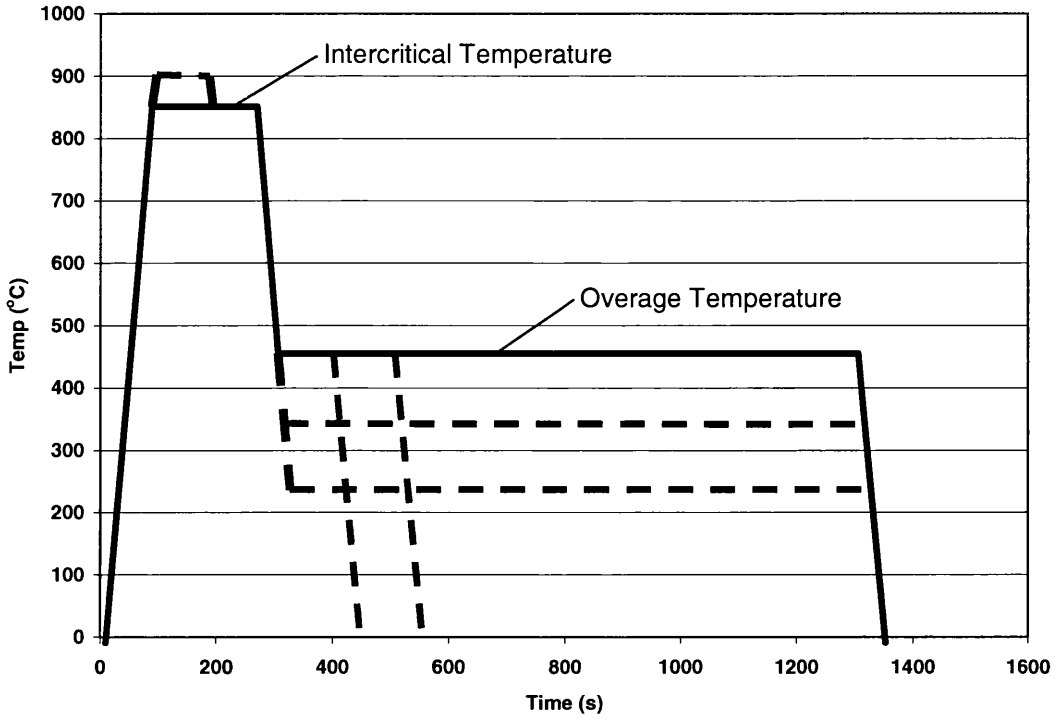

Figure 4.1: Gleeble annealing cycles

4.2.2 Continuous Annealing Simulator (CASIM)

The CASIM was used to simulate a range of heat treatments similar to that as described in the work on the Gleeble. A range of over-ageing times and temperatures were used based on the Corus ZODIAC annealing route of an intercritical temperature of 850°C and an over-age temperature of 460°C for 370seconds (table 4.3). Other variables were also looked at such as heating rates. As there was much more material available for the casts VS4378-VS4381, the CASIM was chosen over the Gleeble to simulate the annealing routes, as the larger samples used allowed for a wider range of mechanical testing to be performed. There was, however, enough material left of casts VS4296-VS4303 to allow a run on the CASIM to simulate a typical ZODIAC cycle and provide additional tensile data to complement the data taken from the Gleeble testing.

Table 4.3: The annealing cycles used on the CASIM

Intercritical Temperature (^{O}C)	Over-age Temperature (^{O}C)	Over-age Time (^{O}C)
CASTS VS4378-VS4381		
850	250	370
850	350	370
850	460	370
850	460	200
850	460	100
850	460	50
Casts VS4296-VS4303		
850	460	370

The CASIM (figure 4.2) is used to simulate different heat treatments upon steel samples through the use of resistance heating. Samples are cut to 400 by 100mm from the cold rolled plate, and then thoroughly cleaned of all grease and dirt so that it is not burnt off at the high temperatures used. The sample is then placed between two copper clamps making sure that it is kept level to ensure even heating. Five thermocouples are welded to the surface in a diamond pattern (figure 4.3) to record the temperature across the sample so that any variation in temperature can be observed. A control thermocouple is placed in the centre of the sample and is used by the machine to adjust the heating temperature.

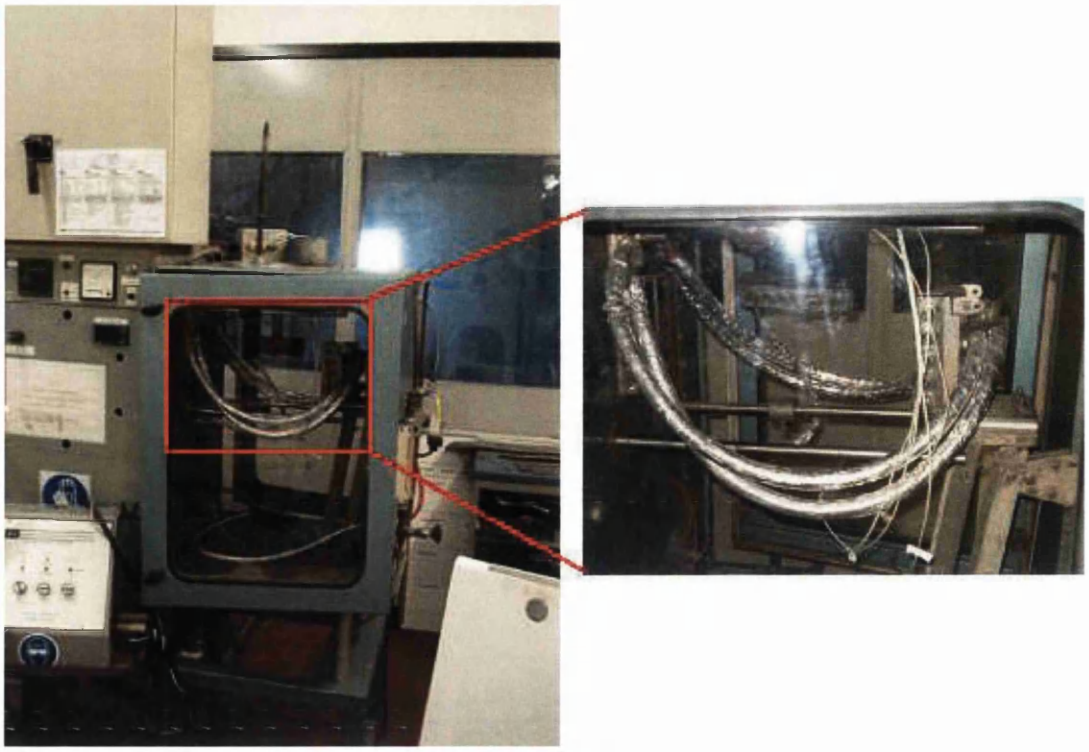

Figure 4.2: The continuous annealing simulator

The user is able to create an annealing regime by inputting target temperatures and times into a computer program that is then uploaded to the machine. The sample is encased in a metal chamber with a Perspex viewing window and a cut off switch on the door for safety purposes. Once set up the current is switched on and the annealing program is started. The sample is heated and kept at temperature by passing a high current through the sample and is cooled through air jets directed at the steel surface. The amount of current that can be passed through the material is restricted as well as a safety cut off if the clamps get too hot. This prevents damage to the CASIM as well as ensuring the sample is not melted.

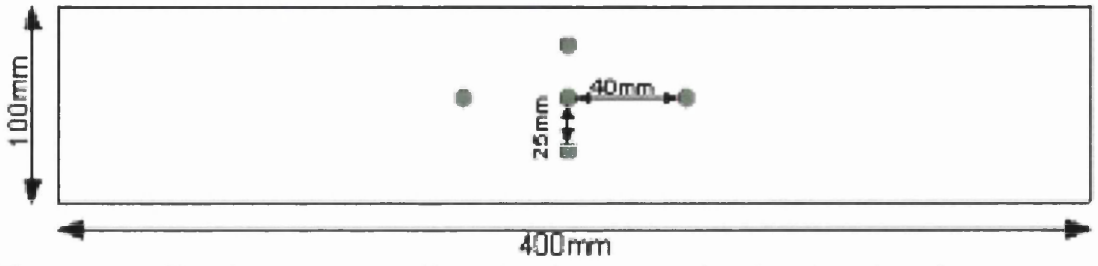

Figure 4.3: Continuous annealing simulator sample showing the placement of the thermocouples.

While the annealing cycle is being run, a computer program is used to monitor the temperatures across the sample using the attached thermocouples. The sample is only removed once it has cooled to room temperature and the current turned off. Only the material towards the centre of the sample is useable, as the extreme edges of the sample will not have fully achieved the target temperatures.

4.3 Metallurgical Analysis

4.3.1 Sample Mounting

Samples are cut using a pair of hand shears (figure 4.4) to a size roughly of 20mm by 5mm. The samples are then mounted using the hot mounting Predopress. Samples are held in place using plastic multi clips, with up to five samples being mounted together where markers are used to identify individual samples. Polyvinylec Formvar powder is poured over the samples to act as the mounting medium. A piece of paper with details of the samples is also included to be mounted into the bottom of the sample. The forming cycle is set for forty minutes including cooling time. Once mounting is complete, the sample is removed and the sharp edges are ground off for safety.

Figure 4.4: Hand shears used to cut microscopy samples.

Using a hot resin to mount the samples was used for the first few test samples during the learning period. Once the bulk of the testing began this was switched to cold mounting. This was due to a concern that the temperatures involved in the hot mounting method (~200^{O}C) had the potential to affect the microstructure, as these steels are quite sensitive to the annealing route. In addition, it was more time efficient to prepare many samples and let the mounting medium cure overnight rather than individually mounting each sample in the Predopress.

For cold mounting the sample, preparation is essentially the same except that a two-part mixture of fifteen parts Epofix resin to two parts Epofix hardener is used as the mounting medium which is left for around eight hours to set, usually overnight.

The samples are then prepared by grinding using the Rotopol grinding machine. The grinding is manually done through four stages of 120, 320 coarse grinding and 500, 1000 fine grit grinding. The samples are thoroughly cleansed between each stage to prevent any cross contamination. The purpose of grinding the samples is initially to remove the surface deformation layer from the hand shears, and then to remove scratches left from each subsequent grinding stage.

The samples are then polished using automatic polishing machines with Struers Blue lubricant and diamond suspension being applied manually. The polishing is done in two stages being polished for approximately ten minutes, using six micron diamond suspension, followed by approximately ten minutes using one micron diamond suspension. Again, the samples are thoroughly cleansed between each stage. Lubrication is applied to make sure sticking of the wheel and samples does not occur. However, over lubrication can result in the diamond polishing sliding off the wheel.

4.3.2 Etching

Several etchants have been used to assess the microstructures. The general procedure is to use a freshly polished surface to increase the effectiveness of the etching. The samples are immersed in the etchant where the amount of time for immersion is dependent upon the etchant being used. The samples are then carefully rinsed with water followed by a rinse of alcohol and then dried under a hand drier making sure no streaks are left behind. Extra care is taken when using a tint etchant during rinsing to make sure that the deposited layer is not disturbed.

When using an attack etchant it should be used soon after polishing. This is because the specimen will develop a passive layer if left for more than a couple of hours. The specimen should be completely immersed face up in the etchant. The etchant can be either prepared just before etching or taken from premixed stock solution. A slight colouration should be seen on the surface as the reaction takes place, and slight agitation should be used to let fresh etchant reach the exposed specimen surface. Generally an etching time of 15 to 30 seconds is used to make sure a clear definition of the phases is present. A shorter etching time should be used initially, as a repeat etch can be done if under-etched. This is easier than re-polishing an over etched specimen. After etching, the specimen should be washed in running water to flush away the remaining etchant.

A freshly mixed solution is needed for tint etching and so they cannot be stored for future use. In addition, a freshly polished surface is needed so that there is no passive layer present. The surface of the specimen needs to be carefully observed while etching, as the proper colour is needed from the tint etchant. Knowing what the proper colour is for each etchant comes with experience. The specimen surface should not be agitated as this can disturb the fragile deposited film, for the same reason the surface should not be swabbed. If the specimen is under-etched, it will have to be re-polished and etched again. Successive etching will not work, as a clean surface is needed for the reaction to take place. After etching, it should be immersed in a beaker of water and rinsed with a minimal amount of alcohol.

Colour etching in general gives a very good colour contrast. However, a difficulty of their use is that it is not always clear which phase appears in a certain colour and what is the cause of these coloration differences. The appearance of the etching can vary depending on many different factors. First, there are the properties of the steel such as chemical composition, dislocation density, texture and phases present. This can vary from steel to steel and in some cases locally on the steel surface. The etching conditions will also influence the colorations such as etching time, temperature, and

freshness of the solution. Due to this, using tint etchants can give varying results even when used on the same sample of steel.

If the etchant has a short etching response time, it may result in a loss of reproducibility as well as an increased chance of over etching. Therefore, for accurate and reliable image analysis as well as a high degree of reproducibility a slow etching response is desirable.

Table 4.4 shows the etchants used to reveal the micro phases present within the multiphase steel. Each of the etchants differed in the elements of the microstructure that they picked out as well as there overall effectiveness and reproducibility. In fact, the ability of the tint etchants to produce a reproducible image in terms of individual phase colouration over a range of steel chemistries and conditions was a major factor in etchant choice.

Table 4.4: Standard etchants used to look at the multiphase steel microstructures.

Etchant	Chemical Composition	Etching Time	Properties
Nital 2%	2 ml HNO_3 98 ml ethanol	5 seconds	Reveals ferrite grain boundaries
Picral 4%	4 g Picric acid 100 ml ethanol	40 seconds	Doesn't reveal grain boundaries, used for ferrite and carbide structures
Le Pera	**Part A:** 1% aqueous sodium Metabisulphite **Part B:** 4% Picral Mix equal parts of A and B	50s Pre etch with 2% Nital for 5 seconds	Ferrite: Brown Martensite: White Austenite: White Cementite: Black Bainite: Black Pearlite: Black
Klemm	**Part A:** 100 ml saturated aqueous sodium thiosulfate **Part B:** 2g potassium Metabisulphite Mix part A and B together Stock solution: 300ml distilled water	60-90 seconds	Ferrite: blue to Brown Austenite: White Martensite: Brown
Sodium - Metabisulphite	8 to 20g sodium Metabisulphite Dilute in 100 ml water	40 Seconds – one minute	Ferrite: off white Bainite: dark Martensite: dark Austenite: White

4.3.2.1 Le Pera

Le Pera is supposed to show a predominantly light brown ferrite phase. However, as can be seen in the samples etched with Le Pera (figure 4.5) they seem to show a much darker brown for the ferrite phase, there is also a blue tint coming through. Tint etchants are very dependent on environmental conditions and the steel chemistry; any variance in these can affect the

shades of colour and the etching time needed to produce a good image. When using Le Pera (figure 4.5) it was found to be too inconsistent to get comparable images between steel samples.

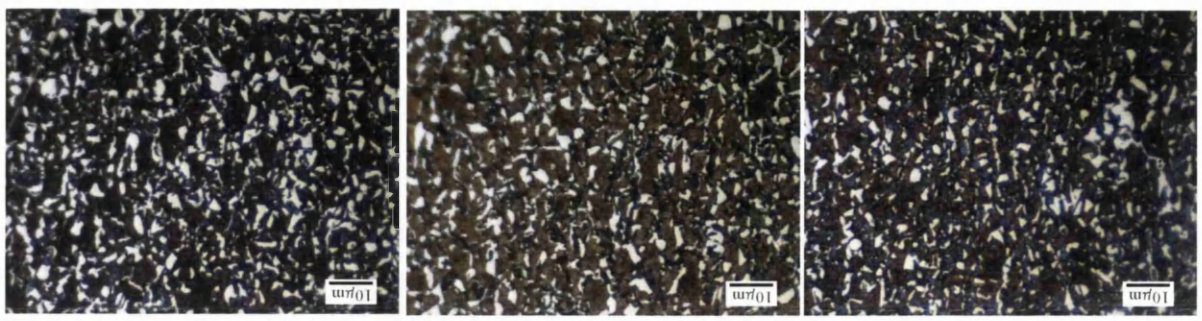

Figure 4.5: Images of TRIP steel etched with Le Pera. Ferrite: brown. Martensite and austenite: white. Cementite, bainite and pearlite: black.

4.3.2.2 Klemm

Again with the Klemm tint etchant (figure 4.6) as with Le Pera there can be seen a variation between the shades of colour resulting in the same difficulties. Klemm did prove to be a better etchant in terms of consistency however as can be seen in the left most image blurring can occur with the tint on the ferrite phase if slightly over etched. Although most of the phases present can be clearly defined there did seem to be a lot more of the white austenite phase in some of the images than expected and when compared to XRD results.

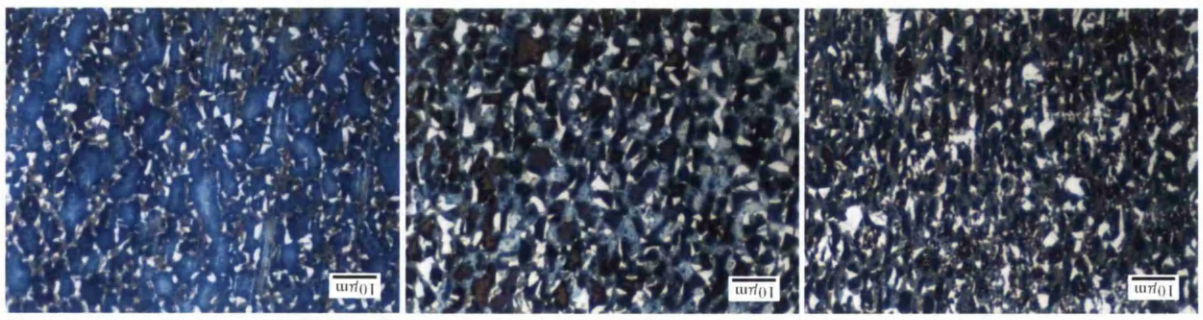

Figure 4.6: Images of TRIP steel etched with Klemm. Ferrite: blue to brown. Austenite: white. Martensite: brown.

4.3.2.3 Picral and Sodium Metabisulphite

This is a two stage etch (figure 4.7). First etching with Picral acid, for one minute followed by a five second etch with sodium metabisulphite. This was one of the most promising tint etchants. Although there is still some variance in colour shades, it was not quite as pronounced as the previous etchants. It also clearly defined the separate phases. In addition, with careful timing so as not to under or over etch it was possible to differentiate between the austenite and martensite phases.

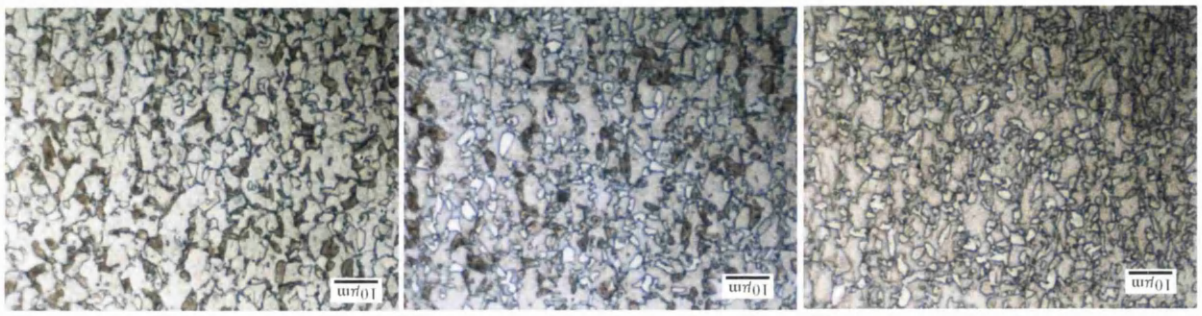

Figure 4.7: Images of TRIP steel etched with Picral and Sodium Metabisulphite. Ferrite: off white. Bainite: dark. Martensite: dark. Austenite: white

4.3.2.4 Metabisulphite

This was another Metabisulphite etchant (figure 4.8), which proved to give very consistent colouring when compared to the other etchants looked at. However it did not give quite the same degree of separation between phases as the previous metabisulphite etchant.

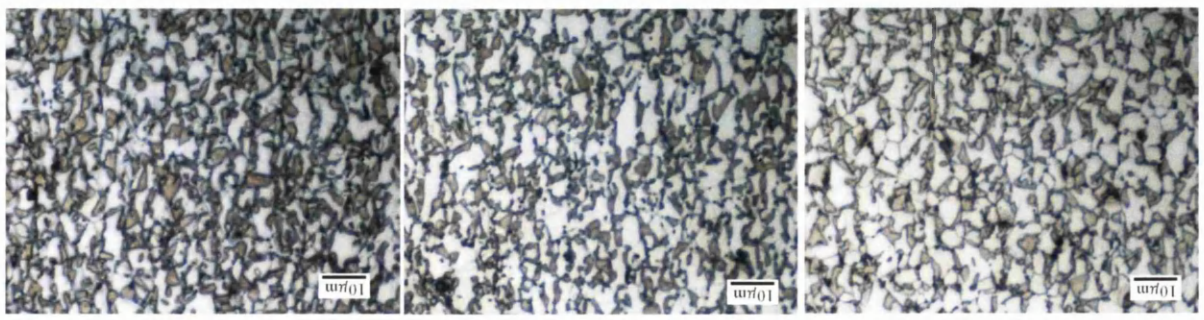

Figure 4.8: Images of TRIP steel etched with Metabisulphite. Ferrite and austenite: off white. Bainite: dark. Martensite: dark.

4.4 Microscopy

The microstructures were observed using a Reichert Polyvar 2 light optical microscope (figure 4.9), which enabled magnifications up to 2000 times to be used which was needed to see the fine microstructures produced. A digital camera was used to capture images of the microstructure. These images were then used for micro structural analysis. Samples were taken horizontal to the rolling direction. Images were taken both before and after tensile testing to get a good indication of the austenite to martensite transformation that occurs during strain for TRIP steels. Therefore, samples were taken as close to the break point from tensile pieces to ensure that micro structural analysis was taken in the area of maximum strain and therefore maximum transformation.

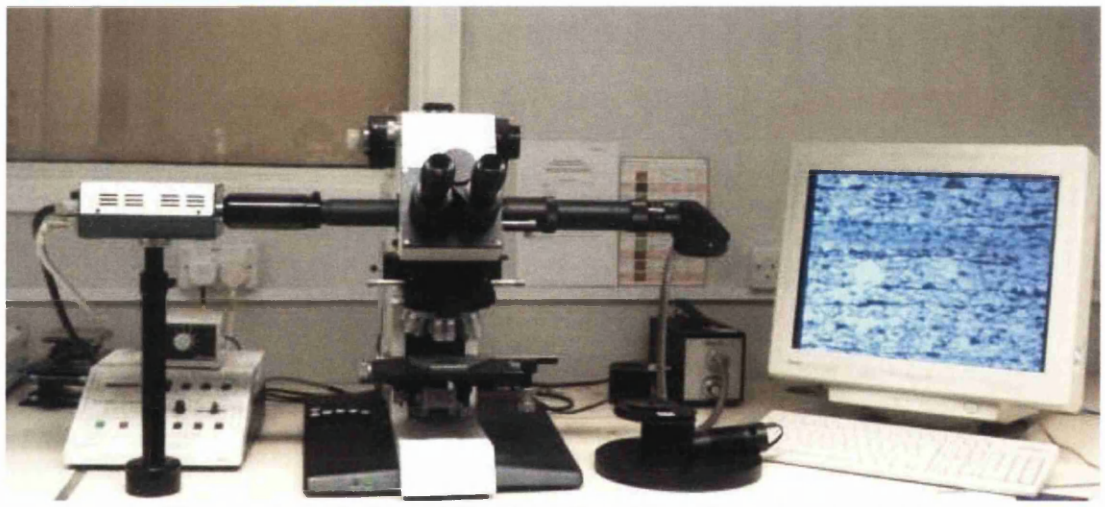

Figure 4.9: Reichert Polyvar 2 light optical microscope.

4.4.1 Volume Fraction

4.4.1.1 Point Counting Method

The point counting method described in ASTM standard E 562[101] was used to calculate the volume fraction of phases present. This is a good method for estimating the volume fraction of phases in a microstructure and is relatively easy to perform. The point counting was performed using a two dimensional grid with one hundred points to give the best accuracy. Using a higher point

count of two hundred and four hundred points was tested but similar results and accuracy were found. To find the volume fractions of each phase, the phase that lies under each grid point is recorded and then final percentage calculated. Measurements were performed by taking the average of ten micrographs per steel specimen. This helped take into account any variation in microstructure across the specimen as well as any differences in colouring and effectiveness of the tint etchant.

By revealing the microstructure it helps to interpret what is happening during the processing of the TRIP steel and how making changes in the processing route changes the microstructure and ultimately how this affects the properties observed. By doing this it will help to increase the understanding of the TRIP steels and what variables to change to optimise the properties.

4.4.1.2 X-ray Diffraction

One well established technique to measure austenite in steels is X-ray diffraction (XRD). When irradiated by x-rays, crystalline substances produce characteristic diffraction patterns. Quantitative determination of the relative volume fraction of austenite can then be made from such x-ray diffraction patterns, because the x-ray intensity diffracted from each phase is proportional to the volume fraction of that phase[102].

The maximum diameter of the area to be analysed is 23mm and can be no thicker than 3mm. The surface to be analysed must be flat. Samples must be cut down to as close to this sample size as possible. Alternatively, a number of smaller samples from the same origin can be grouped together to provide sufficient sample area for analysis. Two 25×25mm square specimens were cut from the each of the as received sheets using hand shears. The sample surface is prepared by electro polishing. The analysis was performed in Corus Swinden Technology Centre using a Philips PW1830 generator with PW1710 diffractometer controller operating at 50kV and 40mA using Mo radiation. The multiline (8 lines in total) method was used and is the method that forms

ASTM E 975-95[103] standards for determination of austenite content. A relative error to within ± 10% or an absolute error to within ± 1% which ever is the greater, is associated with all quoted results. The retained austenite results were extracted using Corus in-house produced software that was based on the methods described in ASTM E 975-95[103] and Jatczak et al.[102]. The software scans for the following peaks: 111γ/110α, 200γ, 200α, 220γ, 211α, 311γ, 420γ, 321α and 411α as seen in figure 4.10.

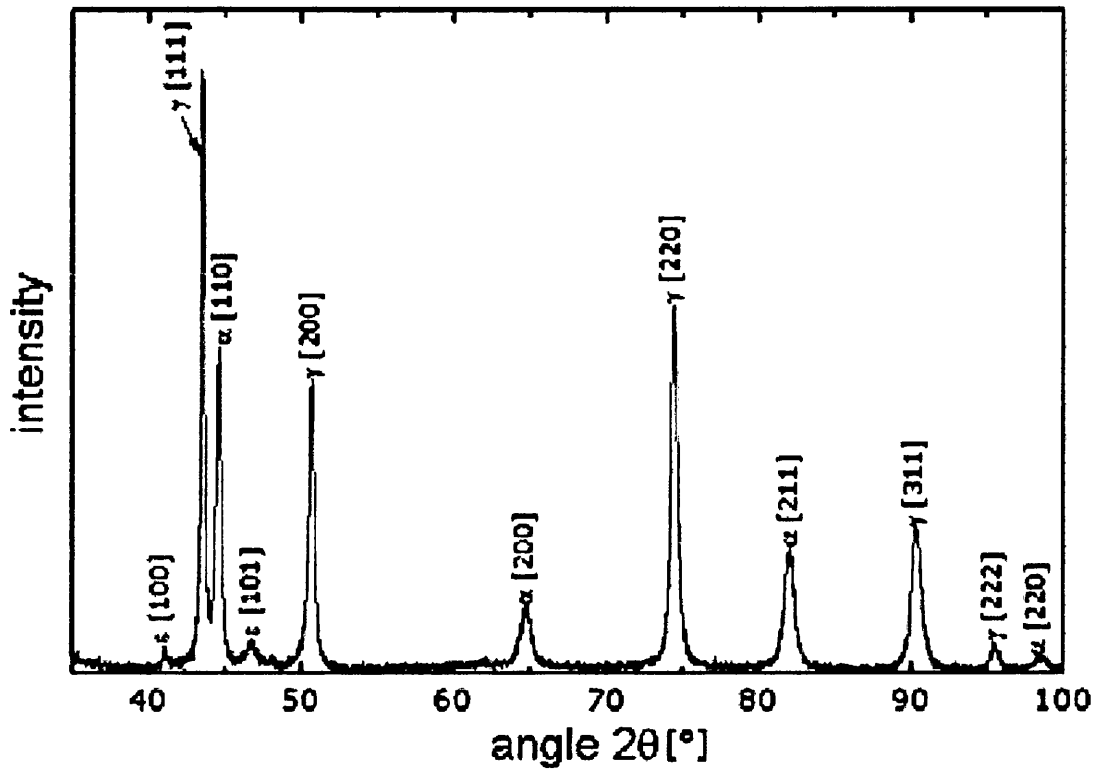

Figure 4.10: Typical X-ray diffraction pattern.

4.5 Mechanical Testing

4.5.1 Tensile Testing

Tensile tests were performed on 50mm tensile coupons under static loading conditions using a Zwick 1474 tensile testing machine incorporating a 100kN load cell (figure 4.11). Testing was performed in accordance with BS EN 10002-1:2001[104]. There was enough material to produce two tensile specimens from each of the CASIM samples produced, one from the top and one from the bottom. This would give a better account of the properties of the steel sample being tested, as there could be variation of heating rates and temperatures across the sample. The average of the properties taken from the tensile tests could be used. Samples were taken in the longitudinal direction.

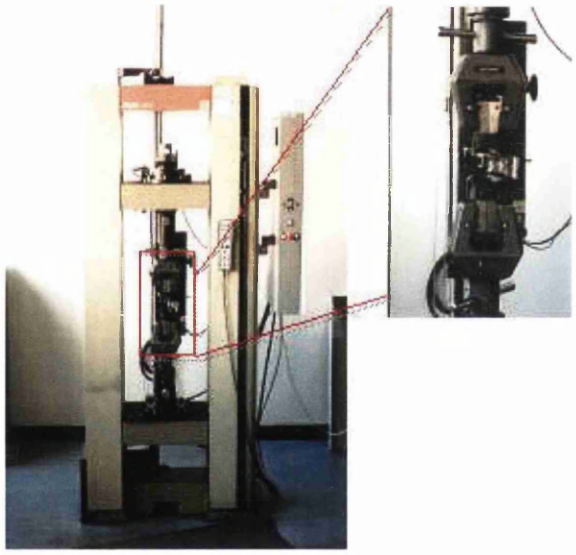

Figure 4.11: Zwick 1474 tensile testing machine

The samples were machined to specification. They were then pickled to remove any scale form the samples. The gauge and width of each sample was measured by taking three readings across the sample and taking the average.

The software package used to operate the tensile testing machine automatically measured all readings and produced an engineering stress strain graph.

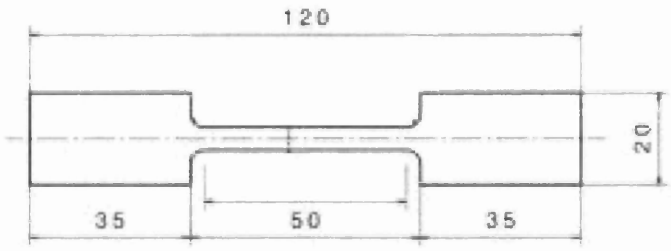

Figure 4:12: Typical tensile sample.

From the tensile data the strain-hardening exponent (n-value) can be obtained. The n-value can be found in the relationship $\sigma = KE^n$, where σ is the true stress; E is the true strain n is the n-value. The n-value is equal to the slope of the true stress/true strain curve up to maximum load, when plotted on log-log coordinates. The n-value relates to the ability of a sheet material to be stretched. The higher the n-value, the better the formability/stretch-ability.

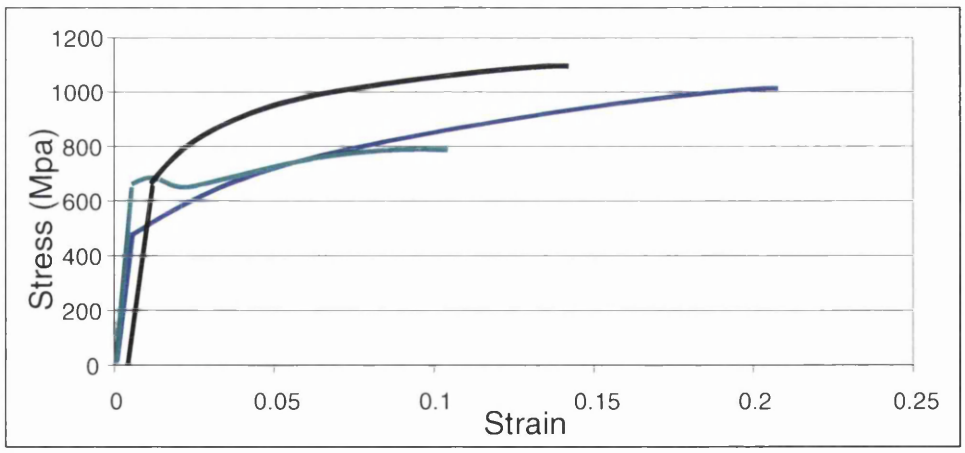

Figure 4.13: Typical stress strain curves.

The proof stress is measured by drawing a line parallel to the elastic portion of the stress/strain curve at a specified strain, this strain being a percentage of the original gauge length. In this work the proof stress is calculated at a stress of 0.2%.

4.5.2 Vickers Hardness Testing

Hardness measurements are taken using the Leco Micro Hardness Tester Model: M-400-G2 (figure 4.14). The sample is placed upon the stage making sure that the surface is parallel. Bringing the samples surface into focus under the 25x low power lens brings the stage to the right height. The load duration timer is set to 15 seconds and the desired weight in grams is set. The turret is then rotated to bring the indenter into position and the test started.

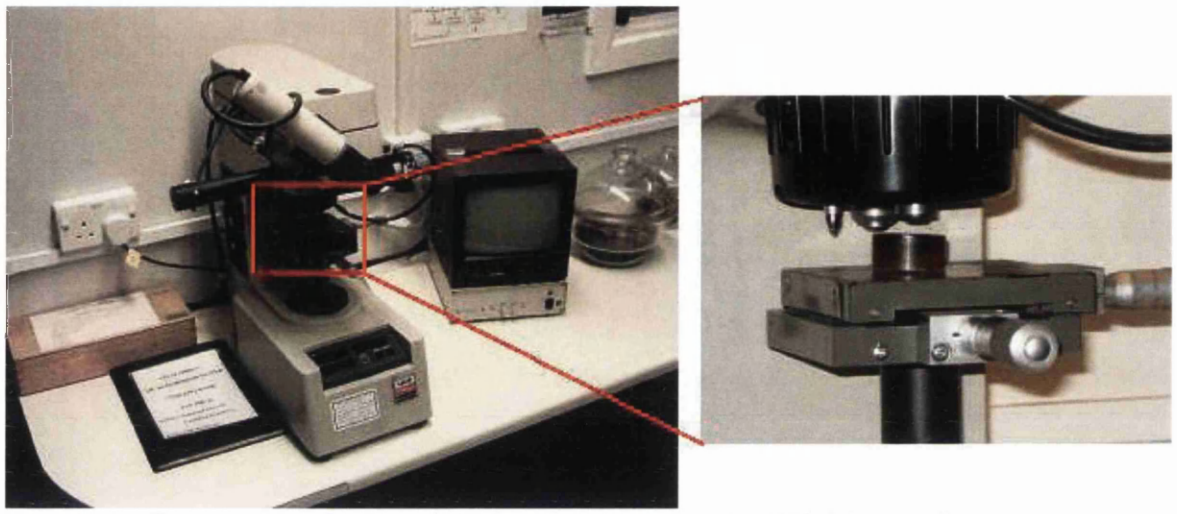

Figure 4.14: Leco micro hardness tester model: M-400-G2

The turret is then rotated again to bring the measuring fifty five times objective lens into place. The indentation is brought into focus so that the corners are most clearly defined. The left hand measuring bar is then brought in so that the inside edge of the bar is just touching the left corner of the indent. The right hand measuring bar is then brought in so that the inside edge of the bar is just touching the right corner of the indent. The reading of the diagonal measurement is then taken. The measuring ocular is then turned through ninety degrees and the above process is repeated for the top and bottom corners of the indent. Figure 4.15 shows the indenter and the indent that is measured in the material. The Vickers hardness value can be calculated by $Hv = 1.854F/d^2$ where F is the is the force applied on the indenter and d is the average length of the diagonal left by the indenter

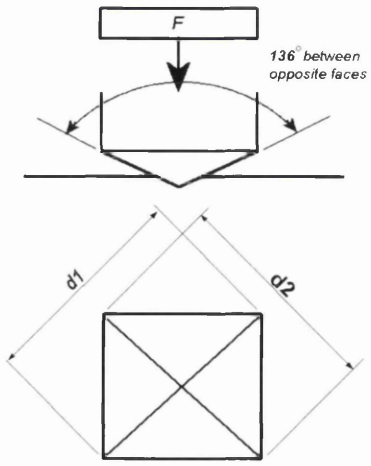

Figure 4.15: Indenter and resulting indent of the Vickers hardness tester.

Verification procedures are carried out every six months though it has been found that the equipment maintains good levels of error (~5%) and repeatability without adjustment. Individual users also verify the accuracy of the equipment with each use; using standard micro hardness test blocks traceable to the original ASTM standards.

Hardness results are taken as the average hardness of the microstructure by taking several measurements across the sample. Attempts were made to take hardness measurements of the individual phases within the microstructure. The lowest load that could be used to produce the indent was 10 grams and this was not a low enough load to make sure that the indent is contained within one phase (figure 4.16)

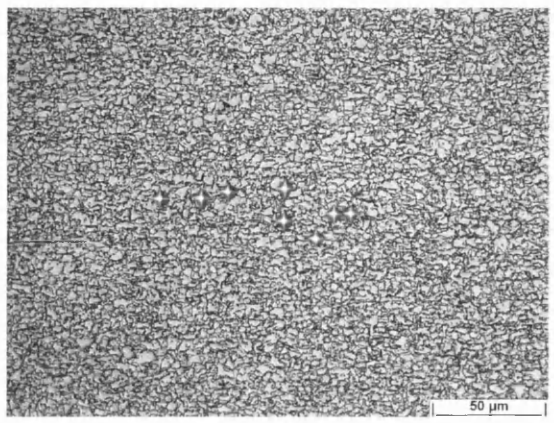

Figure 4.16: Microscopic image showing the size of the indents compared to the grain size of a typically obtained microstructure.

5. RESULTS

5.1 Gleeble Work on Steels VS4269-VS4303

Figures 5.1 and 5.2 show Vickers hardness values for increasing alloying content whilst being held at 460°C during the over-age section for different times. Figure 5.1 shows this for increasing manganese alloying content of 1.35, 1.55, 1.72 and 1.91wt%. It can be seen that there is a general increase in hardness with increasing manganese content. When held for 100 seconds in the over-age section it increases from 242Hv at 1.35wt%Mn to 304Hv at 1.91wt%Mn, giving a total increase of 52Hv. When held for 200 seconds it increases from 262Hv at 1.35wt%Mn to 331Hv at 1.91wt%Mn, Giving a total increase of 69Hv. When held for 1000 seconds it increases from 260Hv at 1.35wt%Mn to 321 at 1.91wt%Mn, giving a total increase of 61Hv.

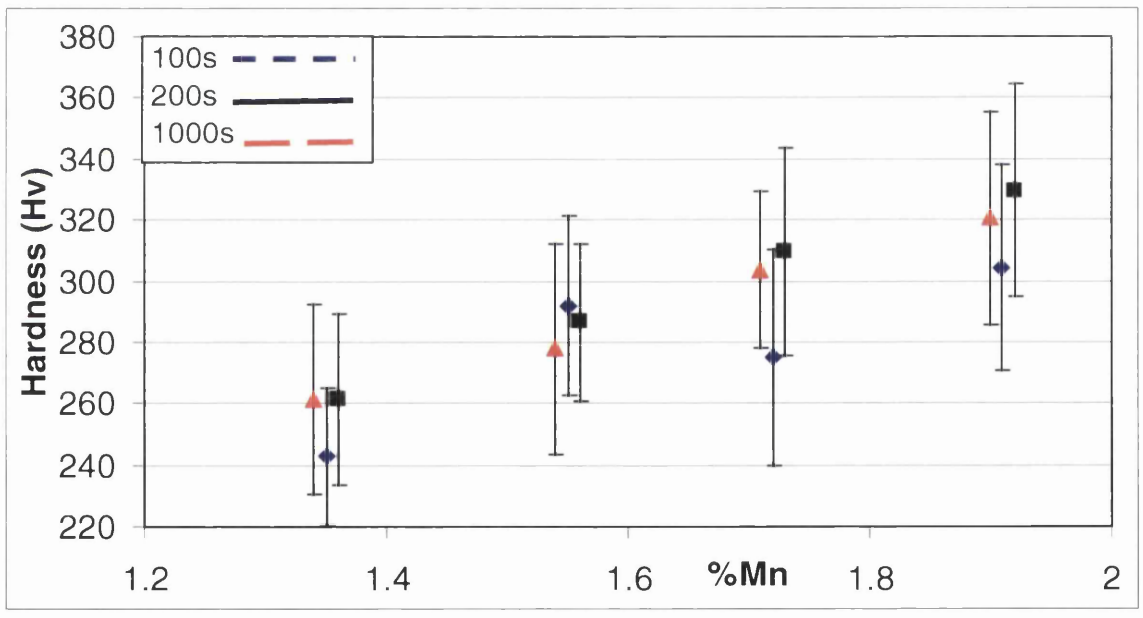

Figure 5.1: Hardness with increasing Mn alloying additions.

Figure 5.2 shows Vickers hardness values for increasing amount of aluminium alloying content at 0.36, 0.64, 1.01 and 1.57wt%. Hardness values for three different over-age times of 100, 200 and 1000 seconds are shown. For 100 seconds there is an increase from 300Hv at 0.36wt%Al to 341Hv at 1.57wt%Al, giving a total increase of 41Hv. For a holding time of 200 seconds, there is an increase in hardness from 314Hv at 0.36wt%Al to 363Hv at 1.57wt%Al, giving a total increase of 49Hv. For a holding time of 1000 seconds there is an increase from 286Hv at 0.36wt%Al to 313Hv at 1.57wt%Al, giving a total increase of 27Hv.

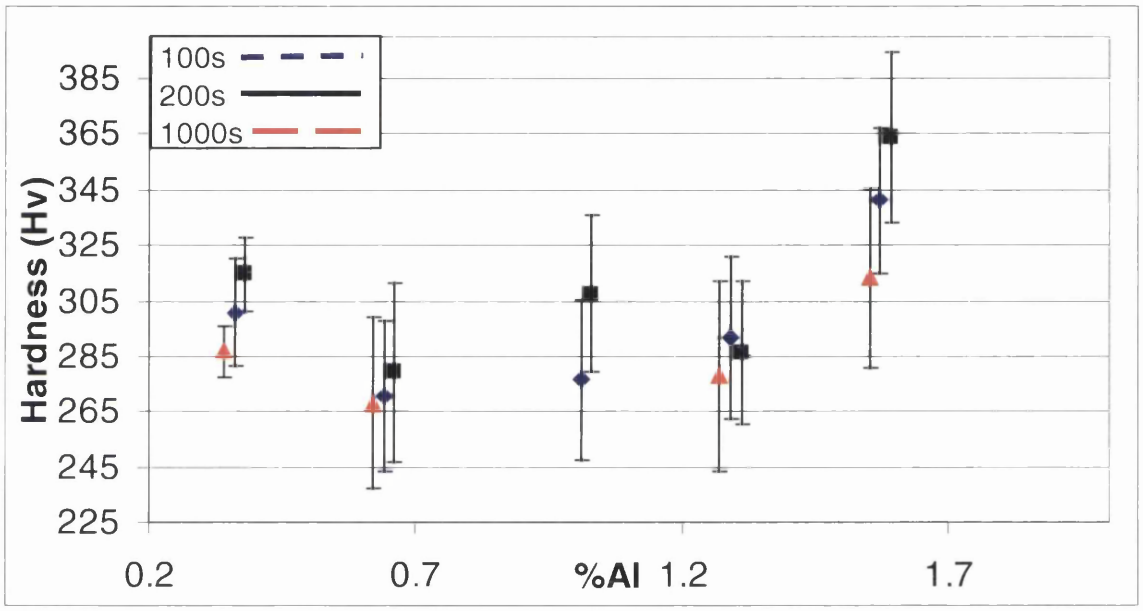

Figure 5.2: Hardness with increasing Al alloying additions.

Figure 5.3: shows the volume fraction of retained austenite within the final microstructure after an annealing route based on the ZODIAC cycle (850°C intercritical temperature, isothermal hold of 460°C for 200 seconds) at different levels of manganese alloying additions. Manual measurements are shown based on point counting for manganese additions of 1.35, 1.55, 1.72, 1.91wt%. X-ray diffraction measurements are also shown for manganese additions of 1.35, 1.72, 1.91wt%. In total, there is an increase in retained austenite of 3.9% from 18.6% at 1.35wt%Mn to 22.5% at 1.91wt%. This gives an average of a 7% increase in retained austenite per 1wt%Mn increase. The increase is not linear with an initial increase of 0.9% from 1.35 to 1.55wt%Mn

followed by a larger increase of 1.8% from 1.55 to 1.72wt%Mn and then a smaller increase of 1.2% from 1.72 to 1.91wt%.

For the X-ray diffraction results, there is a total increase of 3.9% from 1.35 to 1.91wt%Mn the same as was measured for the manual point counting method. Again, this increase is not linear with an increase of 1.4% from 1.35 to 1.72wt%Mn and an increase of 2.5 from 1.72 to 1.91wt%Mn. The manual point counting measurements show an increase of 8-9% over the X-ray diffraction results.

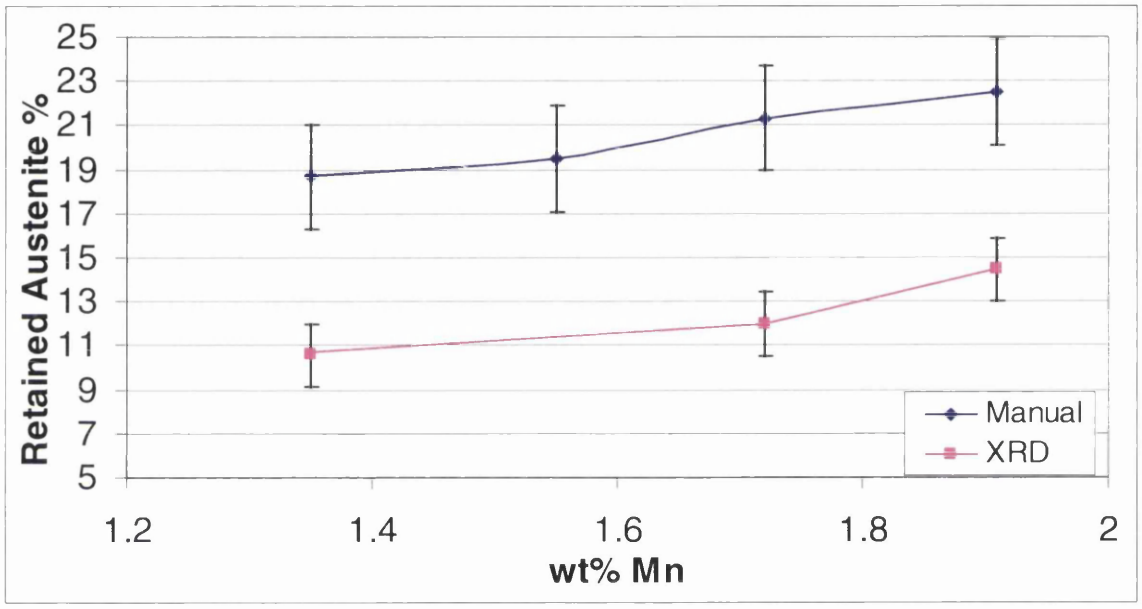

Figure 5.3: Volume fraction of retained austenite for increasing manganese alloying additions.

Figure 5.4 shows the volume fraction of retained austenite within the final microstructure after an annealing route based on the ZODIAC cycle (850°C intercritical temperature, isothermal hold of 460°C for 200 seconds) at different levels of aluminium alloying additions. Measurements were taken using manual point counting method. Overall, there is an increase of retained austenite of 3.3% from 18.2% at 0.36wt%Al to 21.5% at 21.5wt%Al. This gives an average of a 2.7% increase in retained austenite per 1wt%Al increase. Again, this is not linear; there is a small increase of 0.3% retained austenite from 0.36 to 0.64wt%Al. A larger increase of 2% up to 1.01wt%Al. This is followed by a drop of 1% up to 1.29wt%Al and finally an increase of 2% up to 1.57wt%Al.

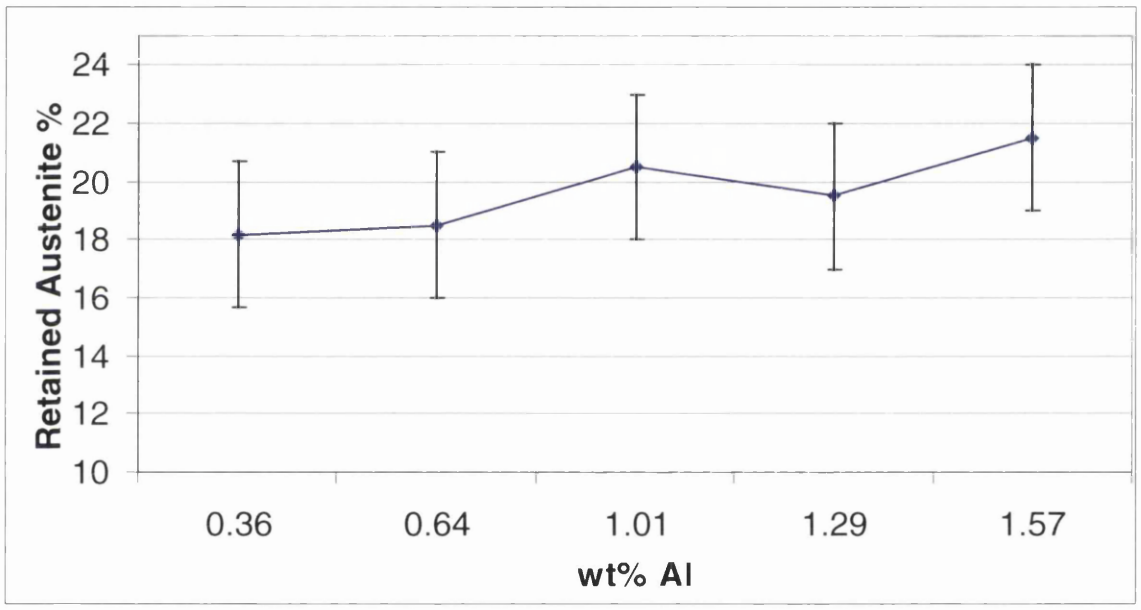

Figure 5.4: Volume fraction of retained austenite for increasing aluminium-alloying additions.

Figure 5.5 shows the general trend of the Vickers hardness values with different over-ageing times of 100, 200 and 1000 seconds. The individual points are made up of all the Gleeble tests on each of the materials at different over-ageing temperatures for each of the over-age times. This shows the overall effect that over-age time has on hardness for these TRIP steels in general. At an over-age time of 100 seconds, the average hardness is 328Hv. This increases by 13Hv at 200 seconds to 341Hv. As the over-age time is increased to 1000 seconds, the hardness decreases by 24Hv to 317Hv.

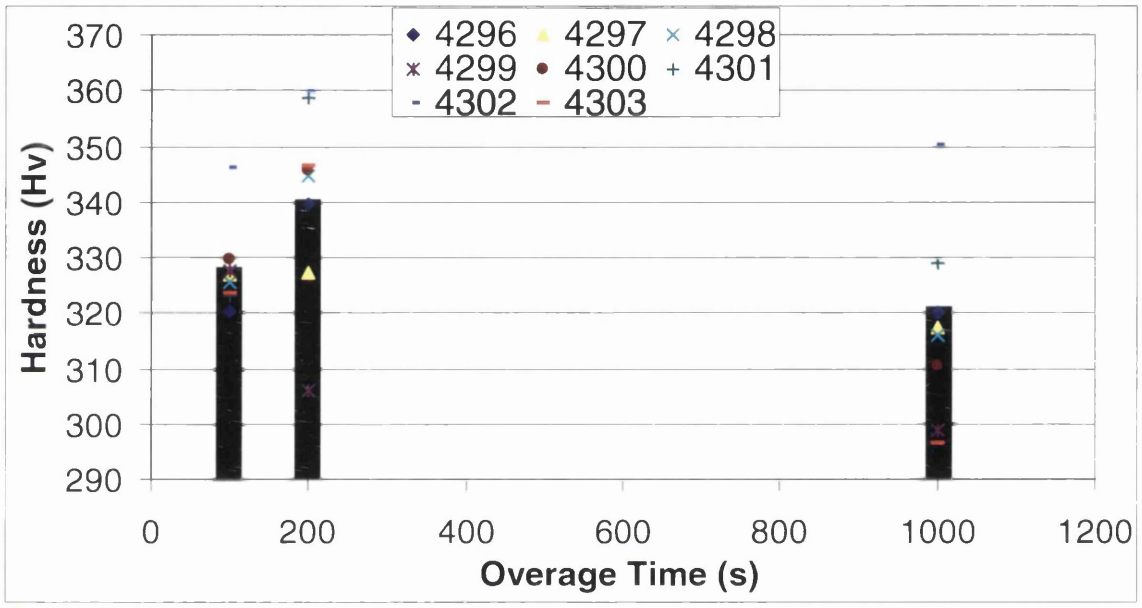

Figure 5.5: General trend for Vickers hardness values with differing over-age times at a temperature of 460°C.

Figure 5.6 shows the general trend of the Vickers hardness values with different over-ageing temperatures of 250, 350 and 460°C seconds. Again the individual points are made up of all the Gleeble tests on each of the materials and at different over-ageing times for each of the over-age temperatures to give the general overview of how hardness changes with over-age temperature. The three bars show the average hardness at those times. At an over-age temperature of 250°C, the average hardness is 326Hv. This decreases by 4 to 322Hv at 350°C. At 460°C, the hardness has increased by 17 to 339Hv.

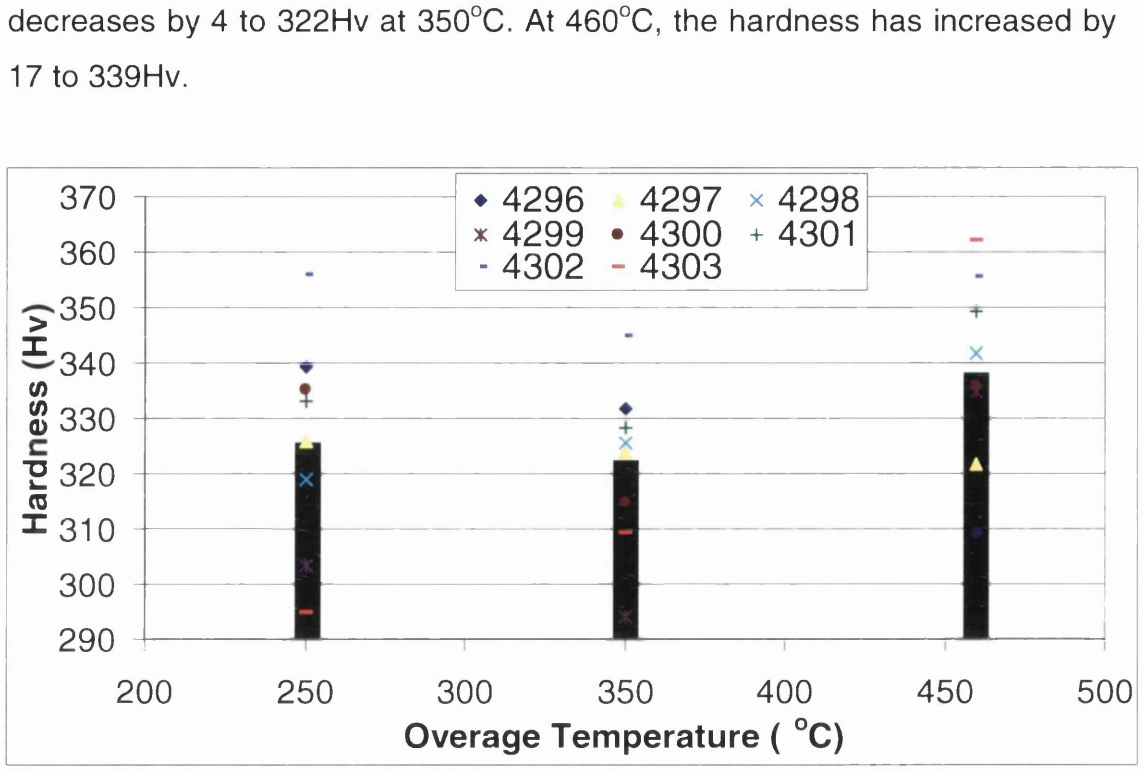

Figure 5.6: General trend for Vickers hardness values with differing over-age temperatures.

Figure 5.7 shows the volume fraction of both retained austenite and bainite, measured by point counting, with increasing over-age time. In these graphs the square points are retained austenite and the diamond points are bainite. Again as above the individual points are made up of all the Gleeble tests on each of the materials and at different over-ageing temperatures for each of the over-age times to give the general overview of how the volume fraction changes with over-age time. For the retained austenite (RA), it starts at 19% at an over-age time of 100 seconds and rises by 2% to 21% by 200 seconds where it then falls by 6 to 15 at an over-age time of 1000 seconds. The volume fraction of bainite starts at 8% at 100 seconds, increases by 2% to reach 10% at 200 seconds. Finally, it continues to rise by another 4% to reach 14% at 1000 seconds.

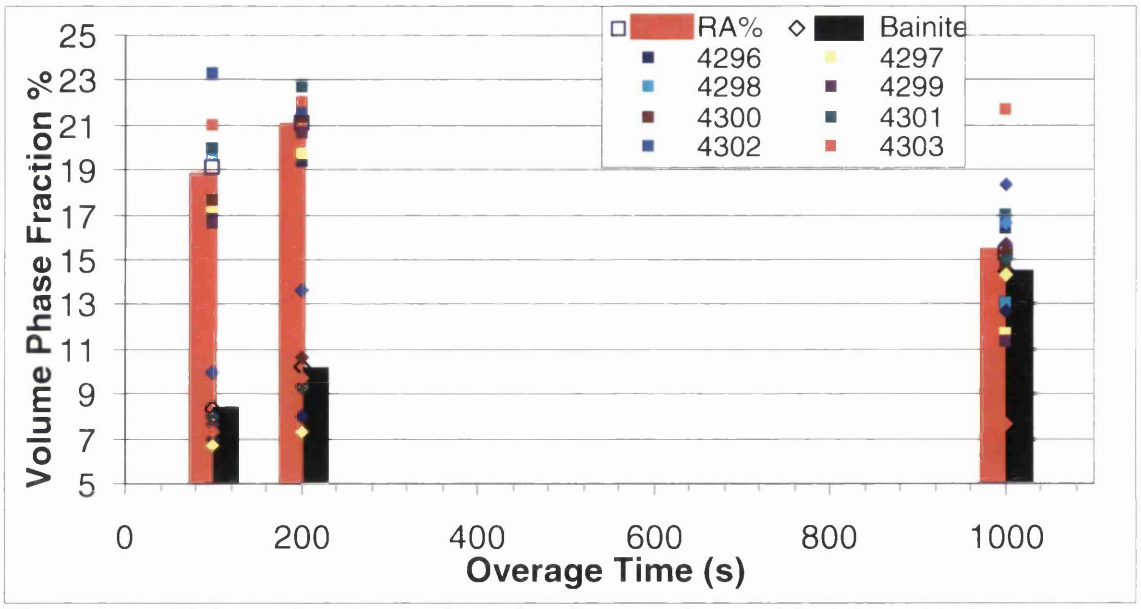

Figure 5.7: Volume fractions of retained austenite and bainite with increasing over-age time.

Figure 5.8 shows the volume fraction of both retained austenite and bainite, measured by point counting, with increasing over-age temperature. Again as above the individual points are made up of all the Gleeble tests on each of the materials and at different over-ageing times for each of the over-age temperatures to give the general overview of how the volume fraction changes with over-age temperature. The retained austenite starts of at 19% at an over-age temperature of 250°C, and remains at 19% at an over-age temperature of 350°C. The volume fraction of retained austenite then slowly drops off by 2% to 17% at an over-age temperature of 460°C. For the volume fraction of bainite, it starts at 9% at 250°C and rises by 2% to 11% at 350°C. Finally, it keeps on rising by another 1% to reach 12% at 460°C.

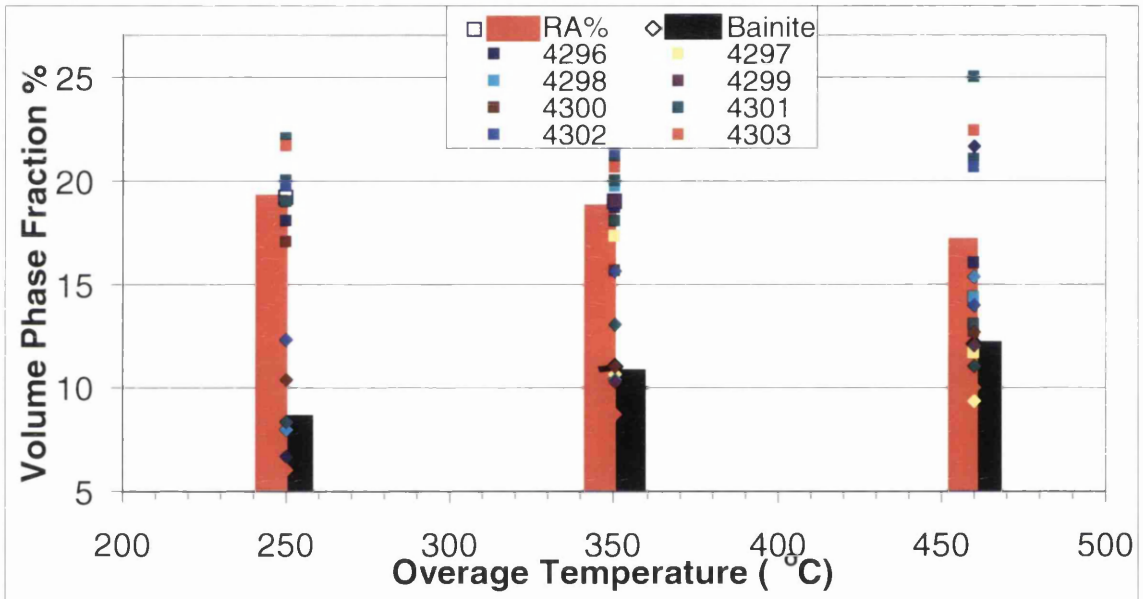

Figure 5.8: Volume fractions of retained austenite and bainite with increasing over-age temperature.

5.2 CASIM Work on Steels VS4269-VS4303

Figure 5.9 shows how the tensile strength changes with increasing alloying content of aluminium and manganese. In both cases, an increase in alloying content gives an increase in strength. For aluminium, it starts of at 675MPa at 0.36wt%Al. There is an increase in strength of 16.5MPa between 0.36 and 0.64wt%Al, which is a 59MPa increase per 1wt%Al. This rate increases to 84MPa per 1wt%Al up to 1.01wt%Al, which is a rise of 31MPa. Finally, it increases by another 35MPa up to 1.57wt%Al which is a rate of 63MPa per 1wt%Al giving a final tensile strength of 757MPa. In total, there is an increase of 83MPa, which is a rate of 68MPa per 1wt%Al.

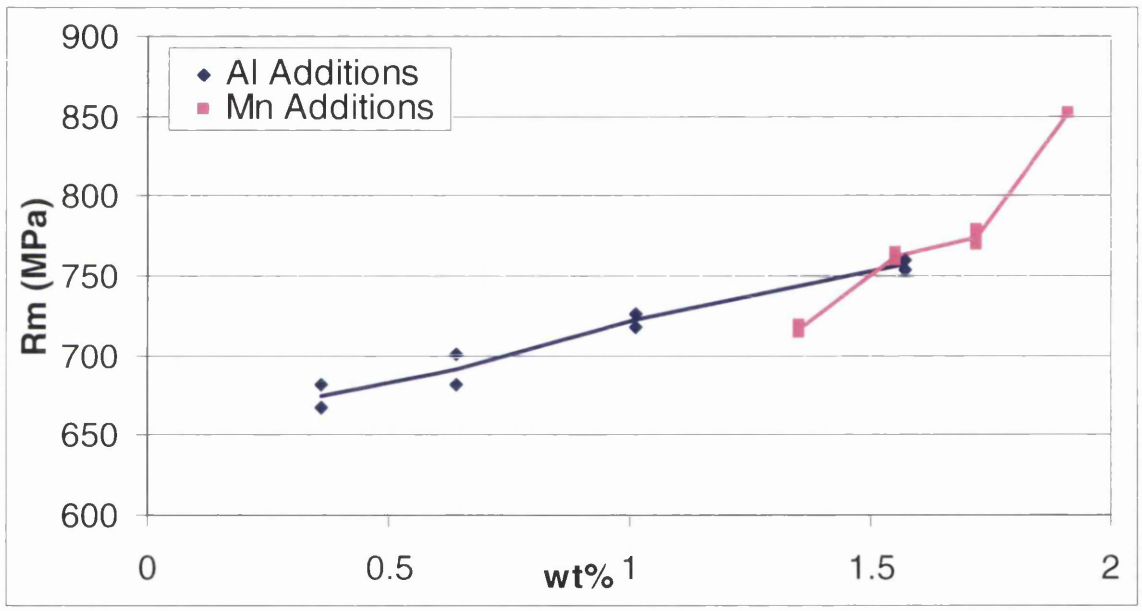

Figure 5.9: Tensile strength with increasing alloying content.

For manganese, the tensile strength for the lowest alloying content of 1.35wt% is 242MPa. The tensile strength increases by 46MPa to 762MPa when the alloying content is increased to 1.55wt%Mn. This is a rate of 228MPa per 1wt%Mn. The rate of increase then levels of to 68MPa per 1wt%Mn so that for an alloying addition of 1.72wt%Mn there is an increase of 11.5MPa giving a tensile strength of 774MPa. The rate of strength increase then rapidly rises again to 413MPa per 1Wt%Mn so that for the alloying

addition of 1.91wt%Mn it raised by 79MPa giving a final tensile strength of 852MPa, which overall is an increase rate of 242MPa per 1wt%Mn.

Figure 5.10 shows the proof stress with increasing alloying content. It can be seen that in general the proof stress increases with increasing aluminium alloying content. However, with increasing manganese alloying content the proof stress decreases. Looking at the increasing aluminium content, with an aluminium content of 0.36wt%Al the proof stress is 440MPa. This increases to 463MPa when the aluminium content increases to 0.64wt%Al. As the aluminium content is increased further to 1.01wt%Al the proof stress decreases down to 448MPa. Finally when the aluminium content is increased to 1.57wt%Al the proof stress reaches 472MPa.

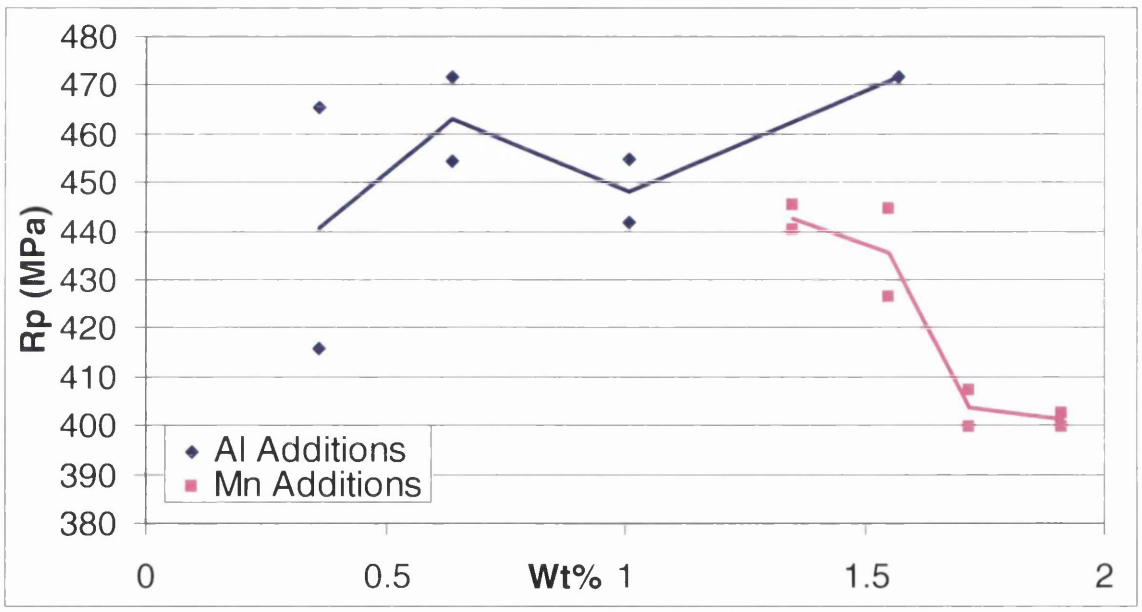

Figure 5.10: Rp with increasing alloying content

For manganese additions whilst the manganese alloying content is at 1.35wt%Mn the proof stress is 443MPa. When the manganese is increased to 1.55Wt%Mn the proof stress drops to 436MPa. As the manganese is increased again, to 1.72wt%Mn the proof stress drops much more rapidly down to 403MPa. The rate at which the proof stress drops with increasing manganese alloying content levels off after this dropping to 401MPa at an manganese alloying content of 1.91wt%Mn.

Overall, the proof stress increases by 31MPa when the aluminium alloying content is increased from 0.36 to 1.57wt%Al, which is a rate of 26MPa per 1wt%Al. For manganese, there is a total decrease of 42MPa from 1.35 to 1.91wt%Mn, which is a rate of 74MPa per 1wt%Mn.

Figure 5.11 shows how the amount of elongation changes with increasing alloying content of both aluminium and manganese. This graph uses the same tensile data as figure 5.9 and 5.10. For aluminium, the total elongation is 14.3% at 0.36wt%Al. This increases by 9.1% so that it is 23.4% at aluminium content of 0.64wt% this is a rate of 32.5% per 1wt%Al. This slows up to a rate of 11.7% per 1wt%Al so that at 1.01Wt%Al there is a total elongation of 27.7%, which is a rise of 4.3. The elongation then decreases by 1.9% to 25.8% at 1.57wt%Al which is a rate of 3.4% per 1wt%Al. overall there is an increase of 11.5%.

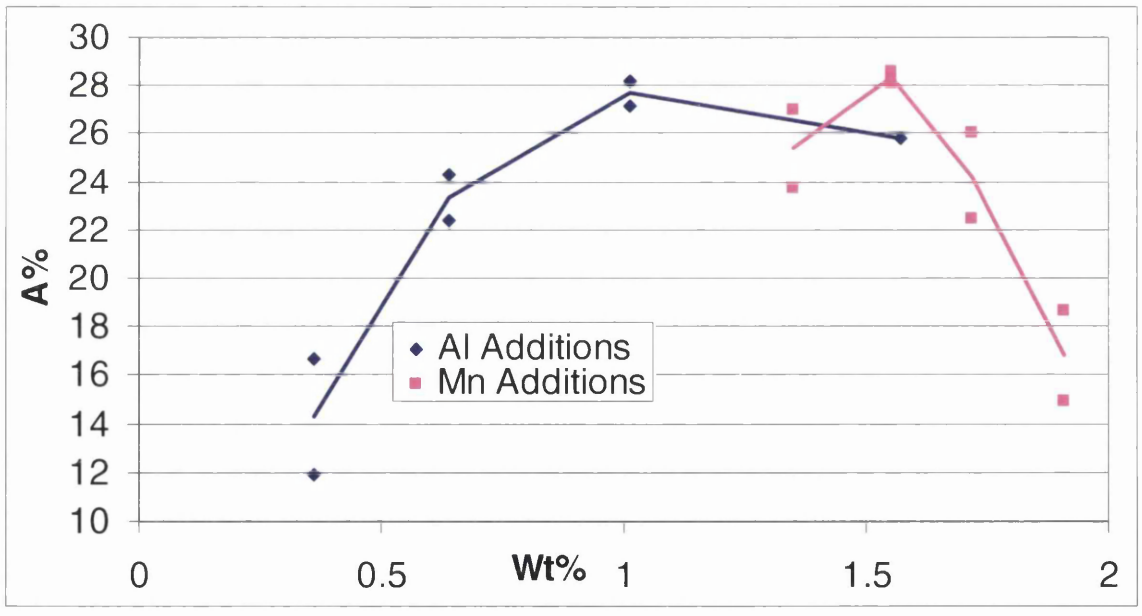

Figure 5.11: Elongation with increasing alloying content.

For manganese alloying additions, it begins at a total elongation of 25.4% at 1.35wt%Mn. This initially increases by 3 to 28.3% at 1.55wt%Mn, which is a rate of 14.8 per 1wt%Al. However after this the elongation decreases with increasing manganese alloying content. Increasing the manganese content to

1.72wt% results in a elongation drop of 4.1% giving a total elongation of 24.2% which is a decrease rate of 24.2% per 1wt%Mn. Finally by increasing the manganese content to 1.91wt% the elongation drops by 7.4% to a total elongation of 16.8% which is a faster drop of 39% per 1wt%Mn.

Figure 5.12 show the n-value with increasing alloying content. Again, these values are taken from the same samples as in figures 9, 10 and 11. For increasing aluminium alloying content there is an n-value of 0.229 at a aluminium content of 0.36wt%Al. This increases to 0.266 at an alloying content of 0.64wt%Al and continues at the same rate to 0.312 at an alloying content of 1.01wt%Al. It peaks at this point however and decreases down to an n-value of 0.238 at an allying content of 0.238wt%Al. Overall from an allying content of 0.36 to 1.01wt%Al the n-value increases by 0.083 which is a rate of 0.128 per 1wt%Al. It then decreases by 0.074 from 1.01 to 1.57wt%Al, which is a rate of 0.132 per 1wt%Al.

For increasing manganese alloying additions, there is an n-value of 0.316 at 1.35wt%Mn. This increases to and peeks at 0.364 at 1.55wt%Mn. The n-value then decreases with further manganese alloying additions down to 0.312 at 1.72wt%Mn. The manganese finally drops down to 0.236 at 1.91wt%Mn. So overall there is an increase of 0.048 between 1.35 and 1.55wt%Mn, which is a rate of 0.24 per 1wt%Mn. It then decreases by 1.278 from 1.55 to 1.91wt%Al, which is a rate of 0.354 per 1wt%Mn.

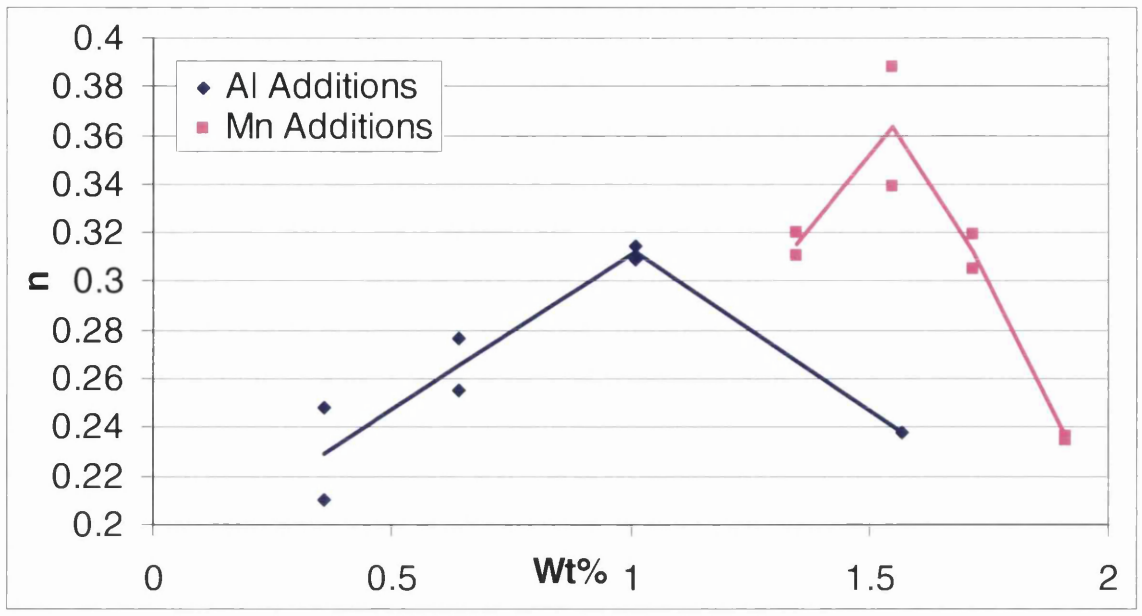

Figure 5.12: n-value with increasing alloying content. Measurements taken from two samples over-aged at 460^{O}C for 370s for each alloying content.

From figure 5.13 it can be seen that by increasing the amount of aluminium manganese alloying content both result in increasing amounts of retained austenite in the final microstructure. For aluminium there is an initial gradual increase raising by approximately 2% from 0.36wt%Al to 1.01wt%Al. it then increases more rapidly reaching 25% retained austenite at 1.57wt%Al. this gives a total increase of 10% which is a rate of 8.3% retained austenite per 1wt%Al. After tensile testing, there is a general reduction for austenite present in the microstructure. It shows a similar trend as before tensile testing with increasing aluminium alloying content. Starting at 12% retained austenite at 0.36wt%Al alloying content there is a small drop off to 11% retained austenite at 0.64wt%Al. It then increases to 11.5% retained austenite at 1.01wt%Al and a further increase to 17% at 1.57wt%Al. Looking at the amount of retained austenite in the microstructure, before and after tensile testing, with increasing aluminium alloying content, there is an average decrease of 29.6% retained austenite after tensile testing.

Overall, manganese increases the amount of retained austenite in the microstructure by 2% from 22 to 24% when the manganese is increased from 1.35wt% to 1.91wt%, which is an increase of 3.6% retained austenite per

1wt%Mn. After tensile testing, there is again a general reduction for austenite present in the microstructure. Starting at 11% retained austenite at 1.35wt%Mn alloying content there is an increase to 16% retained austenite at 1.55wt%Mn. It then increases further to 18% retained austenite at 1.72wt%Mn where it remains at 18% to 1.91wt%Mn. Looking at the amount of retained austenite in the microstructure, before and after tensile testing, with increasing manganese alloying content, there is an average decrease of 30.9% retained austenite after tensile testing.

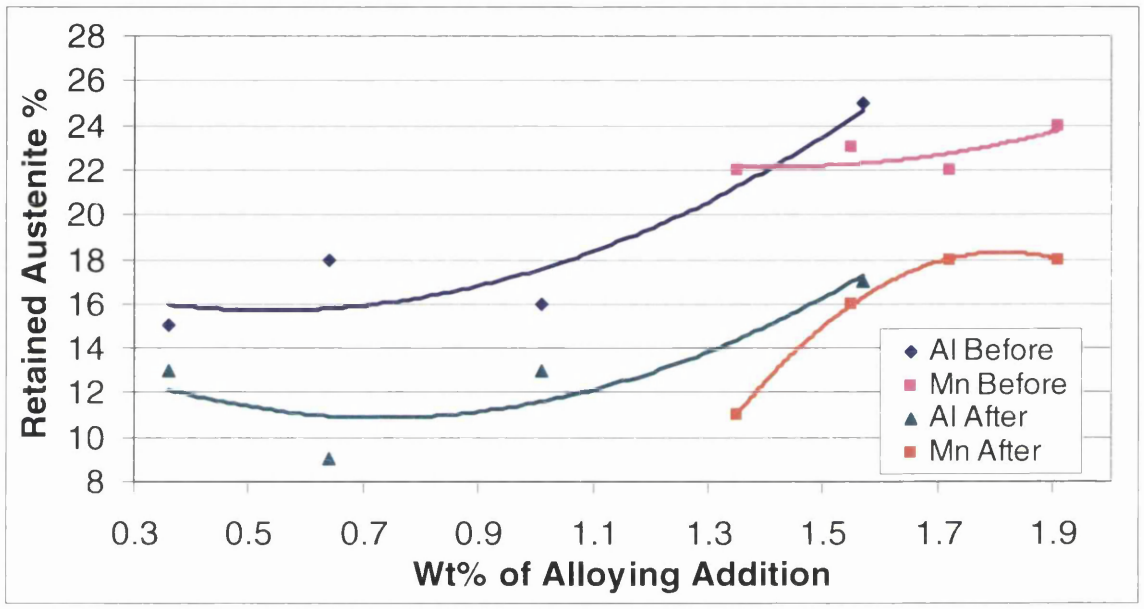

Figure 5.13: The amount of retained austenite in the final microstructure and after tensile testing with increasing alloying content of aluminium and manganese.

Figure 5.14 shows the fraction of retained austenite from the final microstructure after undergoing deformation from tensile testing. This graph was calculated form figure 5.13 to give a better graphical representation of the amount of retained austenite that transforms during straining and therefore shows how stable the retained austenite is. It can be seen that as aluminium additions increase form 0.36wt% to 1.57wt% the amount of retained austenite remaining after deformation drops from 76% down to 66% at 1.01wt%Al levelling out at 70% at 1.57wt%Al. For increasing manganese alloying content there is a large increase in the amount of retained austenite remaining after

deformation form 49% at 1.35wt%Mn peaking around 80% at 1.72wt%Mn and then dropping again slightly to 76% at 1.91wt%Mn.

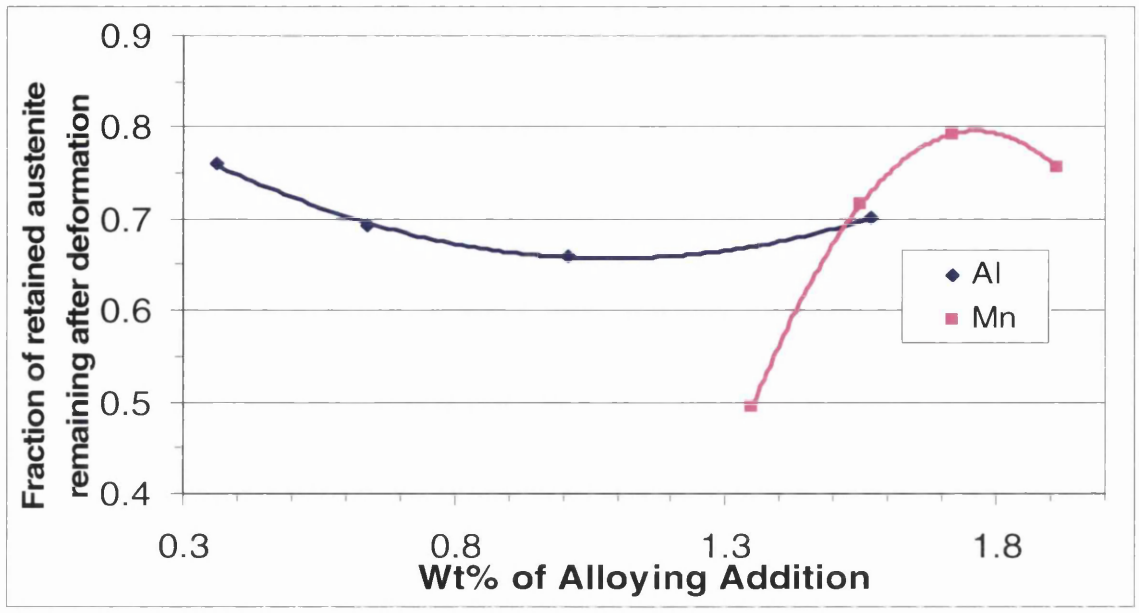

Figure 5.14: The fraction of retained austenite left in the microstructure after deformation (tensile testing).

5.3 CASIM Work on Experimental Casts

Figure 5.15 shows the range of stress strain curves that was seen for the experimental steels. The more formable steels with increased aluminium alloying additions can be seen to the left with lower ultimate tensile strengths. Where the higher strength higher manganese steels can be seen to the right with much lower strain values.

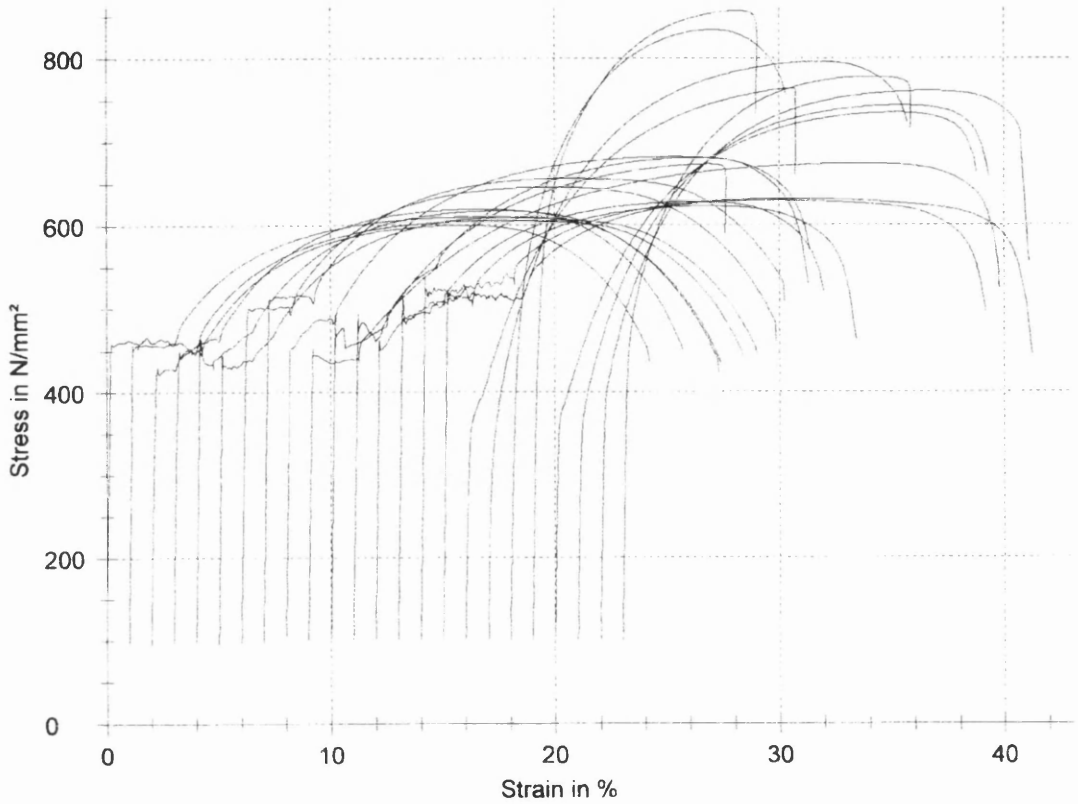

Figure 5.15: Typical stress-strain curves for the experimental casts. Curves ranging from the increased aluminium steel on the left to the increased manganese steel on the right.

5.3.1 Over-age Time

Figure 5.16 shows the ultimate tensile strength that was achieved from the four experimental casts over a range of over-ageing times. The black line that crosses the graph at 790MPa is the target requirement for a TRIP 800. The over-age temperature was 460°C for all points plotted. The base steel examined starts off with a tensile strength at 660MPa at an over-age time of

50 seconds. This decreases to 651MPa at 100 seconds and continues to decrease to 643MPa at 370 seconds. This is an overall decrease of 17MPa so that the rate of decrease is ~0.05MPa per second. For the steel with the increase of 0.5wt%Al, there is an overall increase in strength over the base steel. At 50 seconds, over-age time the tensile strength was 699MPa. This decreases down to 678MPa at 100 seconds but increases back up to 693MPa at 200 seconds. The tensile strength finally drops down to 675MPa at 370 seconds.

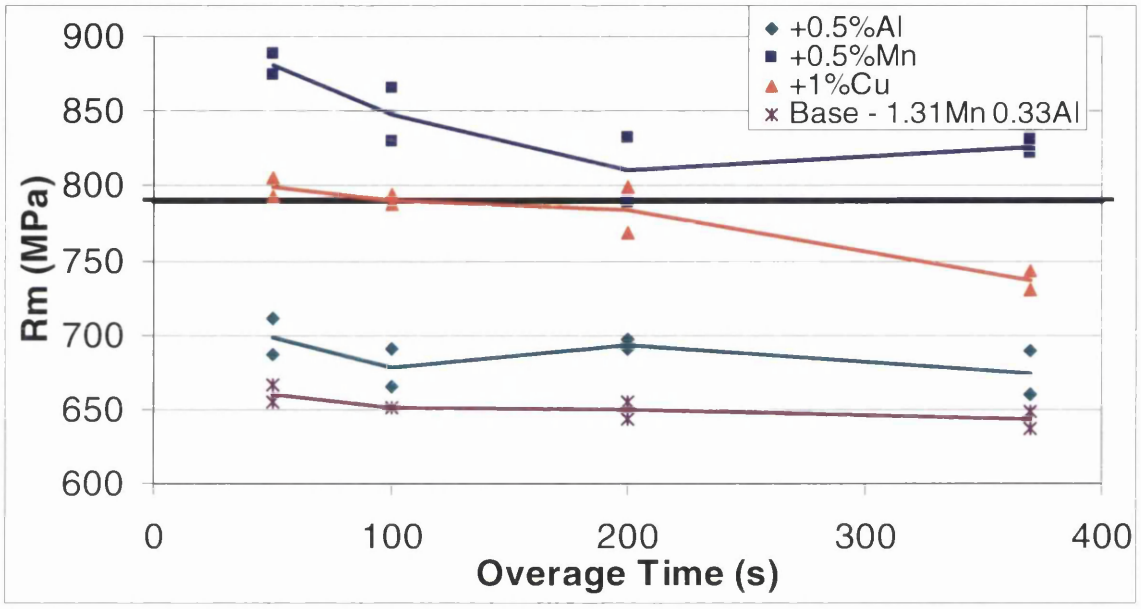

Figure 5.16: Tensile strength achieved over a range of over-age times for the experimental TRIP steel chemistries.

For the steel with the additional of 1wt%Cu, there is a much bigger jump in overall tensile strength over the base steel. There is a continuous decrease in tensile strength with increasing over-age time. Starting at 799MPa at an over-age time of 50 seconds dropping down to 790MPa at 100 seconds, further decreasing to 784MPa at 200 seconds. Finally decreasing down to 737MPa at 370 seconds. This is an overall decrease of 62MPa which is ~0.2MPa per second. Finally, for the steel with the increase of 0.5wt%Mn there is again an overall increase in tensile strength and is the steel chemistry that achieves the highest values. As with the other steels it achieves higher tensile strength at lower over-age times with 881MPa at 50 seconds, decreasing down to

848MPa at 100 seconds. Decreasing further to 811MPa at 200 seconds. However there is an increase as the over-age time is increased to 1000 seconds achieving 827MPa.

Figure 5.17 shows the proof stress that was achieved from the four experimental casts over a range of over-ageing times. The black lines that cross the graph at 440MPa and 560MPa are the limits for a TRIP 800. The over-age temperature was 460°C for all points plotted. For low over-ageing times the steel with the additional aluminium is just below the minimum requirements for a TRIP 800 steel, with a proof stress of 436MPa at an over-ageing time of 50 seconds and 434MPa at an over-ageing time of 100 seconds. This then increases to 457MPa at an over-age time of 200 seconds with a slight drop off at 370 seconds down to 449MPa, both of which lie within the TRIP 800 requirements.

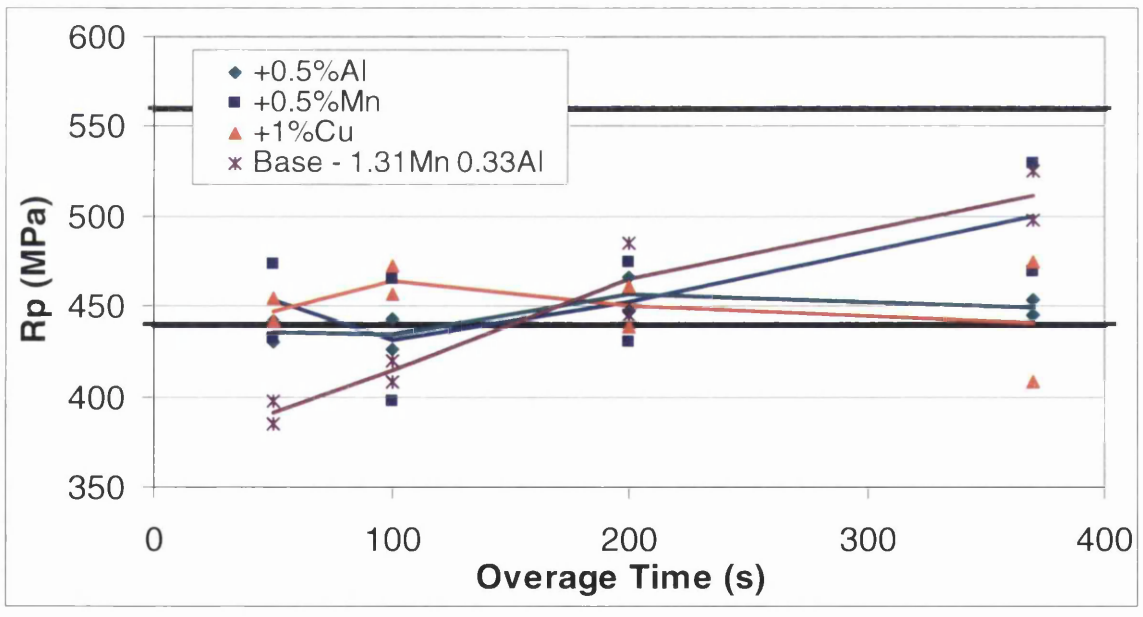

Figure 5.17: Proof stress with increasing over-ageing time

For the increased manganese alloyed steel, it has a proof stress of 453MPa at an over-age time of 50 seconds. This drops to 431MPa at an over-age time of 100 seconds, dropping below the TRIP 800 limit. However, with an over-age time of 200 seconds it crosses back over increasing to 452MPa. Finally, with an over-age time of 370 seconds a further increase in proof stress gives

a value of 499MPa. For the steel with increased copper alloying content, the proof stress stays within the requirements needed for a TRIP 800 steel at all over-ageing times looked at. With an over-age time of 50 seconds, the proof stress is 447MPa. At an over-ageing time of 100 seconds, this increases slightly to 464MPa. Once an over-ageing time of 200 seconds is used this decreases back down to 450MPa. There is then a smaller further drop to 441MPa at an over-ageing time of 370 Seconds. The base steel starts with the lowest proof stress of 391MPa at the over-ageing temperature of 50 seconds. This increases to 414MPa at an over-ageing time of 100 seconds. However, this is still below the requirements for a TRIP 800 steel. At an over-ageing time of 200 seconds, the proof stress increases to meet the standards for TRIP800 steel. Finally, at an over-age time of 370 seconds the base steel chemistry achieves the highest proof stress of 512MPa.

Figure 5.18 shows the total elongation that was achieved from the four experimental casts over a range of over-ageing times. The black line that crosses the graph at 20% is the target requirement for a TRIP 800 steel. The over-age temperature was 460^{o}C for all points plotted. The base steel starts of fat an elongation of 25%. It stays relatively constant with only minor fluctuations with increasing over-age time. 26% at 100 seconds, 25% at 200 seconds and 26% at 1000 seconds. The steel with a 0.5wt%Al addition gives improved elongation values over the base material. Starting at 26% at an over-age time of 50 seconds. There is then a relatively large improvement increasing to 33% at 100 seconds. However, this then drops off to 27% at 200 seconds, decreasing still further to 26% at 1000 seconds. At all over-age times both these steels are above the target elongation value of 20%. For the steel with an additional 1wt%Cu the elongation is 10% at an over-age time of 50 seconds. This then rapidly increases to 22% at 100 seconds finally levelling off to give 20% at 200 seconds and 19% at 1000 seconds. The steel with 0.5wt%Mn follows a similar trend staring low at 16% for 50 seconds over-age time. Increasing to 22% at 100 seconds then dropping off again to 17% at 200 seconds and 14% at 1000 seconds. For these last two steels only an

over-age time of 100 seconds gives elongations that are above the target value for the TRIP 800.

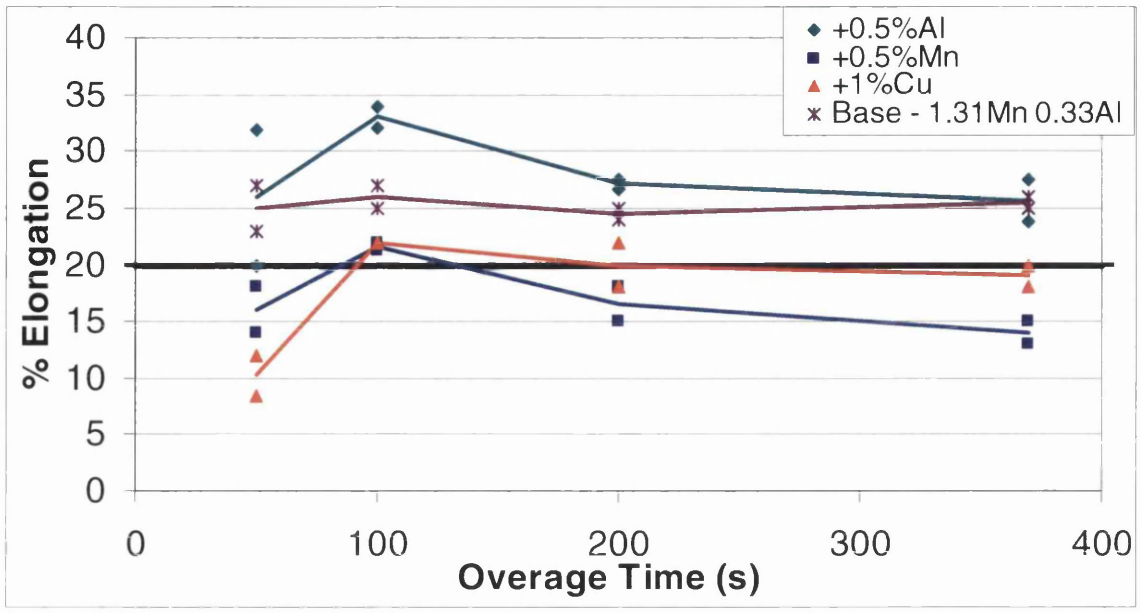

Figure 5.18: Elongation achieved over a range of over-age times for the experimental TRIP steel chemistries.

Figure 5.19 shows the n-value that was achieved from the four experimental casts over a range of over-ageing times. The black line that crosses the graph at 0.14 is the target requirement for a TRIP 800 steel. The over-age temperature was 460°C for all points plotted. Each of the steels for all the over-ageing times achieve n-values higher then the minimum needed for a TRIP 800 steel.

The steel with increased aluminium content has an n-value of 0.289 at an over-age time of 50 seconds. This steadily decreases with increasing over-age time, dropping to 0.284 at an over-age time of 100 seconds. Dropping further to 0.276 at an over-age time of 200 seconds. Finally decreasing down to 0.248 at an over-age time of 370 seconds. Overall, this is a total drop of 0.042, which is 0.013 per 100 seconds. The base steel also shows a continuous drop with increasing over-age time. Its n-value at an over-age time of 50 seconds is 0.242. This drops to 0.231 with an over-age time of 100 seconds. Dropping further to 0.207 at an over-age time of 200 seconds.

Finally, at 370 seconds it reaches an n-value of 0.193. Overall, this is a total drop of 0.050, which is a rate of 0.015 per 100 seconds. The steel with increased manganese content has an n-value of 0.191 at an over-age time of 50 seconds. This increases up to 0.210 at an over-age time of 100 seconds. It increases again slightly at an over-age time of 200 seconds up to 0.216, which is where it peeks. At an over-age time of 370 seconds, the n-value has dropped to 0.171. For the steel with an increased copper content, an n-value was not recorded at the over-age time of 50 seconds. However, from the other points plotted a general upward trend can be seen with increasing over-age time. At the over-age time of 100 seconds, the n-value is 0.198. This increases to 0.205 when an over-age time of 200 seconds is reached. Finally, it reaches its highest point at an over-age time of 370 seconds where a value of 0.209is achieved. There only seems to be a small increase with the total increase being 0.012, which is a rate of 0.004 per 100 seconds.

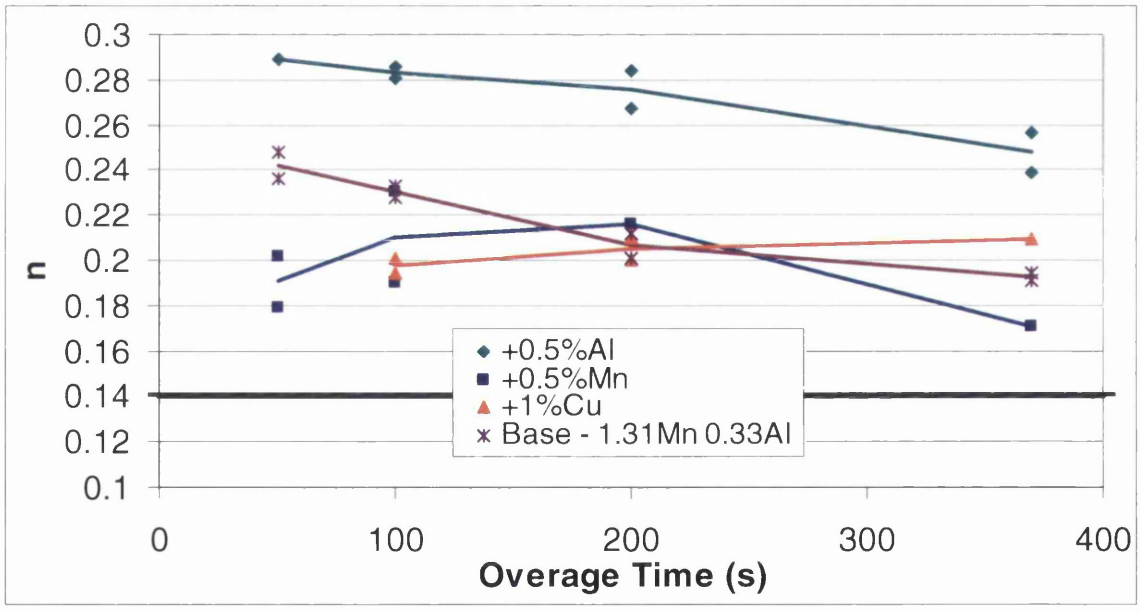

Figure 5.19: n-value with increasing over-ageing time

5.3.2 Over-age Temperature

Figure 5.20 shows the ultimate tensile strength that was achieved from the four experimental casts over a range of over-ageing temperatures. The black line that crosses the graph at 790MPa is the target requirement for a TRIP 800 steel. The over-age time was 370 seconds for all points plotted. The base steel starts with an ultimate tensile strength of 682MPa at an over-age temperature of 250°C. This then gradually decreases as over-age temperature increases giving a tensile strength of 660MPa at 350°C and 643 at 460°C this is a total drop of 39MPa which is a rate of ~0.18MPa per 1°C.

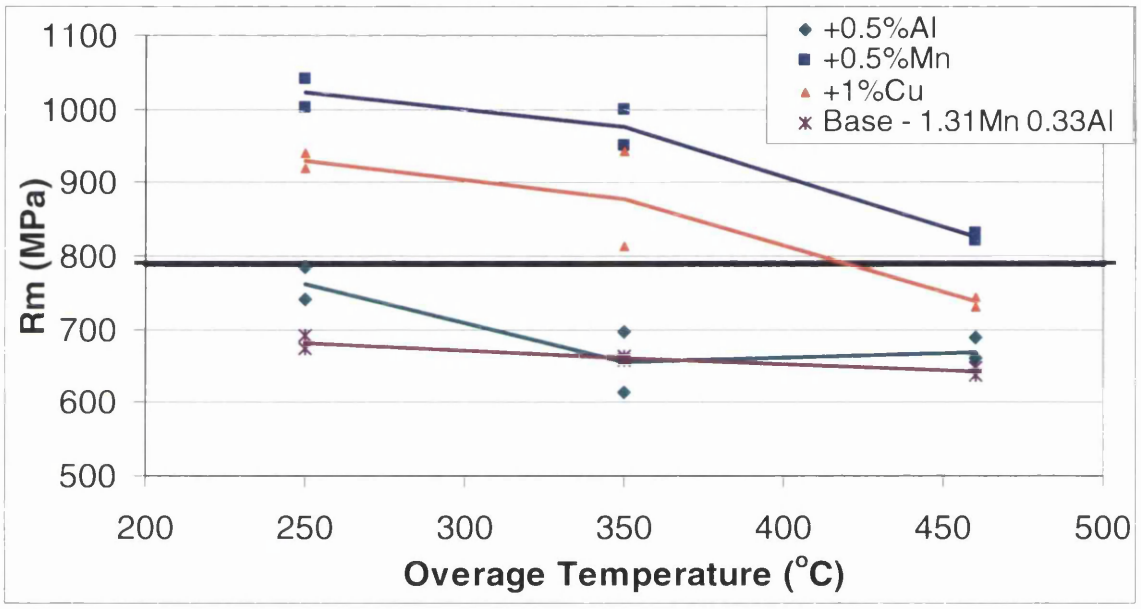

Figure 5.20: Tensile strength achieved over a range of over-age temperatures for the experimental TRIP steel chemistries.

The steel with an additional 0.5wt%Al gives slightly improved tensile strength starting at 761MPa at an over-age temperature of 250°C. This then drops to 655MPa at 350°C, similar to the base steel. However, it does increase slightly to 669 at 460°C. The increased copper and manganese steels both show improved tensile strength. The steel with copper additions has a tensile strength of 929MPa at an over-age temperature of 250°C. This decreases to 877MPa at 350°C and down to 737MPa at 460°C. This is a total decrease of 192MPa which is a rate of ~0.9MPa per 1°C. The steel with additional

manganese shows a similar trend starting at 1022MPa at an over-age time of 250°C. This decreases to 975MPa at 350°C further decreasing to 826MPa at 460°C. This is a total decrease of 195MPa which is a rate of ~0.9MPa per 1°C. Only the steel with increased Mn additions gives tensile strength above the target value of 790MPa for all temperatures and the copper steel achieves strengths above the target for over-age temperatures of 250 and 350°C.

From the proof stress with increasing over-age temperature (figure 5.21), it can be seen that the increased aluminium and copper steels show a similar trend as do the base and increased aluminium steel. For figure 5.21, the over-age time was 370 seconds for all points plotted. The two black lines crossing at 440 and 560MPa are the limits, which the proof stress must fall between for a TRIP 800 steel.

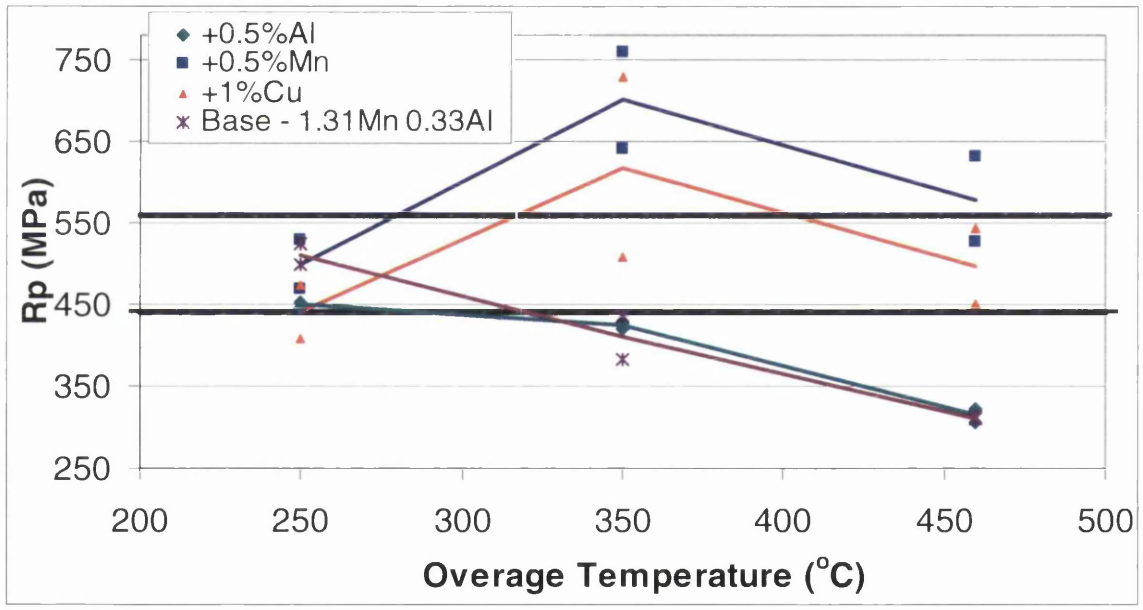

Figure 5.21: Rp with increasing over-age temperature.

For the base steel, there is an almost constant decrease in proof stress as the over-age temperature increases. With an over-age temperature of 250°C, the proof stress is 512MPa. This is the only point that the base steel lies between the limits required for TRIP 800 steel. At an over-age temperature of 350°C the proof stress of the base steel chemistry drops to 409MPa and finally drops further down to 311MPa at an over-age temperature of 460°C. For the base

steel there is a total drop of 200MPa in proof stress, which is a rate of 0.95MPa per 1°C. The steel with increased aluminium content shows a similar trend to the base steel. At 250°C the proof stress is 449MPa, which just meets the target requirement for TRIP 800 steels of 440MPa. Again, as with the base steel, this is the only time that the increased aluminium steel meets the requirements. There is then a slight drop when the temperature is increased to 350°C with a proof stress of 423MPa. This is followed by a larger drop down to 315MPa at an over-age temperature of 460MPa. Overall, the increased aluminium content steel drops by 134MPa, which is a rate of 0.64MPa per 1°C. For the steel with increased manganese content, it has a proof stress of 499MPa at an over-age temperature of 250°C this lays within the requirements for a TRIP 800. However, it is again the only time it meets the requirements. It increases past the upper limit reaching 701MPa at an over-age temperature of 350°C. It peeks at this point and drops down to 579MPa at an over-age temperature of 460°C. The steel with the increased copper content follows a similar trend as the increased manganese steel. At an over-age temperature of 250°C it has a proof stress of 441MPa just meeting the requirements for TRIP 800 steel. At an over-age temperature of 350°C it increases to and peeks at 618MPa. It then decreases down to 496MPa at an over-age temperature of 460°C, which falls back between the limits required for TRIP 800 steel.

Figure 5.22 shows the total elongation that was achieved from the four experimental casts over a range of over-ageing temperatures. The black line that crosses the graph at 20% is the target requirement for a TRIP 800. The over-age time was 370 seconds for all points. The base material starts with an elongation of 28% at an over-age temperature 250°C this decreases by two down to 26% at an over-age temperature of 350°C this continues to decrease but at a slower rate down to 25.5% at an over-age temperature of 460°C. This is a total drop of 2.5% which is a rate of ~0.01% per 1°C. The steel that has the additional 0.5wt%Al starts below the base steel at the over-age temperature of 250°C with an elongation of 25.6%. However, this increases above the base steel at an over-age temperature of 350°C and peeks at an

elongation of 30.4%. The elongation then falls back down to 25.6% when the over-age temperature increases to 460°C. The steel with an increase of 0.5wt%Mn shows the lowest elongation values. Starting at 10% elongation at an over-age temperature of 250°C. This decreases further down to only 6% elongation at an over-age temperature of 350°C. However, once the over-age temperature increases to 460°C the elongation for this steel reaches its highest point of 14%. The steel with the additional 1wt%Cu follows a similar trend as the steel with the extra manganese addition. Starting at 13% at an over-age temperature of 250°C. Dropping down to 8% at an over-age temperature of 350°C. Again as with the higher manganese steel it reaches its highest elongation value at an over-age temperature of 460°C giving 14% elongation.

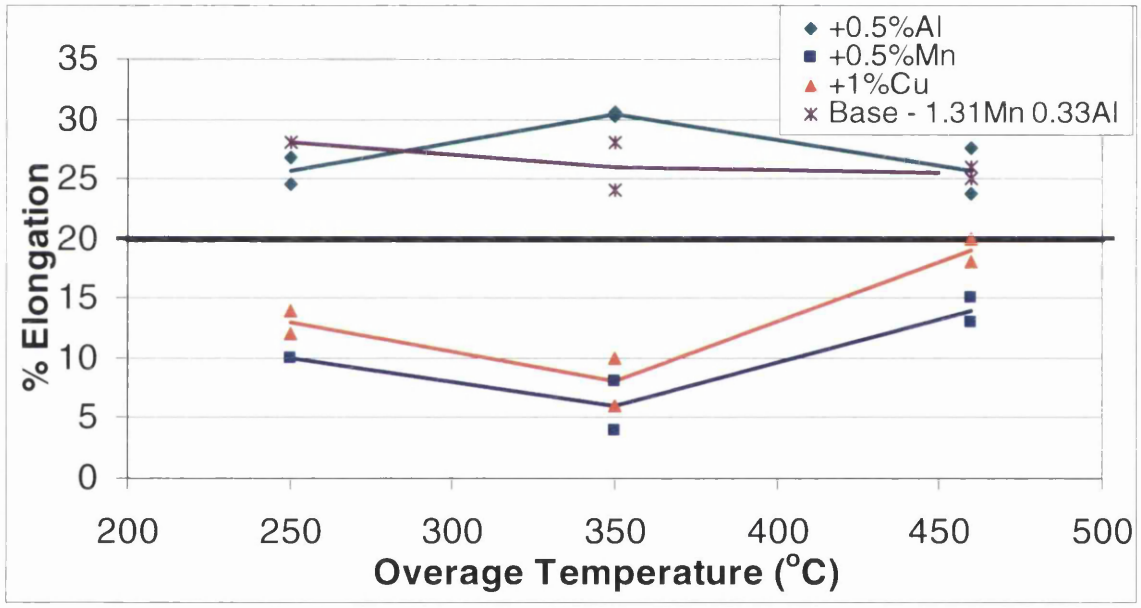

Figure 5.22: Elongation achieved over a range of over-age temperatures for the experimental TRIP steel chemistries.

Figure 5.23 shows the n-value with increasing over-age temperature. For the steels with increased manganese and copper alloying content, an n-value was only obtained at an over-age temperature of 250°C. These along with all other results were above the required n-value for a TRIP 800 steel, which is marked on figure 22 at 0.14. It can be seen from the other two steels, the base steel and increased aluminium steel, that there is a general increase in n-value with increasing over-age temperature. The base steel has an n-value of 0.193 at an over-age temperature of 250°C. This increases to 0.227 at an over-age temperature of 350°C. It then continues to increases though to a lesser degree up to 0.246 at 460°C. Overall, there is a total increase of 0.054, which is a rate of 0.025 per 100°C. For the steel with increased aluminium content, it has an n-value of 0.248 at an over-age temperature of 250°C. This increases slightly to 0.250 at an over-age temperature of 350°C. Once the over-age temperature is increased to 460°C, there is a larger increase in n-value up to 0.288. Overall, this is a total increase of 0.041, which is a rate of 0.019 per 100°C.

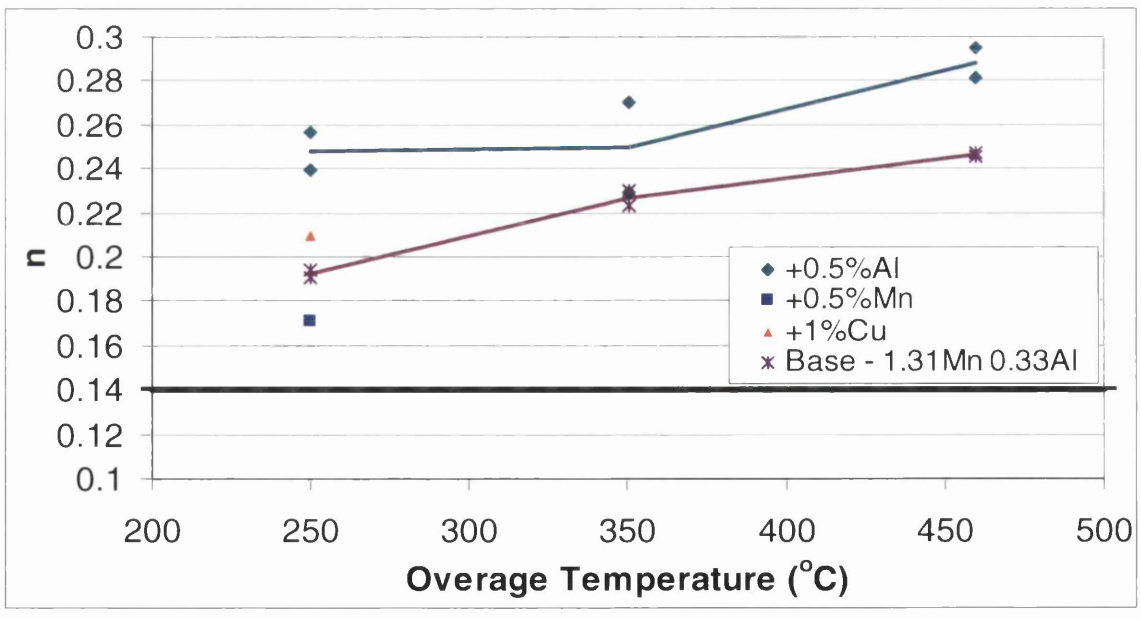

Figure 5.23: n-value with increasing over-ageing temperature.

Figure 5.24 shows the amount of bainite and retained austenite within the final microstructure as the over-age time is increased. The effects are similar as to what was seen for the Gleeble samples. For the retained austenite there is a volume fraction of 20% within the final microstructure at an over-age time of 50 seconds this increases by 1% up to 21% retained austenite when the over-age time is increased to 100 seconds. As the over-age time is increased to 200 seconds, the amount of retained austenite in the final microstructure begins to decrease down to 18.5%. Once the over-age time is increased to 370 seconds the amount of retained austenite in the microstructure decreases by 2.5% to 16%.

The volume fraction of bainite is 11% with an over-age time of 50 seconds. As the over-age time is increased to 100 seconds the amount of bainite within the final microstructure increases by 3.5% to 14.5%. From here, the amount of bainite stays relatively stable with a level of 14% at an over-age time of 200 seconds and then dropping only slightly to 13% at an over-age time of 370 seconds.

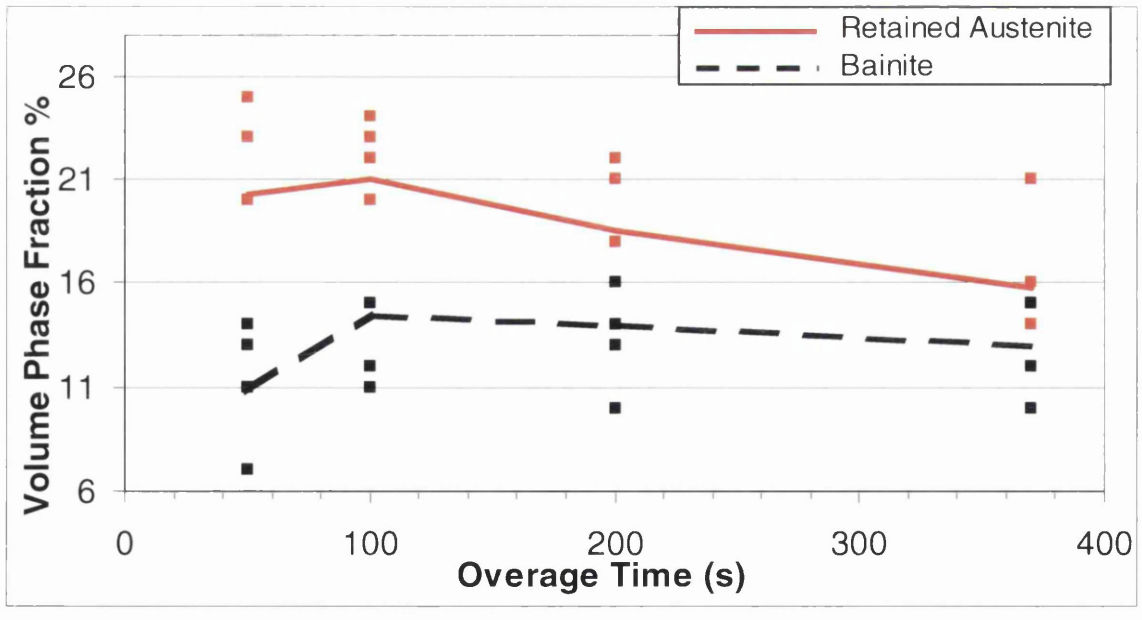

Figure 5.24: Volume fraction of bainite and retained austenite in the final microstructure with an over-age temperature of 460°C for a range of times.

Figure 5.25 shows the amount of bainite and retained austenite within the final microstructure as the over-age temperature is increased. The amount of retained austenite is at its highest at the lower over-ageing temperatures at 250°C it is 19.5%. There is a very small increase when the over-age temperature is increased to 350°C up to 19.75%. Once the over-ageing temperature is increased further up to 460°C there is a large decrease in the amount of retained austenite present in the final microstructure dropping down to 15.75%. For the amount of bainite found in the final microstructure with increasing over-age temperature there is very little change. At an over-age temperature of 250°C, there is 14.5% bainite. At an over-age temperature of 350°C, there is a slight decrease in the amount of bainite down to 13.75%. It then drops to 13% when the over-age temperature is increased up to 460°C

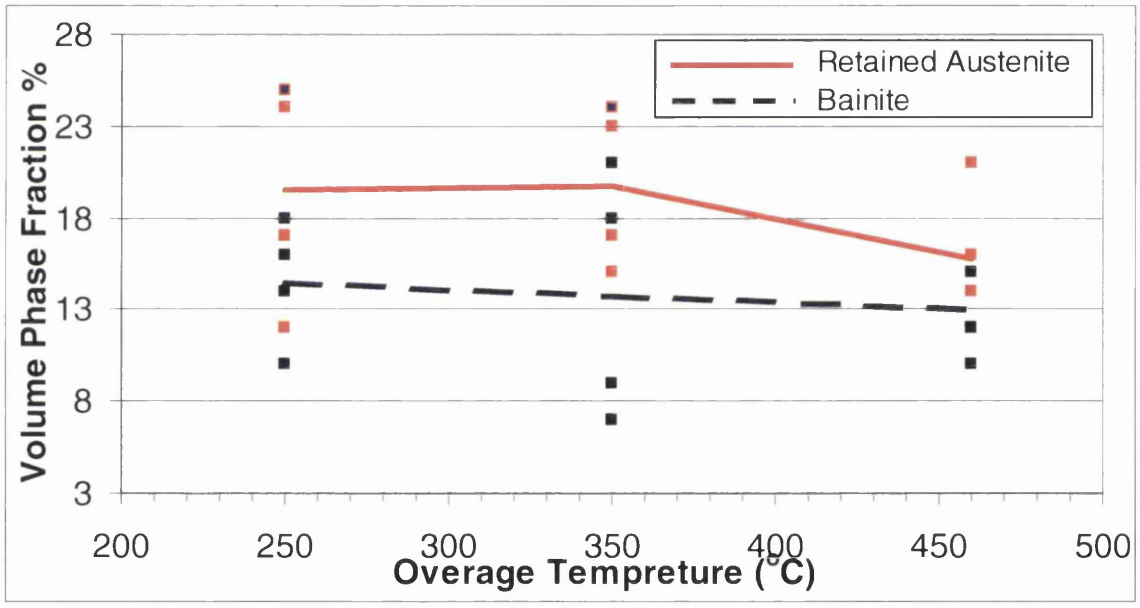

Figure 5.25: Volume fraction of bainite and retained austenite in the final microstructure with an over-age time of 370 seconds for a range of temperatures.

Figure 5.26 shows the ultimate tensile strength that was achieved from the four experimental casts as the intercritical heating rate is increased from 1°C/s to 40°C/s. The black line that crosses the graph at 790MPa is the target requirement for a TRIP 800 steel. The over-age time was 370 seconds and the temperature was 460°C for all points plotted. In general there seems to be

an increase in the tensile strength as the intercritical heating rate is increased. The base steel starts with an ultimate tensile strength of 630MPa at an intercritical heating rate of 1°C/s. This then gradually increases as the intercritical heating rate increases giving a tensile strength of 643MPa at 20°C/s and drops again to 625 at 40°C/s. The steel with an additional 0.5wt%Al gives slightly improved tensile strength starting at 678MPa at an intercritical heating rate of 1°C/s. This then stays stable with a tensile strength of 675MPa at 20°C/s, and 678MPa at 40°C/s. The increased copper and manganese steels both show improved tensile strength. The steel with copper additions has a tensile strength of 739MPa at an intercritical heating rate of 1°C/s. This remains at 737MPa at 20°C/s then increases to 769MPa at 40°C/s. The steel with additional manganese increases with higher heating rates starting at 780MPa at an intercritical heating rate of 1°C/s. This increases to 827MPa at 20°C/s further increasing to 845MPa at 40°C/s. Only the steel with increased Mn additions gives tensile strength above the target value of 790MPa for intercritical heating rates of 20°C/s and 40°C/s.

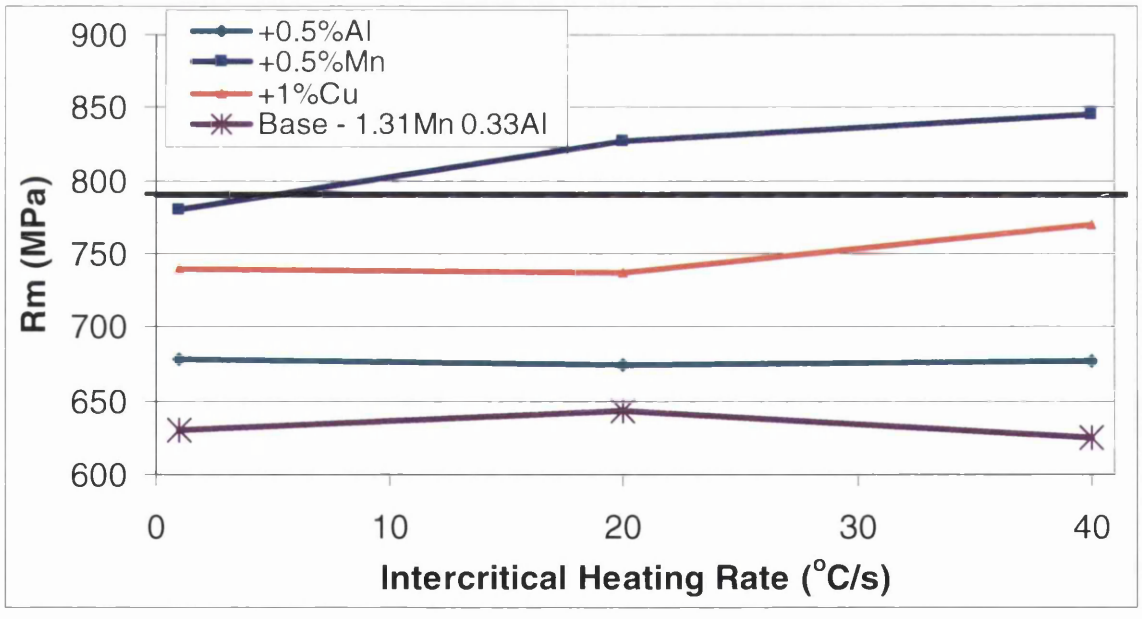

Figure 5.26: Ultimate tensile strength with increasing intercritical heating rate

Figure 5.27 shows the proof stress with increasing intercritical heating rate. The over-age time was 370 seconds and over-age temperature was 460°C for

all points plotted. 440 and 560MPa are the limits, which the proof stress must fall between for a TRIP 800 steel.

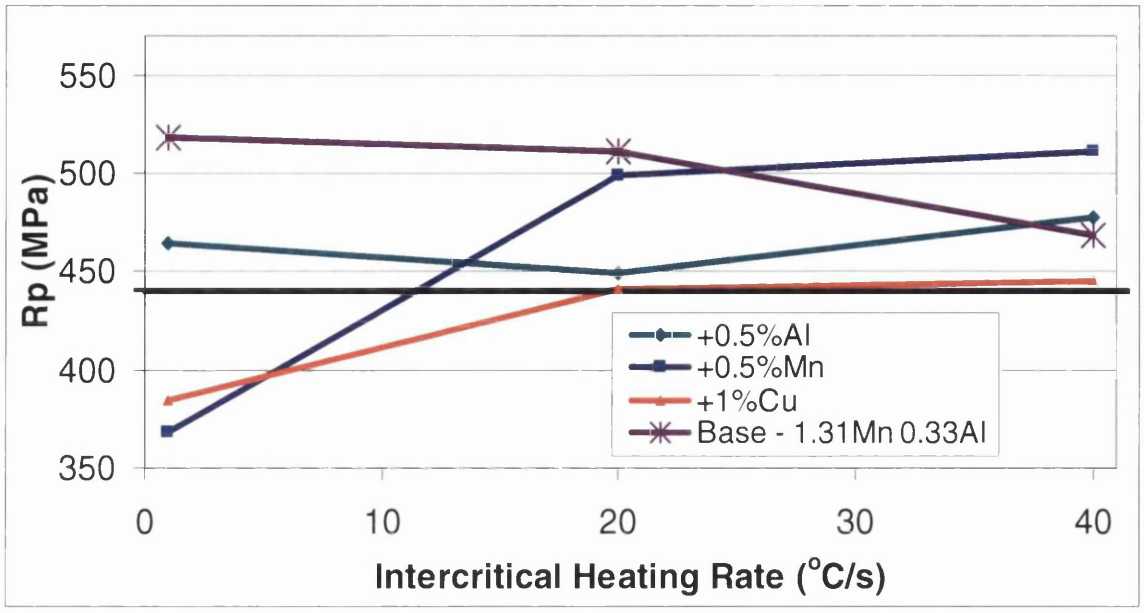

Figure 5.27: Proof strength with increasing intercritical heating rate

For the base steel with an intercritical heating rate of 1°C/s, the proof stress is 518MPa. At an intercritical heating rate of 20°C/s the proof stress of the base steel chemistry drops very slightly to 512MPa and finally drops further down to 469MPa at an intercritical heating rate of 40°C/s. The steel with increased aluminium has a proof stress of 465MPa at an intercritical heating rate of 1°C/s this drops slightly at an intercritical heating rate of 20°C/s with a proof stress of 449MPa. This then increases again to 478MPa at an intercritical heating rate of 40°C/s. For the steel with increased manganese content it starts off below the lower limit for a TRIP 800 with a proof stress of 369MPa at an intercritical heating rate of 1°C/s it then increase rapidly above the lower limit to 500MPa at an intercritical heating rate of 20°C/s, then starts to level off reaching 511MPa at an intercritical heating rate of 40°C/s. The steel with the increased copper content follows a similar trend as the increased manganese steel though at lower stresses. At intercritical heating rate of 1°C/s it has a proof stress of 384MPa again below the requirements for a TRIP 800 steel. At an intercritical heating rate of 20°C/s it increases to 441MPa. Only just

reaching the minimum requirements. It increases slightly further to 446MPa at an intercritical heating rate of 40°C/s.

Figure 5.28 shows the total elongation that was achieved from the four experimental casts over a range of intercritical heating rates. The black line that crosses the graph at 20% is the target requirement for a TRIP 800. The over-age time was 370 seconds and over-age temperature was 460°C for all points plotted.

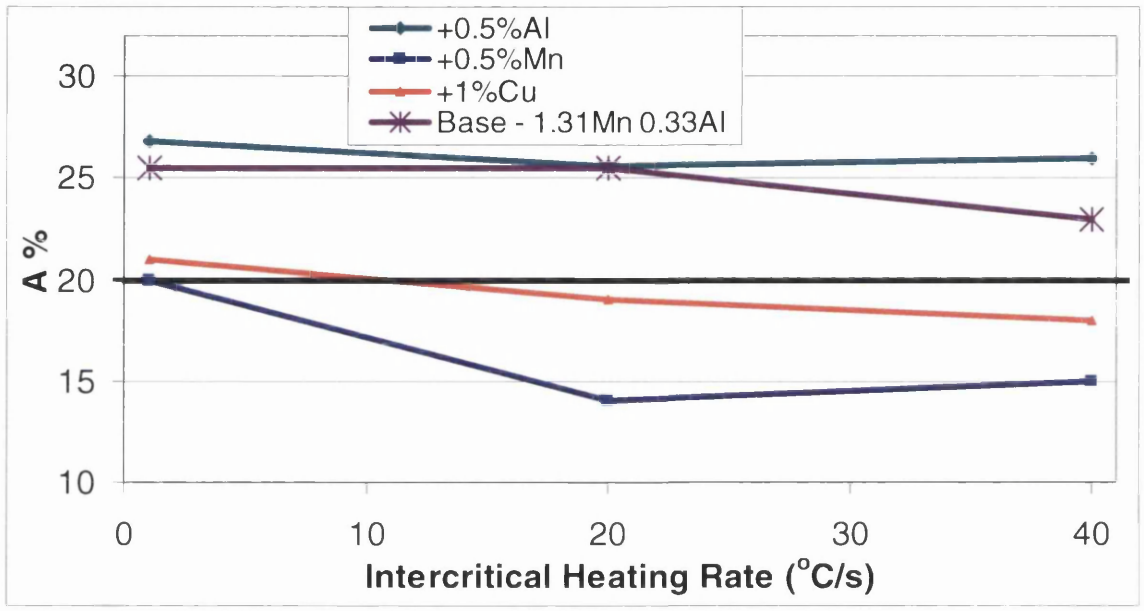

Figure 5.28: Total elongation with increasing intercritical heating rate

The base material starts with an elongation of 25.5% at an intercritical heating rate of 1°C/s remains at 25.5% at an intercritical heating rate of 20°C/s where it then begins to drop to 23% at an intercritical heating rate of 40°C/s. The steel that has the additional 0.5wt%Al reaches similar values with an elongation of 27% at an intercritical heating rate of 1°C/s. dropping to 25.5 at an intercritical heating rate of 20°C/s. then increasing back up to 26% at an intercritical heating rate of 40°C/s. The steel with an increase of 0.5wt%Mn shows the lowest elongation values. Starting at 20% elongation at an intercritical heating rate of 1°C/s. This decreases below the TRIP 800 requirement to 14% elongation at an intercritical heating rate of 20°C/s. then levels off to 15% at an intercritical heating rate of 40°C/s. The steel with the additional 1wt%Cu also starts off above the TRIP 800 requirement with an

elongation of 21 at an intercritical heating rate of 1°C/s then steadily dropping below down to 19 at an intercritical heating rate of 20°C/s and 18 at an intercritical heating rate of 40°C/s.

Figure 5.29 shows the n-value with increasing intercritical heating rate. The required n-value for a TRIP 800 steel is marked at 0.14. The n-value for the base steel stays fairly constant starting at 0.191 at an intercritical heating rate of 1°C/s increasing very slightly to 0.193 at an intercritical heating rate of 20°C/s then dropping very slightly to 0.188 at an intercritical heating rate of 40°C/s.

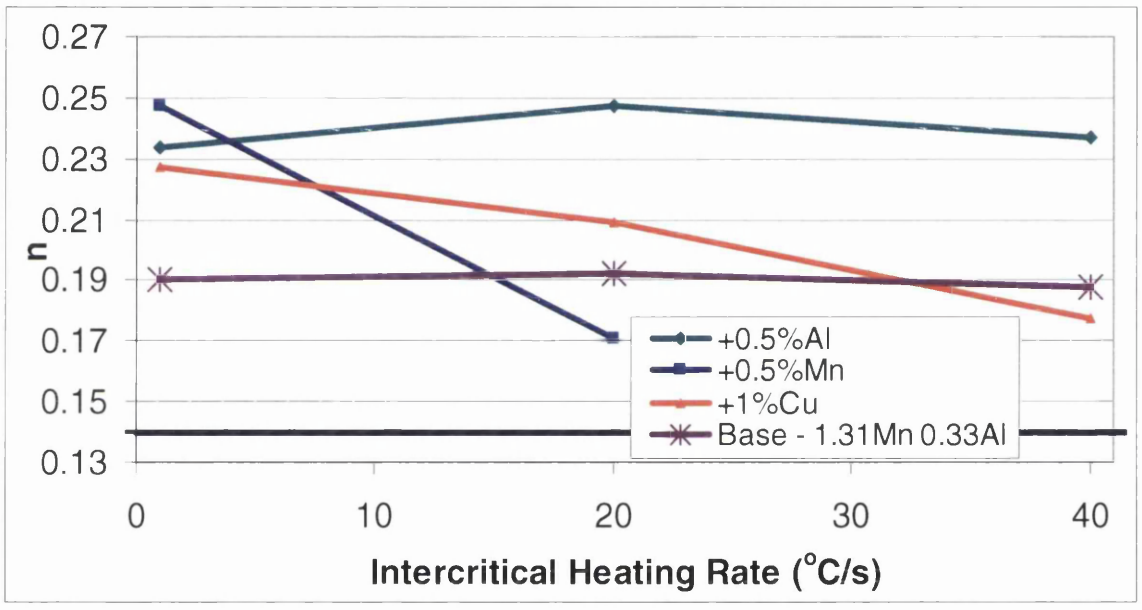

Figure 5.29: Total elongation with increasing intercritical heating rate

The steel with increased aluminium shows the best overall n-value results starting at 0.234 at an intercritical heating rate of 1°C/s increasing further to 0.248 at an intercritical heating rate of 20°C/s then dropping again to 0.237 at an intercritical heating rate of 40°C/s. the increased Copper steel starts off well at 0.227 at an intercritical heating rate of 1°C/s however continuously drops down to 0.209 at an intercritical heating rate of 20°C/s then to 0.178 at an intercritical heating rate of 40°C/s. The increased manganese steel also decreases with increasing intercritical heating rate starting of at 0.247 at an intercritical heating rate of 1°C/s but dropping rapidly to 0.171 at an

intercritical heating rate of 20°C/s. no value was recorded for an intercritical heating rate of 40°C/s.

Figure 5.30 shows the amount of bainite and retained austenite within the final microstructure as the intercritical heating rate is increased. The amount of retained austenite starts off at 13.75 for an intercritical heating rate of 1°C/s. it then peeks to 15.75 at an intercritical heating rate of 20°C/s and drops back down to 14% at an intercritical heating rate of 40°C/s

For the amount of bainite found in the final microstructure it starts with 12.5% at an intercritical heating rate of 1°C/s and only increases very slightly as the heating rate increases to 20°C/s achieving 13% bainite. This then increases quite rapidly to 16.75 at an intercritical heating rate of 40°C/s.

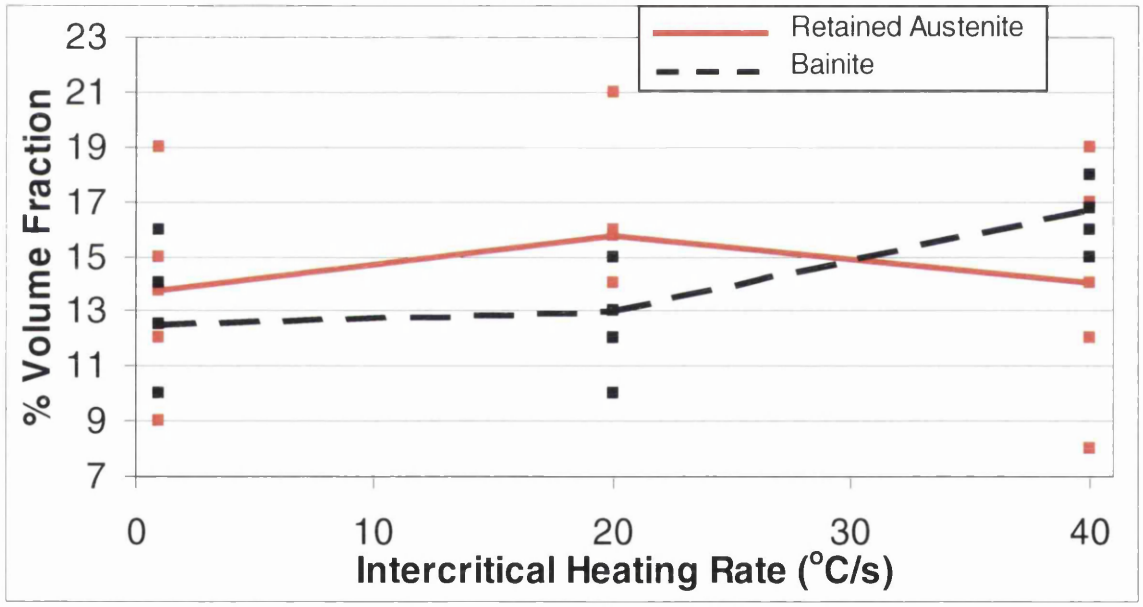

Figure 5.30: Volume fraction of bainite and retained austenite in the final microstructure with increasing intercritical heating rate

5.4 Micrographs

Figure 5.31 shows the hot bans material of the four experimental steels. Depending on the conditions during the etching the ferrite shows as white and/or brown the retained austenite shows as an off white while bainite/martensite shows as black. The four microstructures are similar showing mostly ferrite and the darker bainite/martensite phase. The copper steel seem to show some signs of retained austenite. And the manganese steel shows larger grains of the bainite/martensite phase.

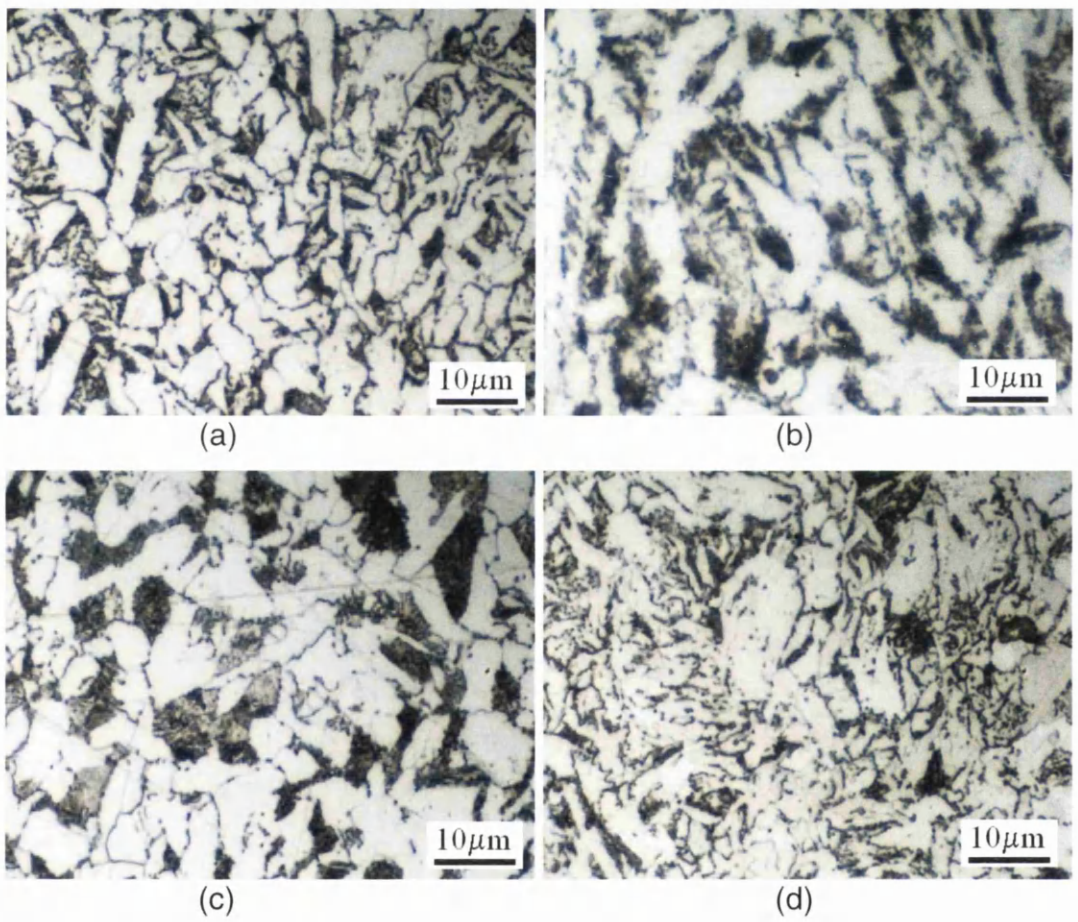

Figure 5.31: Microstructures of the hot band material. (a) base steel (VS4379), (b) +0.5wt%Al (VS4378), (c) +0.5wt%Mn (VS4380), (d) +1wt%Cu (VS4381)

Figure 5.32 shows the microstructures of the TRIP steel as the aluminium alloying content increases. All steels were overaged at 460^{O}C for 370 seconds. All four steels exhibit a fine microstructure, which was typical for these TRIP steels. Due to variances in the conditions whilst etching there will be some differences in coloration. But general there can be seen an increase in the amount of retained austenite with increasing aluminium content.

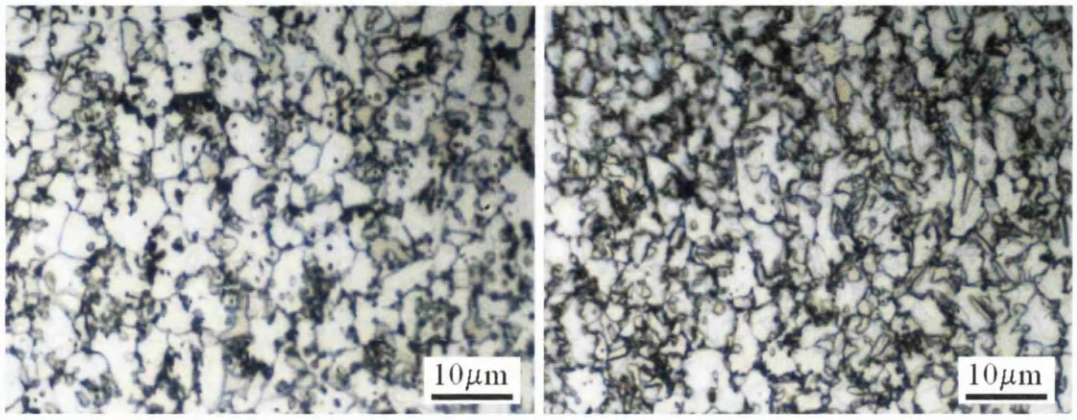

Figure 5.32: Micrographs showing microstructure evolution with increasing Al content. (a) 0.36wt%Al (VS4296), (b) 0.64wt%Al (VS4297), (c) 1.01wt%Al (VS4298), (d) 1.57wt%Al (VS4303)

Figure 5.33 show the microstructures of the TRIP steels as the manganese allotting content is increased. Again all steels were overaged at 460^{O}C for 370 seconds. All four steels again exhibit a fine microstructure, though in this case all four of the microstructures are very similar. The highest manganese steel with an alloying content of 1.91wt%Mn does show slightly more retained austenite.

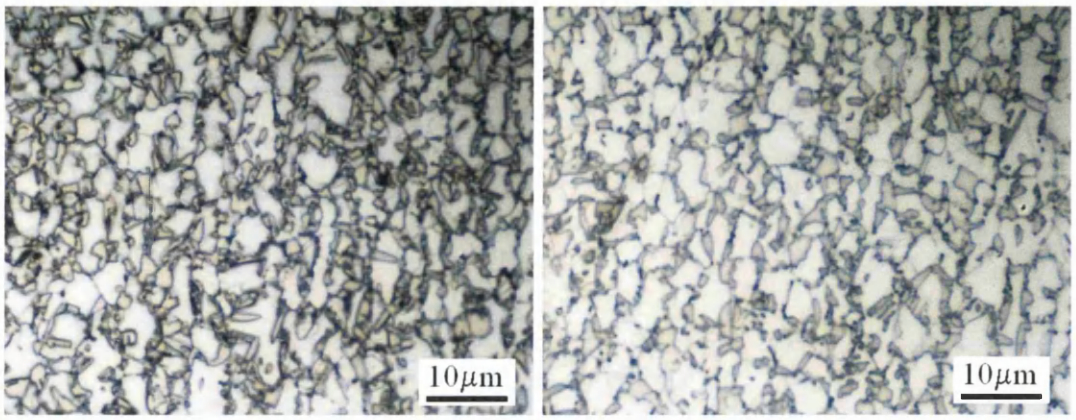

Figure 5.33: Micrographs showing microstructure evolution with increasing Mn content. (a) 1.35wt%Mn (VS4299), (b) 1.55wt%Mn (VS4300), (c) 1.72wt%Mn (VS4301), (d) 1.91wt%Mn (VS4302)

Figure 5.34 shows the microstructures of the four experimental steels when annealed with an over-age temperature of 460°c for 370 seconds. Which is typical of the Corus ZODIAC annealing cycle. The increased aluminium shows higher levels of retained austenite. The increased manganese steel shows much higher levels of the darker martensite/bainite phases along with the copper steel. Along with the increased amount of darker phase in the copper steel there is increased retained austenite compared to the manganese steel.

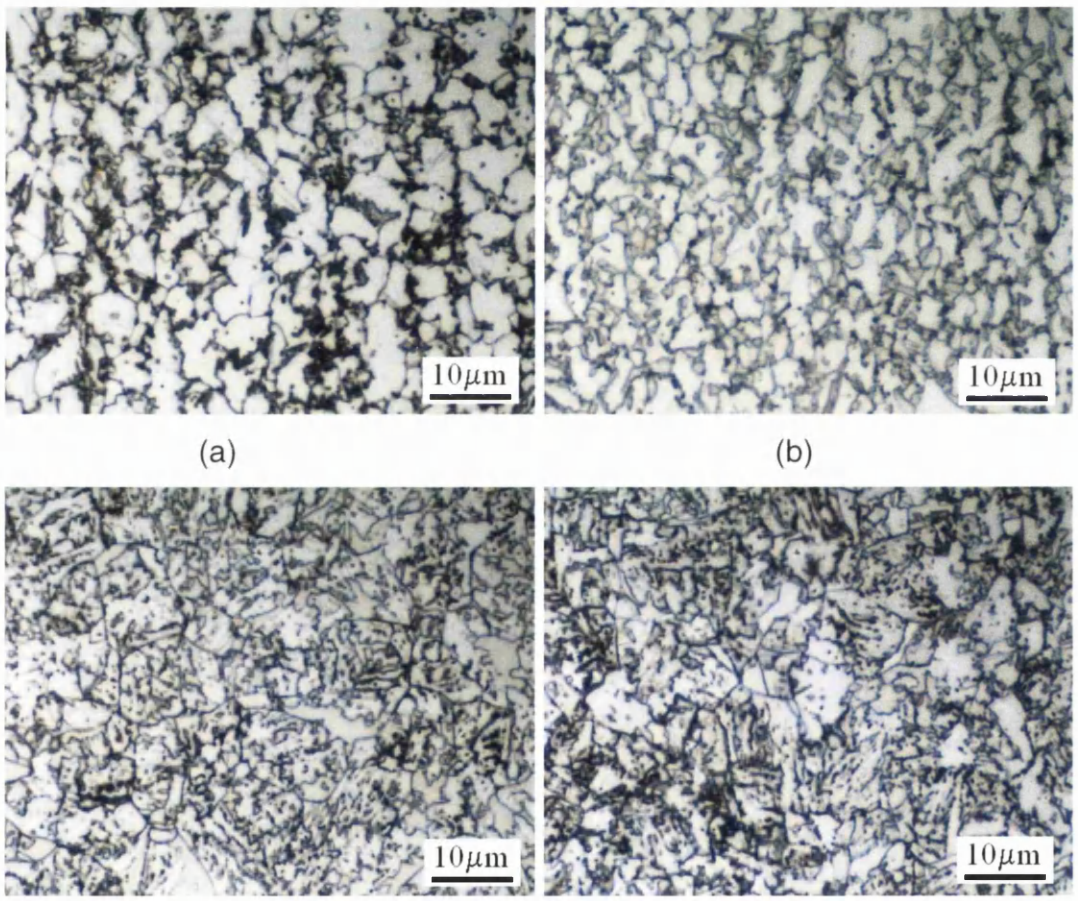

Figure 5.34: Microstructures of a typical ZODIAC cycle (over-aged at 460°c for 370s). (a) base steel (VS4379), (b) +0.5wt%Al (VS4378), (c) +0.5wt%Mn (VS4380), (d) +1wt%Cu (VS4381)

In figure 5.35 the microstructures of the four experimental steels can be seen all over-aged at 460°c for a shorter time of 50s compared to figure 5.34. It can be seen that the increased aluminium produces higher levels of retained austenite. The increased manganese steel shows much higher levels of the darker martensite/bainite phases with less retained austenite. Again the increased copper steel shows more of the darker phases but increased retained austenite compared to the manganese steel. Overall compared to figure 5.34 there is slightly less of the darker phase suggesting the shorter over-age time has produced less bainite.

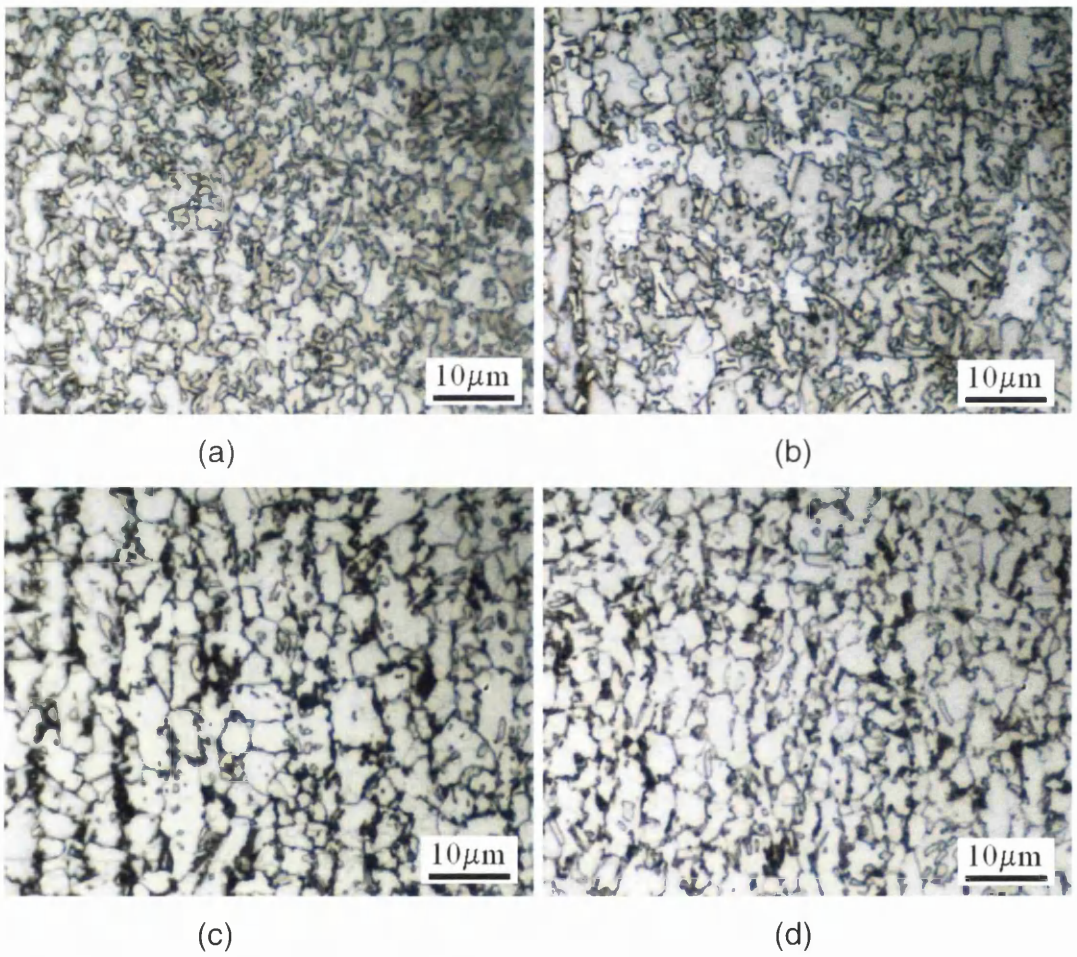

Figure 5.35: Microstructures when annealed with a short over-ageing section (over-aged at 460°c for 50s). (a) base steel (VS4379), (b) +0.5wt%Al (VS4378), (c) +0.5wt%Mn (VS4380), (d) +1wt%Cu (VS4381)

In figure 5.36 the microstructures of the four experimental steels can be seen all over-aged at a lower temperature of 250^{O}C compared to the microstructures in figure 5.34 though for the same time of 370 seconds. We can see that in general that there is more of the darker bainite/martensite phase. Looking at the amount of retained austenite the copper steel seems to exhibit the most and there is an increased amount in the aluminium steel compared to the base. However the manganese steel seem to show very little.

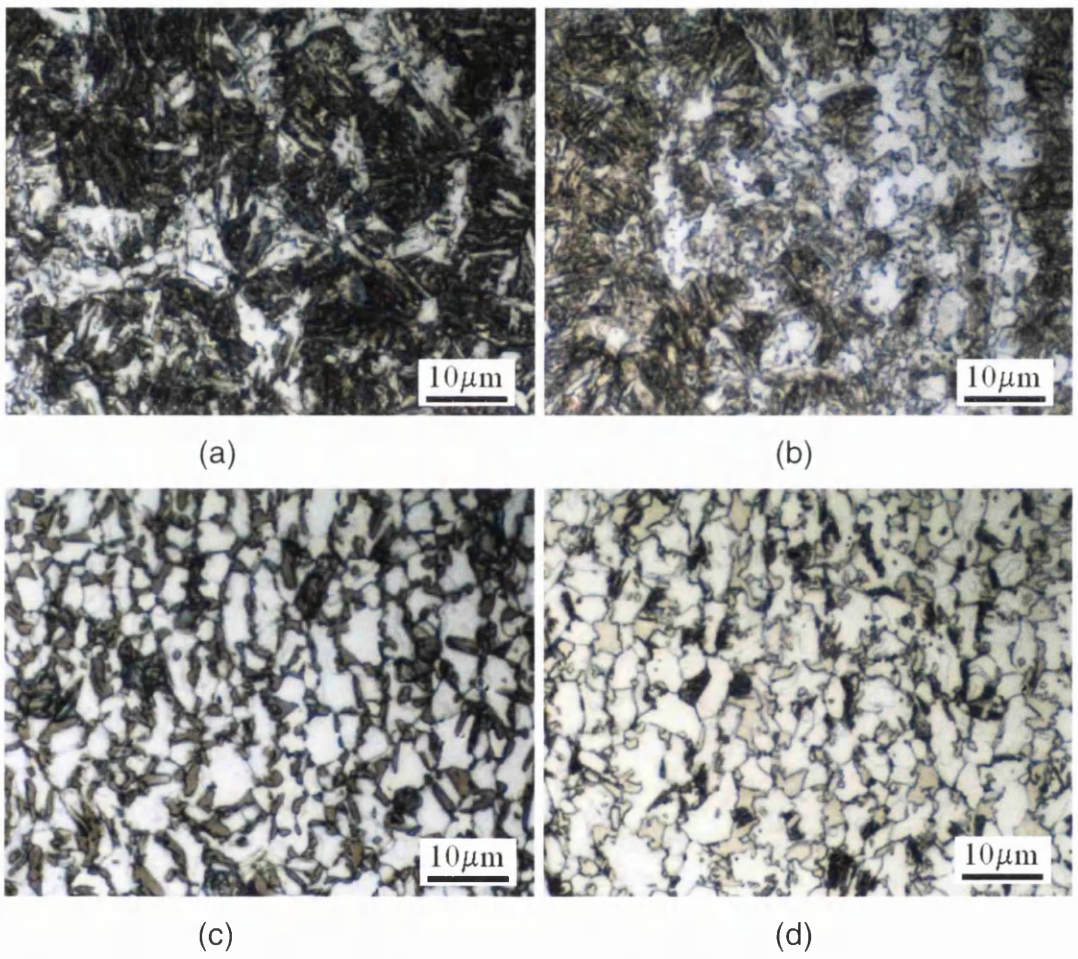

Figure 5.36: Microstructures when annealed with a low over-ageing temperature (over-aged at 250^{o}c for 370s). (a) base steel (VS4379), (b) +0.5wt%Al (VS4378), (c) +0.5wt%Mn (VS4380), (d) +1wt%Cu (VS4381)

Figure 5.37 shows the microstructures of the increased aluminium steel at different heating rates in to the initial intercritical heating at the beginning of the annealing cycle. The over-age section was typical for the Corus ZODIAC annealing line with a temperature of 460^{O}C for 370 seconds. The increased heating rate produces a finer microstructure with increased amounts of the darker bainite/martensite phase.

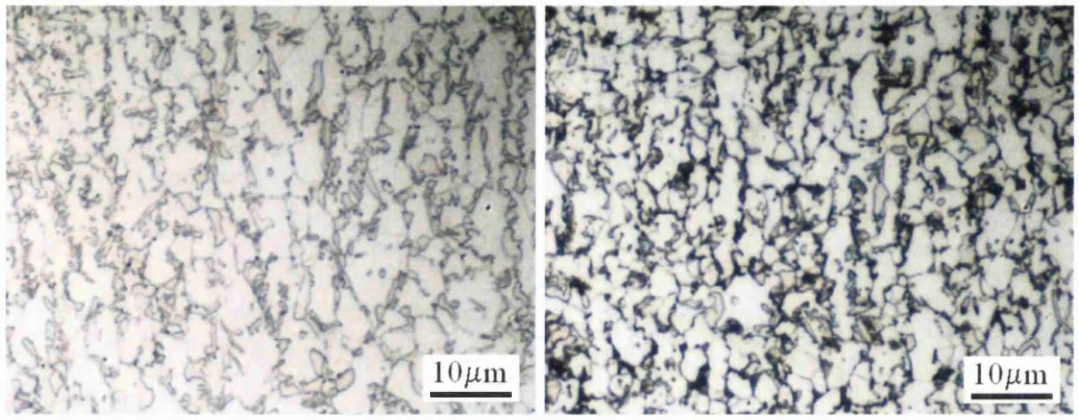

(a) (b)

Figure 5.37: Microstructures of the increased aluminium steel (VS4378) with an intercritical heating rate of (a) 1^{o}C/s and (b) 40^{o}C/s

6. DISCUSSION

6.1 The TRIP Effect.

Throughout this discussion, the TRIP effect will be referred to in terms of explaining the difference in properties shown in the results. The TRIP effect is the transformation of retained austenite to martensite during the application of strain. This transformation will result in an increase in strength due to the increased amounts of the strong martensitic phase present in the microstructure. Combine this with the difficulty of dislocation cross slip in retained austenite and it results in a good work hardening behaviour.

As the TRIP steel undergoes strain hardening, the strain energy builds up due to dislocation pile-up inside the ferrite grains. This accumulated strain provides the mechanical driving force needed for the strain-induced transformation of retained austenite. With the transformation the accumulated energy is absorbed, dislocation pile-up is relaxed, and ferrite grains are again softened. The softened ferrite grains can then be strain-hardened again by the strain-induced martensite. This process will repeat during the strain-induced transformation of retained austenite. It is this process that enhances the formability of TRIP steels.

Therefore, when the TRIP effect is mentioned in the following discussion it is referring to the above process, which is enhancing the strength and elongation properties of the steel.

6.2 ZODIAC Line and its Application for TRIP Steels

All of the annealing cycles were based around the Corus ZODIAC annealing line. The ZODIAC annealing line provides the necessary stages required for producing a TRIP steel with a typical cycle seen in figure 6.1

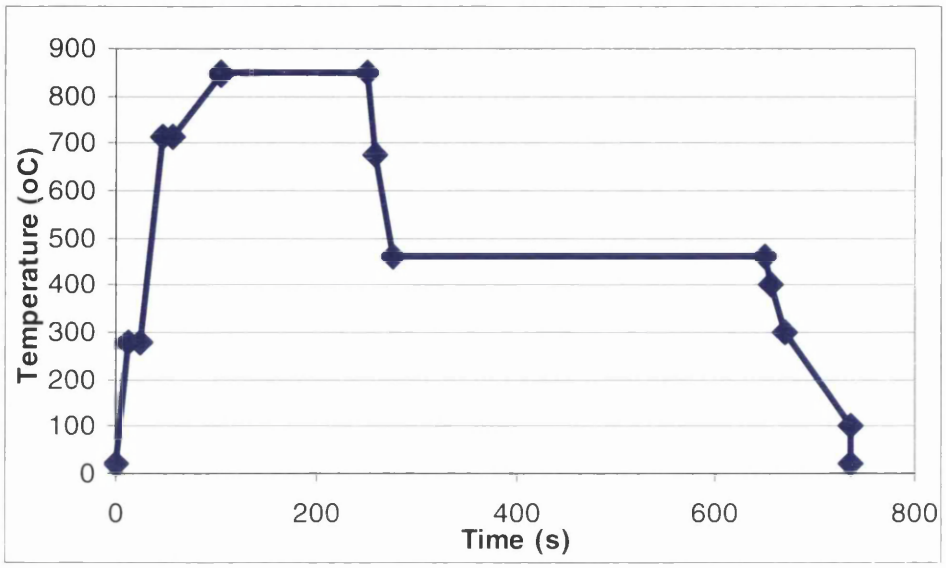

Figure 6.1: Typical ZODIAC annealing cycle

There is also scope to change some of the parameters such as temperatures and line speeds. By basing the annealing routes investigated around an industrial annealing route it gave a good basis to see if a TRIP steel is feasible using existing plant capabilities. It also allows to see how much of a difference there is between what is needed to achieve optimum properties and what is achievable on current capabilities.

6.3 Retained Austenite/Microstructure

6.3.1 The Differences Between Point Counting Method and XRD

Phase fractions were predominantly measured by volume fraction counting. However, some x-ray diffraction (XRD) was also used to detect the volume fraction of retained austenite to confirm the results found manually. Both the results for the amount of austenite present obtained from XRD and manual volume fraction counting showed similar trends. However, results from the XRD method gave retained austenite values at lower levels than the manual point counting method. However, this effect has also been observed in previous work [105].

6.3.2 Effects that the Alloying Content has on the Microstructure.

It can be seen in figures 5.3 and 5.4 that the amount of retained austenite within the microstructure of the samples that were annealed using the Gleeble 3500 shows a general increase with increasing alloying content for both aluminium and manganese. This has been recorded through the use of manual volume fraction counting and x-ray diffraction techniques. This was expected for both alloying elements. Aluminium suppresses carbide formation, therefore resulting in higher levels of carbon within the austenite so that it becomes stable and is retained at room temperature. Manganese is an austeniser, which results in more austenite being formed.

This trend is also shown in figure 5.13 where the amount of retained austenite is shown for increasing alloying content for the samples that were annealed using the CASIM. Again, it can be seen that both the aluminium and manganese alloying additions increase the amount of retained austenite within the microstructure. The aluminium shows a larger difference in the amount of retained austenite within the microstructure compared to the manganese. As aluminium is being investigated here as a partial replacement of silicon the fact that there is a marked increase in the amount of retained

austenite with higher levels of aluminium is encouraging, and shows that aluminium performs well in the role of carbide suppression and subsequent carbon enrichment of the austenite phase. The role that manganese has on the amount of austenite present within the final microstructure is also an additional benefit. Manganese is primarily added as a strengthener though the slight effect it has on the amount of retained austenite will help to increase the TRIP effect.

Looking at the amount of retained austenite left in the microstructure after deformation, in this case tensile testing, and using figure 5.14 to see the fraction of retained austenite remaining, the stability of the retained austenite can be assessed. The stability of the retained austenite is important. It is needed for the retained austenite to undergo the strain induced martensitic transformation to produce the good work hardening effect that TRIP steels are designed for, giving them their good strong and ductile properties. If the austenite becomes enriched with too much carbon and over stabilized, the retained austenite may not transform and therefore reduce the TRIP effect. On the other hand the austenite needs to be stabilized enough so that it is retained at room temperature. In addition, the typical automotive application for TRIP steels is for crash parts. In this case, retained austenite is desirable after part formation, so that the TRIP effect will result in energy absorption during crash situations.

By comparing figures 5.13 and 5.14 it can be seen that with increasing aluminium content there is an increase in the amount of retained austenite however it is less stable as a larger proportion transforms after deformation. Although increasing aluminium increases the amount of austenite within the final microstructure, it may result in the larger amounts of austenite being less enriched with carbon so that although it is enough for it to be retained at room temperature it is less stable.

For the increasing manganese levels, it seems a much more stable retained austenite product is formed with higher manganese alloying additions.

However, manganese is added as a hardener increasing the steels strength through solid solution strengthening. This will result in a potential strong but brittle material. It may be possible that steel failed during the tensile test before it could fully take advantage of the TRIP effect leaving much of the retained austenite untransformed.

Looking at the microstructures as the aluminium content is increased (figure 5.32), it can be seen that there is a fine uniform microstructure in all cases. It can also be visibly seen that there is increased amounts of retained austenite as the aluminium levels increase as was suggested by the properties seen. There can also be seen more of the darker second phase at lower levels of aluminium. This may be slightly higher levels of martensite within the microstructure where all the austenite hasn't been fully stabilized. The austenite grains for the lower aluminium alloyed steels also appear to be slightly smaller which can also contribute to a reduced TRIP effect as grains that are not of sufficient size may not transform during strain. For increasing manganese content (figure 5.33) there is not as much difference between the microstructures as seen for increasing aluminium. Though again with the lowest manganese alloying content an increase in the amount of darker second phase material can be seen.

6.3.3 Effects that the Annealing Route has on the Microstructure.

Figures 5.7 and 5.8 show the amounts of retained austenite and bainite within the final microstructure of the samples annealed using the Gleeble 3500 under different conditions for the over-age section.

Figure 5.7 shows the differences with varying over-age time. As the over-age time is increased, there is a continual increase in the amount of bainite within the final microstructure. This would be expected as the steel is being held in the bainite range of the TTT diagram (figure 2.2). It can be seen that the rate is much faster initially, with the initial formation and growth of the bainite grains. The rate then decreases after an over-age time of two hundred

seconds, as there will still be some growth of the bainite grains. However, continual holding can lead to a tempering effect upon the bainite.

In terms of the amount of retained austenite within the final microstructure, which is desirable for the TRIP effect, there is again an initial increase at 200s along with the initial increase of bainite. As the bainite is formed and grows, it will reject the carbon, which then enriches the austenite allowing it to be retained at room temperature. However, it can be seen that the amount of retained austenite will drop off when held for too long during the over-age section of the annealing route. The bainite forms from austenite therefore with increasing bainite being formed over time there will be less austenite remaining to be retained within the microstructure.

Figure 5.8 shows how the over-age temperature affects the microstructure. In general, higher over-age times result in increased amounts of bainite. This would suggest that the bainite nose on the TTT diagram for these steel chemistries is closer to the higher temperatures data. Looking at the amount of retained austenite in the final microstructure there does not seem to be much change except for the higher over-age temperatures where there is a slight drop off. This can also be put down to the bainite transforming from austenite. If there is more bainite being formed there will be less austenite to be retained in the final microstructure.

This raises an interesting question. If low levels of bainite are formed during the over-age section of the annealing route then there will be more potential austenite to be retained within the final microstructure. However there will also be less carbon rejected from the smaller amounts of bainite formed. This combination of larger amounts of austenite and less carbon rejected from the bainite can lead to the austenite not being stabilized enough to be retained when cooled down to room temperatures. On the other hand, if larger amounts of bainite are formed, then there will be less potential austenite to be retained, and with more carbon rejection from the increase bainite it is more likely to be retained within the final microstructure. In this case, there is the

possibility the austenite will become too stabilized and will not transform upon deformation. This has been shown to happen especially with smaller austenite grain sizes. A good balance needs to be reached so that an optimum amount of retained austenite is produced in the final microstructure that is able to transform during straining and therefore produce a good TRIP effect. In addition, as mentioned above if the steel is being used for crash parts in automotive applications the stability of the retained austenite can be critical.

Figures 5.24 and 5.25 show the amounts of retained austenite and bainite within the final microstructure of the experimental TRIP steels. Looking at the effects of increasing the over-age time. It can be seen that this is similar to what was seen in the Gleeble samples. An initial increase in the amount of bainite is seen up to 100 seconds, and a corresponding increase in retained austenite due to its carbon enrichment. For the Gleeble samples this was after 200 seconds, as this was the shortest over-age time looked at for them. This shows that even less time is needed to produce the amount of bainite required to retain the austenite at room temperatures. After this time the amount of bainite levels off showing that increased holding times will have little beneficial effects, and if any tempering occurs whilst holding the steel at temperature, it may have detrimental effects upon the steel's final properties. It can also be seen that as with the Gleeble samples the amount of retained austenite in the final microstructure decreases after a holding time of 100 seconds, so keeping the over-age time short will maximize the amount of retained austenite and help give optimal properties for the TRIP steel.

6.4 The Effects of Alloying Additions

6.4.1 Increasing Amount of Alloying Additions on Mechanical Properties

In the graphs from the results section (figures 5.1 and 5.2), the effects of increasing the alloy additions of manganese and aluminium have on hardness (which is related to tensile strength) can be seen. These results were taken from the samples that were annealed using the Gleeble 3500. Although there is a lot of scatter it does seem that by increasing the amounts of manganese and aluminium they both have a positive effect in increasing the hardness, where manganese has a larger effect upon the hardness than aluminium.

The increasing hardness with increasing manganese alloying content is due to a solid solution strengthening effect. Aluminium also has an effect on increasing the hardness, though more limited. This effect could also be put down to solid solution strengthening. Although the addition of these elements increases the amount of retained austenite and therefore produces a TRIP effect, it is unlikely that the localised deformation from a hardness test will trigger a significant TRIP effect. Therefore, the majority of the increase in hardness can be put down to solid solution strengthening mechanisms.

The combination of the amount of scatter generated during the hardness testing and that there will be a minimal amount of TRIP effect being produced during a hardness test suggests that this a less than ideal means of testing these steels.

Figures 5.9, 5.10, 5.11 and 5.12 show how increasing the alloying content of manganese and aluminium affects the tensile properties of the TRIP steel. In terms of tensile strength (figure 5.9), a similar trend was obtained as that seen for the hardness values from the Gleeble work on these casts. With both the aluminium and manganese increasing the strength of the material as higher additions are used. Again, it can be seen that the manganese has a larger affect upon the strength of the steel than aluminium. In the case of the tensile

test, the TRIP effect will have taken place as has been shown from the change in the amount of retained austenite before and after the test. Therefore, the TRIP effect will have played a part in the strength levels achieved in these results where it couldn't be certain from the hardness results. Even so it can be seen that there is a similar trend taking place from both sets of results with manganese producing much higher harness values which would suggest that solid solution strengthening mechanisms play a larger role in increasing the strength levels than the TRIP effect.

By examining the proof stress with increasing alloying content (figure 5.10), it can be seen that with increasing aluminium content the proof stress increases. With increasing aluminium there is increase retained austenite and therefore an increase in the TRIP effect. The TRIP effect gives enhanced work hardening, and postpones necking, and will therefore give a higher proof stress. With increased amounts of manganese the proof stress drops off. The manganese has a large solid solution strengthening effect making the material more brittle Because of the increased brittleness the onset of necking will be earlier and so a reduced proof stress will be seen.

From the elongation values with increasing alloying content (Figure 5.11) it can be seen that increasing manganese alloying additions that there is a slight initial increase. Manganese is an austeniser and so can have a slight effect upon the amount of retained austenite present. This can account for this initial increase; with a slight increase in manganese there will be a slight increase in the amount of austenite present, therefore a better TRIP effect and so better elongation of the material. However there is then a rapid drop off as the amount of manganese is increased further. This is due to the solid solution strengthening effect taking over and therefore the typical strength ductility trade off that is associated with this which will override any increase in the ductility achieved from the TRIP effect.

For increasing aluminium additions, we can see that there is an increase in the amount of elongation achieved. This was expected as by increasing the

aluminium content it increases the stability of the austenite therefore retaining more in the final microstructure. This results in a better TRIP effect resulting in better elongation. It can be seen that the amount of elongation with increasing aluminium eventually peeks and starts to drop off at higher aluminium content. This could be due to two reasons either a maximum amount of retained austenite has been achieved and increasing the amount of aluminium added would not increase it further, therefore elongation values level off. Or the retained austenite has become too stabilized, with increased amounts of carbon content in the austenite, with the increased amounts of aluminium present so that it will not transform to martensite during straining. This would result in a reduction in the TRIP effect, therefore a reduction in the amount of elongation that can be achieved.

The n-value is another measure of the formability of the material in particular its stretch-ability in forming process. With increasing alloying content (figure 5.12) it can be seen that there is a similar trend for what was seen for total elongation and therefore the effect on n-value will be for the same reasons.

6.4.2 Hardness/Strength Relationship Between the CASIM and Gleeble Annealed Samples.

Looking at the hardness values taken from the material that was annealed using the Gleeble 3500, and comparing it to the tensile strength of the same material that was annealed in a similar way using the CASIM, it can be seen that there are good similarities within the results. It can be seen that by increasing the manganese content the tensile strength and hardness both increase at a higher rate than with increasing aluminium content. However, where the hardness values from the Gleeble samples show similar values for the manganese and aluminium steels, it can be seen that for tensile strength of the CASIM samples the manganese steels show higher values on average compared to the aluminium steels.

The manganese steels have higher amounts of RA overall compared to the aluminium steels. Looking at the chemistries the manganese steels have an aluminium content on the higher end of the aluminium scale where the aluminium steels have a manganese content on the lower end of the manganese scale used:

An aluminium content of 0.36 to 1.57wt% is used at and the aluminium content of the manganese steels are ~1.28wt%
An manganese content of 1.35 to 1.91wt% is used at and the manganese content of the aluminium steels are ~1.53wt%

Therefore, the manganese steels have more RA as they have higher combined manganese and aluminium content. This also comes out in that the tensile strength of the manganese steels are that much higher compared to the manganese and aluminium hardness values. This further shows that the hardness testing may not fully trigger the TRIP effect. As the tensile strength of the manganese steels are factoring in both solid solution strengthening and TRIP effect. Where the hardness values are mainly based upon the solid solution strengthening effect.

6.5 The Effects of the Annealing Route.

6.5.1 Changing Over-ageing Time on Mechanical Properties

Figures 5.1 and 5.2 were broken down into the different over-ageing times used and it can be seen that an over-age time of 200 seconds produce higher hardness values. The different hardness values that are found at these different over-ageing times can be attributed to the bainite growth during the over-age section. An over-age time of 200 seconds compared to 100 seconds has given more time for the bainite grains to form and grow therefore giving higher hardness values. Again, an over-age time of 1000 seconds gives lower hardness values compared to that of 200 seconds. This can be put down to a tempering effect after being held during the over-age section for an extended period. This can be tied in with what was seen in the microstructure in figure 5.7 with the initial bainite growth up to 200 seconds and although there is still some increase in the amount of bainite up to 1000 seconds the tempering effect is still enough to reduce the hardness.

Figure 5.5 shows this more clearly showing the general trend of the hardness values at different over-ageing times for all the samples examined. Again, it can be clearly seen that there is an increase up to 200 seconds and then a reduction due to the tempering effect as the over-age time is increased to 1000 seconds.

Figures 5.16, 5.17, 5.18, 5.19 show the effects of over-age time upon the tensile properties of the TRIP steels.

Figure 5.16 shows the tensile strength with increasing over-age time for the experimental steels that were annealed using the CASIM. Even though the over-age time was only taken up to 370 seconds rather than the 1000 seconds that the Gleeble samples were, there is still a general overall decrease in strength over time. In fact it can be seen that from 50 to 200

seconds the tensile strength of most of the steel chemistries tested remain relatively level or have already started to decrease. This suggests that there is only a short time from when the bainite is formed to it starting to temper. So that even as new bainite is being formed and growing, the initial bainite is tempering.

By also considering how increasing over-age time affects the total elongation (figure 5.18) it can be seen that there is a marked increase in elongation up to an over-age time of 100 seconds. During this time the bainite is nucleating and rejecting the carbon into the austenite so that it is stabilized at room temperature creating a good TRIP effect. For longer over-age times the elongation decreases slightly and levels off. Again with increasing amounts of bainite nucleating from the austenite there is less to be retained in the first place. And the remaining retained austenite may be too stabilized reducing the TRIP effect and therefore the amount of elongation achieved. Also examining the n-value with over-age time (figure 5.19) it can also be seen that there is a general decrease with increasing over-age time showing that the formability of the steel is decreasing.

By using a lower over-age time of ~100 seconds is optimal. Although even by this time there is a reduction in ultimate tensile strength it is needed to achieve maximum formability. By going over 100 seconds a reduction of strength and formability occurs and so there is a narrow window where optimum properties can be achieved.

6.5.2 Changing Over-ageing Temperature on Mechanical Properties.

Figure 5.6 shows the hardness values with increasing over-age temperature for the Gleeble samples. Investigating the effects of over-age temperature there is a slight increase at higher temperatures. Again, this change in the hardness levels can be attributed to the amount of bainite within the microstructure. If you think about the bainite nose on a TTT diagram, for these particular chemistries the nose peaks around the higher temperatures. This can also be seen in figure 5.8 where there is a slight increase in the amount of

bainite present at the higher temperatures and therefore a slight increase in hardness.

Looking at the ultimate tensile strength of the experimental casts (figure 5.20) we see a difference to what was seen for the Gleeble casts (where temperature only had a slight effect on hardness), with a much higher strength at lower over-age temperatures. This could be because the bainite nose is in fact closer to the lower temperatures for the experimental steels chemistries cast for this work compared to that for the steel that was used for the Gleeble samples and therefore higher amounts of bainite at lower over-age temperatures. Although there is only a small drop off in the amount of bainite at higher temperatures some of the reduction in strength could again be put down to tempering of the bainite. For all the temperatures looked at the holding time was 370 seconds, which has, been shown to give plenty of time for tempering to occur. By holding at higher temperatures for this time it may give a larger tempering effect at higher temperatures.

For elongation (figure 5.22), there is seen high elongations at low temperatures with more bainite more carbon is rejected to stabilize the austenite resulting in more retained austenite and room temperature and so better a TRIP effect. The higher elongation values at higher temperatures could be due to some TRIP effect but also with less bainite in the microstructure there will be less of a strength/ductility trade off. This can be seen more directly in figure 5.23 with n-values increasing showing that the formability of the steels increase with higher over aging temperature.

6.5.3 Changing the Heating Rate on Mechanical Properties

It can be seen that with increasing the heating rate there is a slight increase in the tensile strength of the steels (figure 5.26) and a corresponding reduction in the amount of total elongation (figure5.28) as well as a small drop off in formability (figure 5.29). The effect of this seems to be fairly small especial when compared to other changes within the annealing route. This effect could

be explained by a finer microstructure being produced from the faster heating rates. With the steel being heated up much faster and therefore spending less time in the intercritical region there is less time for the ferrite grains to fully recrystalise and the austenite to fully grow. This refinement within the microstructure will lead to an increase in strength and corresponding decrease in ductility.

Also with smaller austenite grain size they will be les likely to transform during strain, which will result in a reduction of the TRIP effect. This will also have a negative effect upon the final properties of the TRIP steels.

6.6 How do each of the Four Steel Chemistries Perform and Compare to each other?

Table 6.1. The mechanical properties of the four experimental steels showing whether they meet the requirements for a TRIP 800 steel. Green = pass, orange = fail, yellow = only just fail.

	Overage Temperature	Overage Time	Proof Strength	Tensile Strength	Elongation	n-value
			440-560 MPa	>790MPa	>20	>0.14
VS4378	460	370	453	660	28	0.26
VS4378	460	370	445	689	24	0.24
VS4378	460	200	466	690	27	0.27
VS4378	460	200	447	697	28	0.28
VS4378	460	100	443	690	32	0.29
VS4378	460	100	426	665	34	0.28
VS4379	460	370	498	648	26	0.19
VS4379	460	370	525	637	25	0.19
VS4379	460	200	485	643	25	0.20
VS4379	460	200	445	655	24	0.21
VS4379	460	100	420	652	27	0.23
VS4379	460	100	408	651	25	0.23
VS4380	460	370	470	822	13	0.17
VS4380	460	370	529	831	15	0.00
VS4380	460	200	430	789	15	0.22
VS4380	460	200	474	833	18	0.00
VS4380	460	100	397	830	21	0.23
VS4380	460	100	465	865	22	0.19
VS4381	460	370	408	743	20	0.21
VS4381	460	370	474	730	18	0.00
VS4381	460	200	461	799	22	0.21
VS4381	460	200	439	769	18	0.20
VS4381	460	100	456	787	22	0.20
VS4381	460	100	472	794	22	0.19
VS4378	250	370	322	784	25	0.30
VS4378	250	370	307	739	27	0.28
VS4379	250	370	312	673	28	0.25
VS4379	250	370	311	691	28	0.25
VS4380	250	370	526	1002	10	0.00
VS4380	250	370	631	1041	10	-
VS4381	250	370	450	918	14	-
VS4381	250	370	543	939	12	0.00

It can be seen that adding a 0.5wt% of aluminium to the base chemistry has a positive effect on both the tensile strength and elongation. Particularly the elongation and formability values achieved, the increased aluminium steel produced some of the best elongation and n-values at all annealing

conditions. This can be put down to the aluminium helping to stabilize the austenite and therefore increase the amount of retained austenite in the final microstructure resulting in a better TRIP effect. This is what would be expected from higher aluminium levels. There will also be some solid solution strengthening from the aluminium additions giving an additional small increase in strength.

Increasing the manganese, again by 0.5wt%, shows a marked increase in strength producing some of the best tensile strengths achieved out of the four experimental casts however it also produced some of the worst elongation and n-values. This is due to solid solution strengthening effect that manganese has and therefore it associated strength/elongation trade off. The steel with the addition of 1wt% copper also shows an increase in strength and a decrease in formability, though not as extreme as the increased manganese steel Again, this is mostly due to a solid solution strengthening effect. However copper is also an austeniser, therefore should result in increased retained austenite in the final microstructure, therefore a better TRIP effect. This can be seen in that the decrease in elongation isn't as marked as that seen in the increased manganese steel. This is because the TRIP effect helps to off set some of the decrease in elongation that is seen from the solid solution strengthening.

7. CONCLUSIONS

Aim one: To see if a increased aluminium alloying content is feasible, with the intention that reduced silicon levels can be used.

The steel with the additional 0.5wt%Al performs well giving increased strength and very good elongation compared to the base steel, 0.2%C 0.4%Si 1.3%Mn 0.3%Al (VS4379). Combining this with the increase on surface coatability that will arise from being able to reduce the silicon content, it is a good choice. However, the increased aluminium steel still needs additional manganese alloying content in order to meet the strength requirements. By doing this it will remove from some of the good formability characteristics that this steel exhibited. However, with the strength increase that the additional aluminium achieved the amount of additional manganese can be kept at a minimum so that there is less of a reduction in elongation. As the increased aluminium steel had plenty of formability to vary before falling below the requirements and by using the optimum annealing route it should be possible to produce a TRIP 800 steel based on these chemistries.

Aim two: Optimising the TRIP steel chemistry (adjusting elements such as manganese content) with the aim to produce a TRIP 800.

The steel with the 0.5wt% increase in manganese is able to meet the TRIP 800 requirements under certain annealing conditions (over-age temperature of 460^{o}C and over-ageing times of 100 to 200 seconds). The manganese is needed to reach the strength requirements however only the above conditions allowed it to meet the required formability requirements.

Aim three: investigating the effects of other austenising elements such as copper to be able to reduce silicon levels and enhance TRIP steel properties.

The steel with the additional 1wt% Cu meets the requirements for a TRIP 800 steel when an over-age temperature of 460°C and over-ageing times of 100 to 200 seconds are used. It also leaves slightly more margin for error, as the copper is able to increase the strength by solid solution strengthening, similar to manganese whilst having more benefit on retaining austenite and producing a better TRIP effect.

Aim four: Investigate processing route variables such as intercritical temperature and isothermal holding time to see how the aluminium additions affect this. The processing route will also be based on the current industrial capabilities available in South Wales with the aim of eventually producing viable commercial TRIP steel.

To achieve optimum properties in terms of the annealing route using an over-age time of 100 seconds at a temperature of 250°C would produce the best results.

An over-age time of 100 seconds is enough to produce the required amount of bainite to retain enough austenite at room temperature to produce good formability within the steel. It was seen at this over-age time that the best total elongations were achieved and generally better n-values were seen at shorter over-age times. Any less than this and there is a decrease in elongation due to the lack of bainite formation, any more and the strength of the material is effected due to tempering of the bainite.

An over-age temperature of 250°C produced the best tensile strengths. Whilst an over-age temperature of 460°C produced better elongation values particularly for the steels with the increased manganese and copper alloying additions, there was a marked decrease in strength for these temperatures. If

a chemistry was used based upon the aluminium steel, which exceeded the elongation requirements, with additional manganese to increase the strength. Then using lower over-age temperatures will also help increase the strength to meet requirements whilst still meeting the required elongation.

Comparing this with the industrial ZODIAC cycle, which has an over-age section of 460°C for 370 seconds, then formability values that are equal to or perhaps higher than can be achieved; however there will be a marked reduction in the strength of the steel. Therefore additional alloying additions will need to be added to achieve the requirements of a TRIP 800 steel. Also by using a lower over-age temperature of 250°C and shorter over-age time of 100 seconds compared to the industrial ZODIAC annealing cycle there will be a reduction in the amount of time and energy requirements needed to anneal these TRIP steels.

8. FUTURE WORK.

Predominantly TRIP steels will be used in crash critical parts where some forming will be needed. For this role the materials crash performance and energy absorption will be important.

Further work into these areas will be important and investigating how these steels perform in terms of the TRIP/work hardening effect after some initial straining as would be expected form the forming process.

This work set out to find a way to improve the coat-ability of TRIP steels by reducing the amount of silicon. However due to the size of the annealed samples it made comparison of the surface quality of the steels difficult. A full industrial trial would be needed to produce a large enough area to asses any surface defects and to see how well these steels coat.

Another major issue with TRIP steels is their weld-ability due to the high carbon content used. Welding trials and further work to optimise the chemistries used to improve on their welding characteristics will also be useful.

9. REFERENCES

1. M. Y. Sherif, (2003) **Strain Induced Transformation of Very Strong Metal.** University of Cambridge Department of Materials Science and Metallurgy, Cambridge

2. V. F. Zackay, E. R. Parker, D. Fahr and R. Bush. Transactions of the American Society for Metals, 1967, Vol. 60, pp. 252.

3. P. Haasen, editor (1991) **Phase transformation in materials.** Materials Science and Technology, Volume 5, Weinheim (Germany)

4. J.Huang, W.J. Poole and Militzer. **Austenite formation during intercritical annealing**. Metallurgical and Materials Transactions A, 2004, Vol. 35A, pp. 3363-3375.

5. H. K. D. H. Bhadeshia (2001) **Bainite in steels**, 2nd edition, Institute of Materials, London.

6. J. Flamming, D.N. Hanlon. **A feasibility study for 600-800MPa Tensile Strength GA TRIP steels for the ZODIAC hot dip galvanising line.** Internal Corus report 109054, 2003

7. O. Matsumura, Y.Sakuma and H. Takechi. **The developments of cold-rolled TRIP-assisted multiphase steels. Low silicon TRIP-assisted multiphase steels.** 2001, ISIJ international, Vol. 41, pp. 1061.

8. J. Wang and S. van der Zwagg. **Stabilization mechanisms of retained austenite in transformation-induced plasticity steel.** Metallurgical and Materials Transactions A, 2001, Vol. 32, pp. 1527.

9. A.K. Srivastava, S.B. Singh, G. Jha, N. Gope. **Effect of heat treatment on microstructure and mechanical properties of cold rolled C-Mn-Si- TRIP aided steel. Materials characterization.** Materials Characterization, 2006, Vol. 57, pp. 127-135.

10. B.A. Wade. **Development of lower carbon HR TRIP800 steels**. Internal Corus report 113153, 2005.

11. P.J. Jacques **Transformation-Induced Plasticity for High Strength Formable Steels.** Current opinion in solid state & materials science, 2004, Vol. 8, pp. 259-265.

12. D. A. Porter and K. E. Easterling (1981) **Phase Transformations in Metals and Alloys, 2nd edition**, Chapman and Hall, London.

13. S. Zaefferer, J. Ohlert, W. Bleck. **A Study of microstructure, transformation mechanisms and correlation between microstructure and mechanical properties of low-alloyed TRIP steel.** Acta Materialia, 2004, Vol. 52, pp. 2765-2778.

14. O. Matsumura, Y.Sakuma and H. Takechi. **Enhancement of elongation by retained austenite in intercritical annealed 0.4C-1.5Si-O.8Mn Steel.** Transactions of the Iron and Steel Institute of Japan. 1987, Vol. 27, pp. 570.

15. K. Sugimoto, M. Misu, M. Kobayashi and H. Shirasawa. **Effects of second phase morphology on retained austenite morphology and tensile properties in a TRIP-aided dual-phase steel sheet.** ISIJ International, 1993, Vol. 33, pp. 775.

16. B.C. De Cooman. **Structure–properties relationship in TRIP steels containing carbide-free bainite.** Solid state and materials science, 2004, Vol. 8, pp. 285-303

17. Bleck W. **Proceedings of the international conference on TRIP aided high strength ferrous alloys**, Ghent, 2002. pp. 13.

18. Etienne Girault, Anne Mertens, Pascal Jacques, Yvan Houbaert, Bert Verlinden and Jan Van Humbeeck. **Comparison of the effects of silicon and aluminium on the tensile behaviour of multiphase TRIP-assisted steels.** Scripta Materialia, 2001, Vol. 44, pp. 885-892.

19. T. Lung, J. Drillet, A. Couturier and C. Olier. **Detailed study of the transformation mechanisms in ferrous TRIP aided steels.** Steel Research, 2002, Vol. 73, pp. 218-224.

20. A. Wasilkowska, P. Tsipouridis, E.A. Werner, A. Pichler, S. Traint. **Microstructure and tensile behaviour of cold rolled TRIP-aided steels**. Journal of materials processing technology, 2004, Vol. 157-158, pp. 633-636.

21. H.K.D.H. Bhadeshia, **Bainite in Steels**, The Institute of Materials, London, 1992.

22. I.B. Timokhina, P.D. Hodgson. E.V. Pereloma. **Effect of microstructure on the stability of retained austenite in transformation-induced-plasticity steels**. Metallurgical and Materials Transactions A, 2004, Vol. 35, pp. 2331-2341.

23. N.C. Goel, S. Sangal, and K. Tangri. **A theoretical model for the flow behavior of commercial dual-phase steels containing metastable retained austenite: Part I. derivation of flow curve equations.** Metallurgical and Materials Transactions A, 1985, vol. 16, pp. 2013-22.

24. E. V. Pereloma, I. B. Timokhina P.D. Hodgson. **Transformation behaviour in thermomechanically processed C-Mn-Si TRIP steels with and without Nb.** Materials Science and Engineering, 1999 Vol. 273-275, pp. 448-452.

25. Oblak JM, Hehemann FR (1967) **Transformation and hardenability in steels.** Climax Molybdenum Company of Michigan, Ann Arbor.

26. J.R. Tarpani, M.H.P. Braz, W.W.B. Filho and D. Spinelli. Materials Research, 2002, Vol. 5.

27. Olson GB, Cohen M. **A general mechanism of martensitic nucleation: Part I. General concepts and the FCC → HCP transformation.** Metallurgical and Materials Transactions A, 1976, Vol. 7, pp. 1905.

28. Zarei Hanzaki A, Yue S. **Ferrite formation characteristics in Si-Mn TRIP steels.** ISIJ international, 1997, Vol. 37, pp. 583.

29. Zarei Hanzaki A, Hodgson PD, Yue S. **Hot Deformation Characteristics of Si-Mn TRIP Steels with and without Nb Microalloy Additions.** ISIJ international, 1995, Vol. 35, pp. 324.

30. S. van der Zwaag, J. Wang. **A Discussion on the Atomic Mechanism of the Bainitic Reaction in TRIP Steels.** Scripta Materialia, 2002, Vol. 47, pp. 169-173.

31. H. Yan-Qiu, L. Xiu-Hui, Z. Zhen-Hua, L. Jin-guo, **Bainite transformation and TRIP effect in 20Mn2SiVB steel.** Materials Science and Engineering A, 2006, Vol. 438-440, pp. 158-161.

32. S. Zaefferer, J. Ohlert, W. Bleck. **A study of microstructure, transformation mechanisms and correlation between microstructure and mechanical properties of a low alloyed TRIP steel**. Acta Materialia, 2004, Vol. 52, pp. 2765-2778.

33. V.T.T. Miihkinen and D.V. Edmonds. Materials, Science and Technology, 1987, vol. 3, pp. 422-30.

34. Sugimoto KI, Nakano K, Song SM, Kashima T. **Retained austenite characteristics and stretch-flangeability of high-strength low-alloy TRIP type bainitic sheet steels.** ISIJ International, 2002, Vol. 42, pp. 450–5.

35. Lee CG, Kim SJ, Lee TH, Lee S. **Effects of volume fraction and stability of retained austenite on formability in a 0.1C–1.5Si–1.5Mn–0.5Cu TRIP-aided cold-rolled steel sheet.** Materials Science and Engineering A, 2004, Vol. 371, pp. 16.

36. G.R. Speich, V.A. Demarest, and R.L. Miller. **Formation of austenite during intercritical annealing of dual-phase steels.** Metallurgical and Materials Transactions A. 1981, Vol. 12, pp. 1419-28.

37. S.W. Thompson, G.S. Fan, and P.R. Howell. **Phase Transform. Ferrous Alloys, Procedings of International conference.** 1984, pp. 43-47.

38. R. Petrov, L. Kestens and Y. Houbaert. **Recrystallization of a cold rolled TRIP-assisted steel during reheating for intercritical annealing.** ISIJ International, 2001, Vol. 41, pp. 883-90.

39. D.Z. Yang, E.L. Brown, D.K. Matlock, and G. Krauss. **Ferrite recrystallization and austenite formation in cold-rolled intercritically**

annealed steel. Metallurgical and Materials Transactions A, 1985, Vol. 16A, pp. 1385-92.

40. E. Emadoddin, A. Akbarzadeh, Gh. Daneshi. **Effect of intercritical annealing on retained austenite characterization in textured TRIP-assisted steel sheet.** Materials Characterization, 2006, Vol. 57, pp. 408-413.

41. H.K.D.H. Bhadeshia. **Bainite in Steels, Transformation, Microstructure and Properties**, the Institute of Materials, London, 1992, p. 173.

42. A.K. Sinha. **Ferrous Physical Metallurgy**, Butterworth and Co., Stoneham, MA, 1989, p. 315.

43. P. Brozzo, G. Buzzichelli, A. Mascanzoni, and M. Mirabile. Metal science, 1977, vol. 11, pp. 123-29.

44. A. Zarei-Hanzaki. Ph.D. Thesis, McGill University, Montreal, 1994.

45. A. Zarei Hanzaki, P.D. Hodgson, S. Yue, **Retained austenite characteristics in thermo mechanically processed Si-Mn transformation-induced plasticity steels.** Metallurgical and Materials Transactions A, 1997, Vol. 28A, 2405-2414.

46. O. Matsumura, Y. Sakuma, and H. Takechi. **Enhancement of elongation by retained austenite in intercritical annealed 0.4C-1.5Si-O.8Mn steel.** Transactions of the Iron and Steel Institute of Japan. 1987, Vol. 27, pp. 570-79.

47. K. Hulka, W. Bleck, and K. Papamantellos. **Procedings of the 41st mechanical working and steel processing Conference.** 1999, pp. 67-76.

48. Y. Tommita. **Effect of bainitic transformation on mechanical properties of 0.6C-Si-Mn steel.** Journal of Materials Science. 1995, Vol. 30, pp. 105-10.

49. G. Reisner, E.A. Werner, P. Kerschbaummaur, I. Papst, and F.D. Fischer. Journal of metals, 1997, vol. 49, pp. 62-65.

50. M. De Meyer, D. Vanderschueren. and B.C.De Cooman. **The influence of the substitution of Si by Al on the properties of cold rolled C-Mn-Si TRIP steels.** ISIJ International, 1999, Vol. 39, pp. 813-22.

51. M.L. Brandt and G.B. Olson. Ironmaker and Steelmaker, 1993, vol. 20, pp. 55-60.

52. H.C. Chen, H. Era, and M. Shimizu. **Effect of phosphorus on the formation of retained austenite and mechanical properties in Si-containing low-carbon steel sheet.** Metallurgical and Materials Transactions A, 1989, Vol. 20, pp. 437-45.

53. M. Takahashi and H.K.D.H. Bhadeshia. **A Model for the Microstructure of Some Advanced Bainitic Steels.** Materials Transactions, JIM, 1991, Vol. 32, pp. 689-96.

54. I. Tsukatani, S. Hashimoto, and T. Inoue. **Effects of Silicon and Manganese Addition on Mechanical Properties of High-strength Hot-rolled Sheet Steel Containing Retained Austenite.** ISIJ International, 1991, Vol. 31, pp. 992-1000.

55. O. Matsumura, Y. Sakuma, and H. Takechi. **TRIP and its kinetic aspects in austempered 0.4C-1.5Si-0.8Mn steel.** Scripta Metallurgica, 1987, Vol. 21, pp. 1301-06.

56. P.J. Jacques, J. Ladrière, and F. Delanny: Metall. **On the influence of interactions between phases on the mechanical stability of retained austenite in transformation-induced plasticity multiphase steels.** Metallurgical and Materials Transactions A, 2001, Vol. 32, pp. 2759-68.

57. M.H. Saleh, R. Priestner. **Retained austenite in dual-phase silicon steels and its effect on mechanical properties.** Journal of Material Processing Technology, 2001, Vol. 113, pp. 587-593.

58. I. Tamura. Metal Science, 1982, Vol. 16, pp. 245.

59. H. Y. Yu. **A new model for the volume fraction of martensitic transformations.** Metallurgical and Materials Transactions A, 1997, Vol. 28, pp. 2499.

60. M. Cohen. **International summer course on martensitic Transformations.** Leuven department of metals and materials Engineering. KV Leuven, 1.1-1.12.

61. T. Iwamoto, T. Tsuta, Y. Tomita. **Investigation on deformation mode dependence of strain induced martensitic transformation in TRIP steels and modeling of transformation kinetics.** International Journal of Mechanical Sciences, 1997, Vol. 40 pp. 173-182.

62. Y.H. Yan, G.Y. Kai, M.D. Jian. **Transformation behaviour of retained austenite under different deformation modes for low alloyed TRIP-assisted steels.** Materials Science and Engineering A, 2006, Vol. 441 pp. 331-335.

63. B.C. De Cooman, L. Samek, J. Mahieu, J. Van Slycken, P. Verleysen, J. Degrieck, L. Lin, L. Wang, X. Cheng ei, and S. Peng. **Fall meeting of TMS and 45th ISS mechanical working and steel processing conference**, Vancouver, BC, Canada, 2003.

64. J. Van Slacken, P. Valise, J. Derrick. **High strain rate behaviour of low alloy multiphase aluminium and silicon based transformation induced plasticity steels.** Metallurgical and Materials Transactions A, 2006, Vol. 37, 1527-1539.

65. K.P. Staudhammer and L.E. Murr. Materials Science Engineering, 1980, vol. 44, pp. 97-113.

66. Young, C. H. and Bhadeshia. H. K. D. H. Material Science Technology. 1994, Vol. 10, pp. 209.

67. Tvergaard V. **Influence of voids on shear band instabilities under plane strain conditions.** International Journal of Fracture. 1981, Vol. 17, pp. 389.

68. T. Tong, L.I. Lin, B.C. De Cooman, W. Xi-chen, S. Peng. **Effects of temperature and strain rate on dynamic properties of low silicon TRIP steel.** Journal of iron and steel research, international. 2006 Vol. 13, pp. 51-56.

69. Masaaki Itabashi. Kozo Kawata. **Carbon Content Effect on High-Strain-Rate Tensile Properties for Carbon Steels.** International Journal of Impact Engineering, 2000, Vol. 24, pp. 117-131.

70. Wel Xi-cheng,. FU Ren-yu. et al. **Time Dependence of Transformation Processing of Si-Mn TRIP Steel During High- Speed Tensile Impact Testing.** International Conference on TRIP-aided High Strength Ferrous Alloys. Ghent. Belgium. 2002, June 19-21 253-259.

71. We1 Xi-cheng, FU Ren-yu. **Time Dependence of Transformation Processing of Si-Mn TRIP Steel During High- Speed Tensile Impact Testing**. GRIP'S Sparking World of Steel. 2002, Vol. 1, pp. 293-298.

72. K. Sugimoto, N. Usui, M. Kobayashi and S. Hashimoto. **Effects of Volume Fraction and Stability of Retained Austenite on Ductility of TRIP-aided Dual-phase Steels.** ISIJ International. 1992, Vol. 32, pp. 1311.

73. Bleck W. **Proceedings of the International Conference on TRIP Aided High Strength Ferrous Alloys**, Ghent, 2002, pp. 13.

74. Matsumura O, Sakuma Y, Takechi H. Camp-ISIJ. 1985, S1293, 89.

75. Kim SJ, Lee CG, Choi I, Lee S. **Effects of heat treatment and alloying elements on the microstructure and mechanical properties of 0.15 wt pct C transformation-induced plasticity-aided cold rolled steel sheet.** Metallurgical and Materials Transactions A, 2001, Vol. 32, pp. 505-14.

76. J. Maki, J.Mahieu, B.C. De Cooman, S. Claessens. **Galvanisability of silicon free CmnAl TRIP steels.** Materials science and technology. 2003 Vol.19, pp. 125-131.

77. De Meyer M, Vanderschueren D, De Cooman BC. **The influence of the substitution of Si by Al on the properties of cold rolled CMnSi TRIP steels.** ISIJ International, 1999, Vol. 39, pp. 813–22.

78. Jacques PJ, Girault E, Harlet P, Delannay F. **The development of cold rolled TRIP-assisted multiphase steels. Low silicon TRIP assisted multi-phase steels.** ISIJ International, 2001, Vol. 41, pp. 1061–7.

79. L. Gavard. **New metallurgy for micro-alloyed TRIP steels.** Internal Corus report 113918. (2005)

80. Chen HC, Era H, Shimizu M. **Effect of phosphorus on the formation of retained austenite and mechanical properties in Si containing**

low carbon steel sheet. Metallurgical and Materials Transactions A, 1989, Vol. 20, pp. 437-445.

81. W. C. Jeong and J. H. Chung (1992) **HSLA Steels: Processing, Properties and applications**. By G. Tither and Z. Shoubua, minerals metals and materials scocity, Warrendale, PA, 305.

82. A. Pichler, P. Stiaszny, R. Potzinger, R. Tikal and E. Werner: Proceedings of Mechanical Working and Steel Processing.

83. J. Chance and N. Ridley. **Chromium partitioning during isothermal transformation of a eutectoid steel.** Metallurgical and Materials Transactions A, 1981, Vol. 12, pp. 1205.

84. P. Jacques, E. Girault, T. Catlin, N. Geerlofs, T. Kop, S. van der Zwaag, F. Delannay. **Bainite transformation of low carbon Mn–Si TRIP-assisted multiphase steels: influence of silicon content on cementite precipitation and austenite retention.** Materials Science and Engineering A. 1999, Vol. 273-375 pp. 475-479.

85. J. Mahieu, J. Maki, B. C. De Cooman, and S. Claessens. **Al Transformation-Induced Plasticity-Aided Steel.** Metallurgical and Materials Transactions A, 2002, Vol. 33, pp. 3573-3580.

86. M. De Meyer, D. Vanderschueren, B. C. De Cooman. **The influence of Al on the properties of cold rolled C-Mn-Si TRIP steels.** 41st Mechanical Working and Steel Processing Conference Proceedings ISS. 1999 265-276.

87. J. M. Rigsbee and P. J. VanderArend (1977) **Proceedings of the symposium on formable HSLA and dual-phase steels.** Chicago, pp. 56.

88. F. B. Pickering (1978) **Physical Metallurgy and the Design of Steels.** Applied Science Publishers Ltd., London. pp.10.

89. A. Pichler, P. Stiaszny, R. Potzinger, R. Tikal and E. Werner. **TRIP steels with reduced Si content.** 40th Mechanical Working and Steel Processing Conference Proceedings, 1988 ISS. 259-274.

90. H. C. Cheng, H. Era and M. Shimizu. **Effect of phosphorus on the formation of retained austenite and mechanical properties in Si-containing low-carbon steel sheet.** Metallurgical and Materials Transactions A, 1998, Vol. 20, pp. 437-445.

91. M. L. Brandt and G. B. Olson. **Bainitic stabilization of austenite in low alloy sheet steels.** Iron & Steelmaker. 1993, Vol. 20, pp. 50-60.

92. Sung-Joon Kim, Chang Gil Lee, Tae-Ho Lee, Chang-Seok Oh. **Effect of Cu, Cr and Ni on mechanical properties of 0.15 wt.% C TRIP-aided cold rolled steels.** Scripta Materialia. 2003, Vol. 48, pp. 539-544.

93. Im DB, Lee CG, Kim SJ, Park I. J. The Korean Institute of Metals and Materials. 2000, Vol. 38, pp. 447.

94. Koh HJ, Lee SK, Park SH, Kim NJ. **Proceeding of the sixth symposium on phase transformation**. Pohang: Korean Institute of Metals and Material, 1996, pp.157.

95. Yoo JY, Choo WY, Park TW, Kim YW. **Microstructures and age hardening characteristics of direct quenched Cu bearing HSLA steel.** ISIJ International, 1995, Vol. 35, pp. 1034.

96. Chang Gil Lee, Sung-Joon Kima, Tae-Ho Lee, Sunghak Lee. **Effects of volume fraction and stability of retained austenite on formability in**

a 0.1C–1.5Si–1.5Mn–0.5Cu TRIP-aided cold-rolled steel sheet. Materials Science and Engineering A. 2004 Vol. 371, pp. 16–23.

97. H. Stankova, Z. Novy, K. Dalikova, L.W. Meyer, B. Masek. **Expansion of TRIP effect application in incremental deformation forming.** University of West Bohemia, Univerzitni 22, 30614 Pilsen.

98. **Application of high-strength steel sheets for automobiles in Japan** ATS International Steelmaking Conference, Paris, 2000.

99. Cretteur L, Koruk AI, Tosal-Martinez L. Steel Research 2002. Vol. 73, pp. 314–9.

100. J. Mahieu, S. Claessens, M. De Meyer, and B. De Cooman. **Proceedings Galvanised steel sheet forum ± automotive.** London, UK, 2000, The Institute of Materials, 185.

101. Annual Book of ASTM Standards. **Standard recommended practice for determining volume fraction by systematic manual point count.** Part 11, E 562,

102. F. Jatczak, J.A. Larson, S.W. Shin. **Retained austenite and its measurement by X-ray diffraction** sp-453C. (SAE) Society of Automotive Engineers, 1980, ISBN 0-89883-224-1.

103. ASTM Designation. **Standard practice for X-ray determination of retained austenite in steel with near random crystallographic orientation.** ASTM International, E 975 – 95.

104. Tensile testing of metallic materials. Part 1 - Method of test at ambient temperature, BS EN 10002-1:2001.

105. S. Oliver. Eng.D. Thesis, University of Wales Swansea, 2007